



Delft University of Technology

## Molecular dynamics simulation on bulk bitumen systems and its potential connections to macroscale performance: Review and discussion

Ren, S.; Liu, X.; Lin, P.; Gao, Y.; Erkens, S.

**DOI**

[10.1016/j.fuel.2022.125382](https://doi.org/10.1016/j.fuel.2022.125382)

**Publication date**

2022

**Document Version**

Final published version

**Published in**

Fuel

**Citation (APA)**

Ren, S., Liu, X., Lin, P., Gao, Y., & Erkens, S. (2022). Molecular dynamics simulation on bulk bitumen systems and its potential connections to macroscale performance: Review and discussion. *Fuel*, 328(125382), 1-35. Article 125382. <https://doi.org/10.1016/j.fuel.2022.125382>

**Important note**

To cite this publication, please use the final published version (if applicable).

Please check the document version above.

**Copyright**

Other than for strictly personal use, it is not permitted to download, forward or distribute the text or part of it, without the consent of the author(s) and/or copyright holder(s), unless the work is under an open content license such as Creative Commons.

**Takedown policy**

Please contact us and provide details if you believe this document breaches copyrights.

We will remove access to the work immediately and investigate your claim.



## Review article

# Molecular dynamics simulation on bulk bitumen systems and its potential connections to macroscale performance: Review and discussion



Shisong Ren, Xueyan Liu, Peng Lin, Yangming Gao\*, Sandra Erkens

*Section of Pavement Engineering, Faculty of Civil Engineering & Geosciences, Delft University of Technology, Delft, Netherlands*

## ARTICLE INFO

**Keywords:**  
 Bitumen  
 Molecular dynamics simulation  
 Aging  
 Modification  
 Rejuvenation  
 Multiscale evaluation methods

## ABSTRACT

Molecular dynamics (MD) simulation plays an effective role in predicting the critical properties and explaining the macroscale phenomenon at the nanoscale. This review summarized the application cases of MD simulations in various bitumen systems, considering aging, modification, and rejuvenation factors. Meanwhile, the potential relationships between the nanoscale parameters predicted from MD simulations and macroscale properties measured from experimental tests were discussed for the first time. Different molecular models of virgin bitumen, commonly-used Forcefields, and validation parameters for MD simulations on bituminous materials were summarized. Based on the reactive MD simulation outputs, the oxidative aging reaction path at the atomic scale of bitumen molecules was reviewed. Furthermore, the influence of aging (short-term and long-term), modification (polymers, fillers, and bio-bitumen), and rejuvenation (various rejuvenators) on the molecular-scale properties of virgin bitumen models would be evaluated through MD simulations. This review could help us further explore the main functions of MD simulations in different bulk bitumen systems and build an integral multi-scale research method from the molecular design and performance prediction to material optimization and synthesis of bituminous materials without lots of experimental attempts.

## 1. Introduction

Asphalt pavement attracts increasing attention due to its flexible performance and driving comfort [1]. However, there are still many issues to be addressed during the design, construction, and maintenance procedures of asphalt mixtures [2]. From a practical engineering viewpoint, the asphalt pavements with low cost, high performance, long service life, and environmental friendliness are always preferred [3]. To this end, numerous advanced technologies have been proposed, including bitumen modification by adding polymers and waste materials, bio-bitumen, warm-mix asphalt, and rejuvenation of reclaimed asphalt pavement (RAP) [4–9]. Meanwhile, asphalt mixtures always suffer from the heavy loadings, resulting in different failure modes of rutting, raveling, and cracking [10–12]. At the same time, the complicated environmental conditions of temperature, moisture invasion, oxidative reaction, and ultraviolet-light radiation inevitably lead to the performance deterioration of bitumen binder and asphalt mixture [13–17].

Experimental characterization is the first choice for pavement researchers to evaluate modification efficiency, monitor performance

variation, analyze influence factors, determine preparation and construction conditions of bituminous materials, and estimate the recycling potential of RAP materials [18–22]. In addition, various chemical, mechanical, and morphology methods have been utilized to reveal the underlying mechanisms of aging, modification, destructive form, self-healing, and rejuvenation phenomenon [23–30]. However, these macroscale evaluation methods have limitations in fundamentally understanding the static and dynamic behaviors of bituminous materials, such as (1) the oxidative reaction path of bitumen molecules during a thermal aging procedure [31]; (2) the intermolecular interactions between different modifiers and bitumen molecules [32]; (3) the effects of aging and modification on both thermodynamics parameters and structural arrangements of bitumen molecules [33]; (4) the atomic-scale mechanism of cohesion and adhesion failures [34]; (5) the diffusion behaviors of oxygen and moisture substances in bitumen binder and asphalt mixture [35]; (6) the molecular-scale self-healing mechanism of bitumen [36]; (7) the diffusion and blending behaviors of rejuvenators in aged bitumen [37]; (8) the molecular-level reasons for the difference in rejuvenation efficiency between rejuvenators and aged binders [38]. It is challenging to address these gaps with macroscale evaluation

\* Corresponding author.

E-mail address: [Y.Gao-3@tudelft.nl](mailto:Y.Gao-3@tudelft.nl) (Y. Gao).

techniques alone.

Nowadays, a multi-scale bituminous materials characterization (from the nanoscale to macroscale levels) is favored, as illustrated in Fig. 1 [39]. The asphalt mixture is composed of bitumen, aggregate, filler, and sand [40]. The bitumen plays an essential role in bonding aggregates and providing structural stability to the whole asphalt mixture [41]. Hence, it is of significance to comprehensively understand both macroscale and microscale properties of bitumen during the fabrication, modification, aging, and rejuvenation procedures. Previous studies proved that bitumen's rheological and mechanical properties strongly depended on its chemical components [42,43]. However, bitumen with complicated chemical compositions is a heavy oil residue derived from refining crude oil [44]. It is challenging to completely sort out all molecular components in bitumen, but they could be mainly divided into four groups based on molecular polarity and solubility, including the saturate, aromatic, resin, and asphaltene (SARA) fractions [45]. From the perspective of bitumen microstructure, the colloidal structure has been the most popular theory. Asphaltene molecules acting as gel cores are surrounded by resin molecules and dispersed in lighter fractions phase (aromatic and saturate) [46]. Although the chemical mechanisms of bitumen aging and rejuvenation could be interpreted on the basis of SARA fractions' variation, it is also necessary to explore the aging reaction path of each SARA fraction and the intermolecular interactions between various bitumen molecules with polymers, warm-mixing agents, and rejuvenators [47–49]. Identifying the difference in intermolecular force and molecular distribution of bitumen components could determine the physical, thermodynamic, and mechanical properties of bitumen [50]. With a multi-scale investigation method, the underlying mechanism would be explained thoroughly, and thus the innovative anti-aging additives, warm-mixing agents, and rejuvenators could be developed from molecular design to optimization and validation [51].

The MD simulation has been widely performed on various bulk, dynamic, and interfacial systems of bituminous materials [52]. Firstly, different molecular models of bitumen have been developed in line with its chemical characteristics, which were the basic and important input parameters of MD simulations [53]. Afterwards, different thermo-physical [54], thermo-dynamics [55], thermo-mechanical [56], and structural parameters [57] can be outputted from MD simulations, which are seldom measured from macroscale tests because of the restricted scale scope and instrument accuracy. In terms of aging mechanism and influence, MD simulations have been successfully employed to explore the potential oxidative reaction path of bitumen molecules [58] and predict aging impacts on the thermodynamic properties and molecular structures of a whole bitumen model [59]. In addition, it has been proved that the MD simulation could allow us to probe the intermolecular interactions between bitumen molecules with various polymers [60], fillers [61], and rejuvenators [62]. The diffusive behaviors of oxygen, moisture, and rejuvenator molecules in bitumen at an atomic scale have also been monitored with MD simulations [63–65]. Furthermore, the self-healing mechanism was explained from the viewpoint of molecular mobility with different temperatures, aging levels, rejuvenator components and dosages [66]. Last but not limited,

the MD simulations show advantages in predicting the adhesion performance and explaining the intermolecular interaction mechanism between the bitumen and aggregates. All influence factors of bitumen components, aggregate type, temperature, and moisture were considered in MD simulations [67–69], and many time-consuming and laborious experiments were omitted.

There is no doubt that the MD simulation method shows a considerable application potential in bituminous materials, which has significant scientific values in material design, mechanism explanation, and performance prediction. However, there are few review papers summarizing the applications of MD simulations in bulk bitumen systems considering the influence of aging, modification, and rejuvenation. Meanwhile, the bitumen models, Forcefield type, validation indices, and predicted parameters from MD simulations vary considerably for different bituminous materials, which have not been generalized. Further, the potential connections between estimated parameters of bulk bitumen systems outputted from MD simulations and their macroscale performance measured from experiments were hardly discussed.

## 2. Review objective and structure

The main objective of this paper is to comprehensively review the applications of MD simulations on different bulk bitumen systems during aging, modification, and rejuvenation processes. Meanwhile, the input and output parameters in MD simulations on bitumen will be summarized. The review structure and main contents are illustrated in Fig. 2. Firstly, the basic principle and forward-looking characteristics of MD simulations are introduced briefly. Secondly, the molecular models of bitumen, Forcefield types, validation parameters, and predicted parameters during the MD simulations on bulk bitumen systems are generalized and summarized. Thirdly, MD simulation studies on the oxidative reaction mechanisms of bitumen molecules and the aging influence on the molecular-scale characteristics of bitumen are reviewed. Afterwards, MD simulation work on various modified bitumen systems (polymer, filler, and bio-bitumen) are examined. In addition, MD simulation investigations exploring the rejuvenation efficiency and mechanism of rejuvenated bitumen systems at an atomic level are introduced. Lastly, the potential connections between these molecular-scale parameters of bulk bitumen systems outputted from MD simulations and the corresponding mechanical properties measured by macroscale experiments are discussed.

## 3. Molecular dynamics simulations

### 3.1. Basic principles of MD simulations

The molecular dynamics simulation technology composed of theoretical knowledge of quantum mechanics and Newton's classical mechanics probes the material characteristics from a molecular-level viewpoint [50,52]. Fig. 3. demonstrates the basic principles of MD simulations, and it includes the following steps:

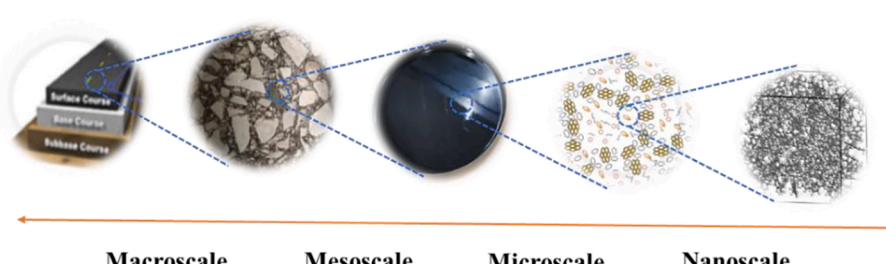


**Fig. 1.** Multiscale illustration of asphalt and bituminous materials.

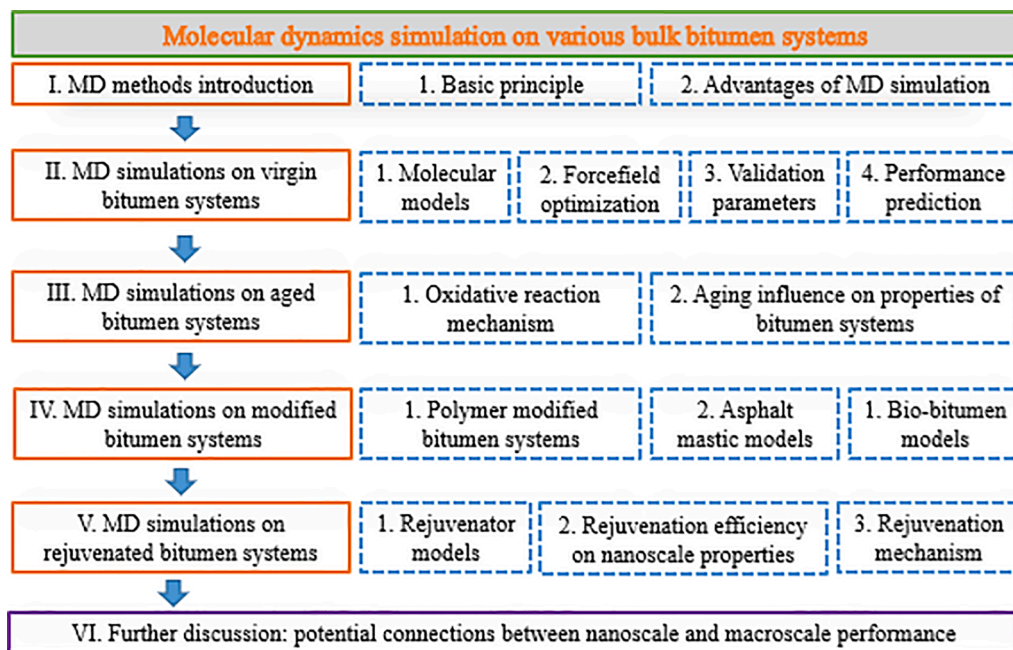


Fig. 2. The review structure and content.

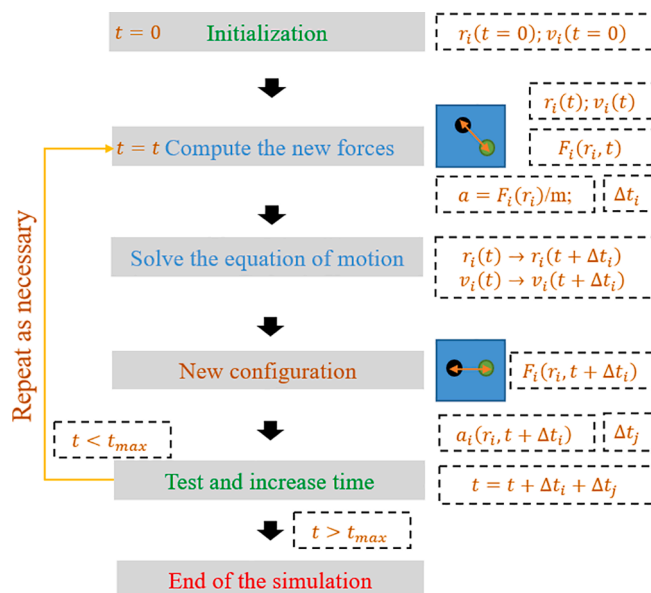


Fig. 3. The basic principle of MD simulation.

- Step 1-Initialization: Before running an MD simulation program (simulation time  $t = 0$ ), the target molecules are incorporated into a simulation system with an initial position  $r_i(t = 0)$  and velocity  $v_i(t = 0)$ ;
- Step 2-Computation of a new force: The intermolecular interaction force  $F_i(r_i, t)$  is estimated under a forcefield.
- Step 3-Solving the equation of motion: The acceleration value of a molecule is estimated using Newton's equation ( $a = F/m$ ). When the time elapses from  $t$  to  $t + \Delta t$ , both the new position and velocity of one molecule change from  $r_i(t)$  and  $v_i(t)$  to  $r_i(t + \Delta t)$  and  $v_i(t + \Delta t)$ , and thus the new configuration at the time  $t + \Delta t$  can be obtained.
- Step 4-Repeating steps 2 and 3: When the simulation time  $t + \Delta t$  is shorter than the set maximum simulation time  $t_{max}$ , steps 2 and 3 are repeated to obtain the equilibrium system and relevant results.

During this step, the interaction force is recalculated, while the molecular velocity and position are renewed.

- Step 5-Ending the simulation: When the time  $t + \Delta t$  reaches the set value ( $t_{max}$ ), the MD simulation will end. At the same time, the trajectories of model configuration and energy during MD simulation are recorded to predict the physical and thermodynamics parameters of the simulated models.

### 3.2. Advantages of MD simulations

The laboratory experiments are usually employed for characterizing the bituminous materials because of the great authenticity [70,71]. Nevertheless, some disadvantages of these conventional tests have been realized, which are listed as follows:

- Some specific experiments are difficult or impossible to perform due to the instrument and material limitations;
- The experimental errors resulted from the difference in both material and instrument factors cannot be avoided, which significantly affect the ultimate experimental results;
- The laboratory evaluation methods are expensive and time/workforce consuming, showing negative influence the parameters optimization and material design;
- The molecular-scale underlying mechanisms are still unclear based on these large-scale experimental results. Moreover, many experimental parameters should be controlled, and it remarkably increases the difficulty and uncertainty of experimental outputs;
- The chemical experiments with hazardous materials and high-risk equipment are dangerous. Meanwhile, the toxic products do harm both human health and environmental quality.

Therefore, the MD simulation method has been developed to address these shortcomings of conventional experiments. It can predict the results by avoiding unnecessary investigations and explain the underlying mechanisms of experimental results from the nanoscale perspective. Here are some perceivable advantages of MD simulation technology:

- We can get an insight into the performance prediction of different materials at an atomic level, which is distinctly valuable to the material design and optimization without unnecessary experiments;
- The experimental conditions could be optimized based on MD simulation outputs. Meanwhile, the region of the simulation environment (e.g. temperature and pressure) can be more controllable than laboratory tests considering the instrument capacity and operational safety;
- The MD simulation method plays an important role as a bridge in connecting the theory and experiments, and it would be beneficial to developing innovative ideas and research methods;
- Furthermore, the atomic-level interaction mechanisms could be provided by MD simulation to explain the experimental phenomena.

#### 4. MD simulations on virgin bitumen systems

The molecular dynamics simulation method has been utilized in bituminous materials to understand the intermolecular interactions between bitumen molecules and predict the crucial physical, thermodynamics, and mechanical properties [72–74]. This section introduces the application cases of MD simulations in virgin bitumen systems without any additive or aging. Fig. 4 displays the overall program of MD simulation on pure bitumen systems. The bitumen models and forcefield are the most critical inputs directly related to the reasonability of simulation outputs. After optimizing the molecular model and forcefield, the MD simulation program could be performed with variable ensemble, temperature (Thermostat control), pressure (Barostat control), time step, and simulation time.

Meanwhile, the trajectories for the equilibrium configurations of bitumen models are recorded to predict the physical and thermodynamics properties. To verify the reliability of both molecular models and

forcefield, it is indispensable to figure out the difference in the chemical and thermodynamics parameters between MD simulation outputs and experimental results. Afterwards, MD simulation procedures are implemented to determine other valuable indications of bitumen systems, including the thermo-physical, thermo-dynamics, mechanical, and structural characteristics. Eventually, it is crucial to link the nanoscale parameters from MD simulations with the corresponding macroscale properties of bituminous materials from experiments. Herein, the potential relationships between nanoscale and macroscale parameters will be discussed briefly in the last section to enlighten and encourage researchers to consider the connection issue when they conduct MD simulation studies on bituminous materials.

##### 4.1. Molecular model development of virgin bitumen

###### 4.1.1. Average one-component molecular model

Bitumen is composed of thousands of hydrocarbon molecules, and it is difficult to determine the integral structure of each bitumen molecule. Initially, one average molecule was adopted to represent a whole bitumen system. In view of the petrochemical knowledge, Jenning et al. [75] proposed the average molecular models of eight core bitumen based on the Nuclear Magnetic Resonance (NMR) spectroscopy results, shown in Fig. 5. These average molecular structures are all composed of aromatic rings, naphthenic rings, alkyl branched chains, and few heteroatoms. Meanwhile, the bitumen source significantly influences the average molecular structures with variable molecular weight, functional group distribution, aromaticity, and branched-chain length. Although Pauli et al. reported that it was possible to predict the density and surface energy of bitumen [76], these average models have neglected the sizeable molecular distribution region characteristic of bitumen. In addition, it is hard to explore the intermolecular interactions between

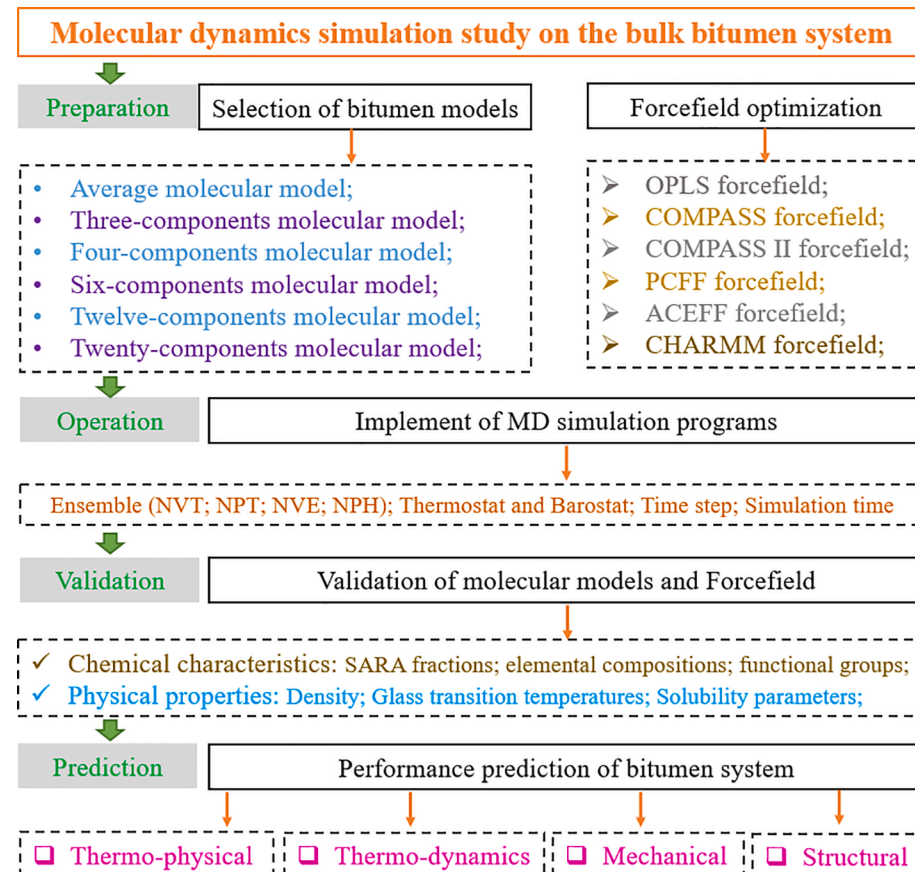
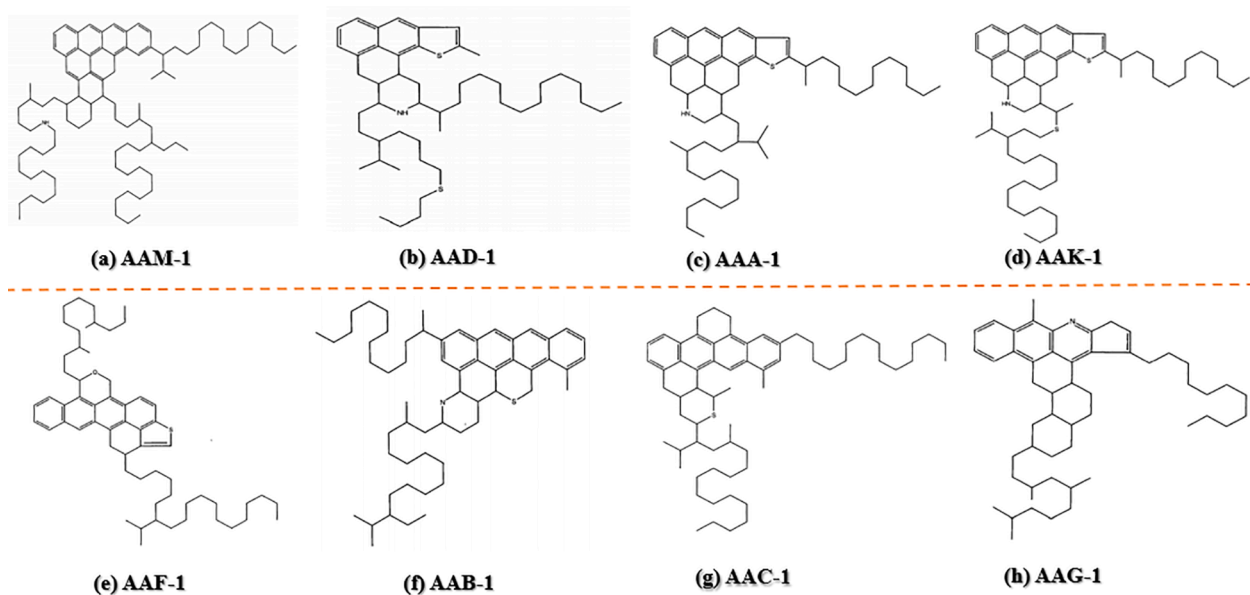


Fig. 4. The overall program of MD simulations on virgin bitumen systems.



**Fig. 5.** The average molecular models of eight SHAP core bitumen.

different SARA fractions of bitumen. In other words, when these average models are adopted, it is impossible to detect the molecular components change in bitumen during various aging, modification, and rejuvenation procedures.

#### 4.1.2. Three-component molecular model

The average model is able to reflect the whole chemical structure of bitumen to some extent, including the aromaticity, hydrogen/carbon (H/C) ratio, and the atomic number of aromatic and aliphatic carbon. However, thousands of molecules with a massive difference in molecular weight, aromaticity, polarity, and functional group distribution are included in one bitumen binder. To this end, these chemical components are divided into four groups: saturate, aromatic, resin, and asphaltene. It should be mentioned that only saturate, resin, and asphaltene fractions were considered in a three-component model. As shown in Fig. 6, the saturate and resin fractions are represented by *n*-docosane and 1,7-

dimethylnaphthalene molecules. Moreover, two typical molecular structures of asphaltene were proposed in a three-component model. Asphaltene I molecule consists of several fused aromatic rings with short alkane branches, while asphaltene II exhibits longer aliphatic chains surrounding a core of fewer aromatic rings. Zhang et al. [77] performed an MD simulation on a three-component bitumen model with the OPLSaa forcefield. They reported the feasibility of three-component bitumen model through predicting the thermo-physical properties of bitumen model, including the density, thermal expansion coefficient, and isothermal compressibility.

However, it should be noted that all molecules in a three-component model come from different bitumen sources, resulting in a considerable difference between MD simulation outputs and experimental results. Ding et al. [78] carried out liquid chromatography (LC) transform combined with Fourier-transform infrared (FTIR) spectroscopy and gel permeation chromatography (GPC) for the purpose of separating and

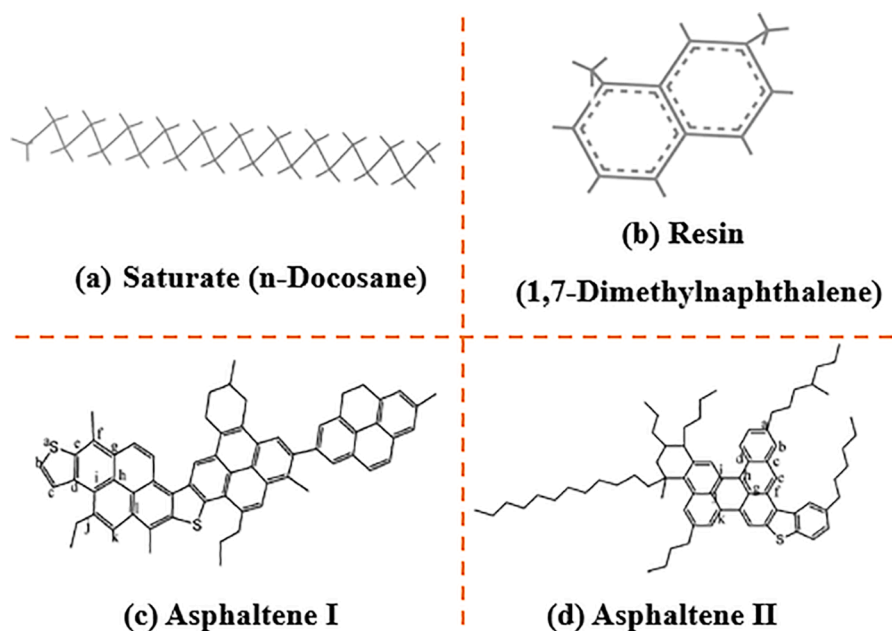


**Fig. 6.** The molecular structure of each fraction in the three-components model.

detecting authentic chemical components in both virgin and aged bitumen. Three categories were identified on the basis of the difference in molecular weight distribution. Afterward, the molecular weight, C/H ratio, and the number of aromatic carbons, aromatic rings, alkane carbons, and branched-chain carbons, as well as the branched chains were calculated. Accordingly, new three-component virgin and aged bitumen models have been constructed, as illustrated in Fig. 7. Finally, the density results revealed that the proposed three-component molecular model was more accurate than the previous model. It should be noted that the model was based on a standard performance grade (PG 64–22) bitumen in Tennessee, USA, and the aging protocol contained a rolling thin film oven (RTFO) test and a standard pressure aging vessel (PAV) test.

#### 4.1.3. Four-component molecular model

The Four-component molecular model was also established based on SARA fractions of bitumen, in which each SARA fraction was represented by one average molecule. Different four-component molecular models were proposed in previous studies, summarized in Fig. 8. The four-component model I was popularly adopted [79–83], in which the representative molecules for asphaltene, resin, saturate, and aromatic were  $C_{53}H_{57}NO_5$ ,  $C_{100}H_{106}$ ,  $C_{22}H_{46}$ , and  $C_{12}H_{12}$ . Meanwhile, the four-component model II was also developed to represent the bitumen models [84–86]. The molecular formula (molecular weight) information was: Asphaltene:  $C_{150}H_{181}N_3O_2S_2$  (2122.24 g/mol); Resin:  $C_{59}H_{85}NO_5$  (856.395 g/mol); Aromatic:  $C_{46}H_{50}S$  (634.966 g/mol); and saturate:  $C_{22}H_{46}$  (310.61 g/mol). Fig. 8c draws the commonly-utilized four-component bitumen model [87–91]. In addition, Zeng et al. developed another four-component bitumen model with the SARA fraction's molecular formula of  $C_{51}H_{92}$  (saturate),  $C_{103}H_{151}N$  (aromatic),  $C_{95}H_{120}O_4$  (resin), and  $C_{66}H_{80}S$  (asphaltene) [92]. Similarly, Ramezani and Rickgauer [93] built a four-component bitumen model through selecting several molecules from the most universal 12-component molecular model initiated by Li and Greenfield [94].

#### 4.1.4. Six-component molecular model

In view of the difference in molecular weight and aromaticity, Qu et al. [33] further subdivided the aromatic molecules into mono-aromatic, diaromatic, and polyaromatic categories. Fig. 9 displays the molecular structures of SARA molecules. In this proposed six-component molecular model, the *n*-docosane ( $C_{22}H_{46}$ ) and 1,7-Dimethylnaphthalene ( $C_{12}H_{15}$ ) were chosen to represent the saturate and mono-aromatic. Besides, Diethyl-cyclohexane-naphthalene (DOCHN,  $C_{30}H_{36}$ ) and Perhydrophenanthrene-naphthalene ( $C_{35}H_{44}$ ) represented the diaromatic and polyaromatic molecules. Moreover, the resin molecule was chosen to be Quinolinohopane ( $C_{34}H_{47}N$ ), and the asphaltene molecular formula was  $C_{73}H_{100}S$ . It was reported that both density and elastic modulus values predicted from an MD simulation on this six-

components model agreed well to the experimental results than the commonly-used 12-component model [95]. It should be mentioned that the six-component model was determined based on NMR, GPC, FTIR spectroscopy tests, and element analysis for one #70–100 bitumen from the Nynas Plant in Venezuela.

#### 4.1.5. Twelve-component molecular model

The twelve-component model, proposed by Li and Greenfield, is the most widespread molecular model of bitumen [94]. The target bitumen binders were AAA-1, AAK-1, and AAM-1 from the Strategic Highway Research Program (SHRP). As illustrated in Fig. 10, bitumen molecules were classified into four groups (saturates, naphthalene aromatics, polar aromatics, and asphaltenes). Meanwhile, 2–5 types of molecules with different polarities and sizes are selected to represent SARA fractions based on previous studies on petroleum geochemistry [96]. In detail, the squalene and hopane molecules were chosen to denote the saturate fraction, while naphthalene aromatics were perhydrophenanthrene-naphthalene (PHPN) and diethyl-cyclohexane-naphthalene (DOCHN). Moreover, the resin fraction was composed of five molecules, including the quinolinohopane, pyridinohopane, thio-isorenieratane, trimethylbenzene-oxane, and benzobisbenzothiophene. Three asphaltene molecules, named asphaltene-phenol, asphaltene-pyrrole, and asphaltene-thiophene, were relocated from the asphaltene structures proposed by Mullins [97,98]. Furthermore, the number of each molecule was determined by the solubility parameters and elemental compositions. After an MD simulation on the 12-component bitumen model with an OPLS Force Field, the predicted outputs in Hansen solubility parameters, density, thermal expansion coefficient, molecular rotational relaxation times, diffusion coefficients, and viscosity were closer to the experimental results than the average and 3-component models.

In addition, Wang et al. [45] proposed a Fifteen-component molecular model for three bitumen Q70, P90, and H90 according to their structural parameters of molecular weight ( $M_n$ ), total hydrogen ( $H_T$ ), total carbon ( $C_T$ ), aromatic carbon ( $C_A$ ), naphthenic carbon ( $C_N$ ), paraffin carbon ( $C_P$ ), aromatic rings ( $R_A$ ), and naphthenic rings ( $R_N$ ) calculated with an improved Brown-Ladner (B-L) method. It was found that the arrangement of SARA fractions was strongly in line with the classic colloidal theory. The asphaltene molecules were dispersed as a core in the maltene phase, mainly resulting in the bee microstructure of bitumen observed from atomic force microscopy (AFM). Xu et al. [99] established a Twenty-component molecular model for fresh bitumen composed of the different SARA fractions from previous literature [42,45,96]. Furthermore, according to the reaction routes of bitumen molecules' initial, fast, and long-term aging reactions, the 25-component molecular models of three fresh and aged bitumen (AD90#, SK90#, and GF90#) were constructed. Both SARA fractions and element compositions in molecular models agreed well with the measured values. It was proved that the model was more appropriate than

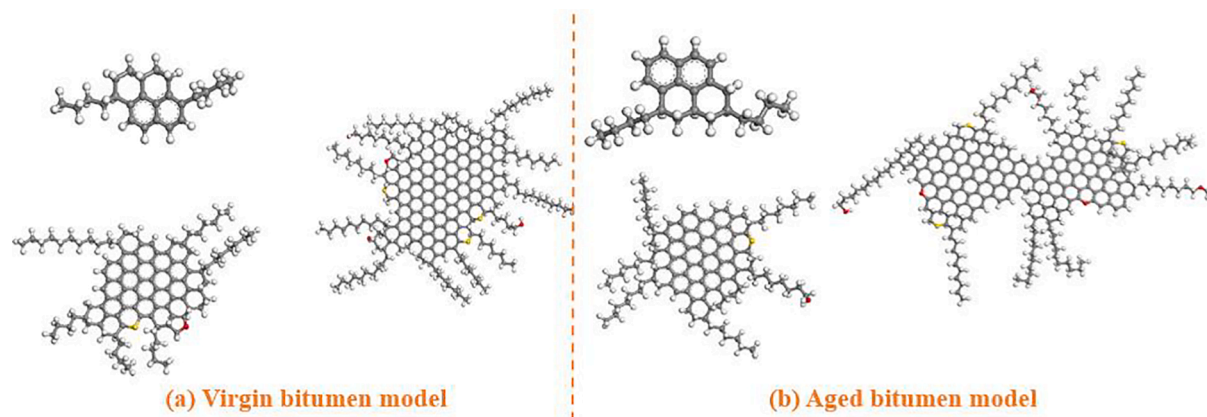


**Fig. 7.** Three-components molecular models for virgin (a) and aged (b) bitumen.

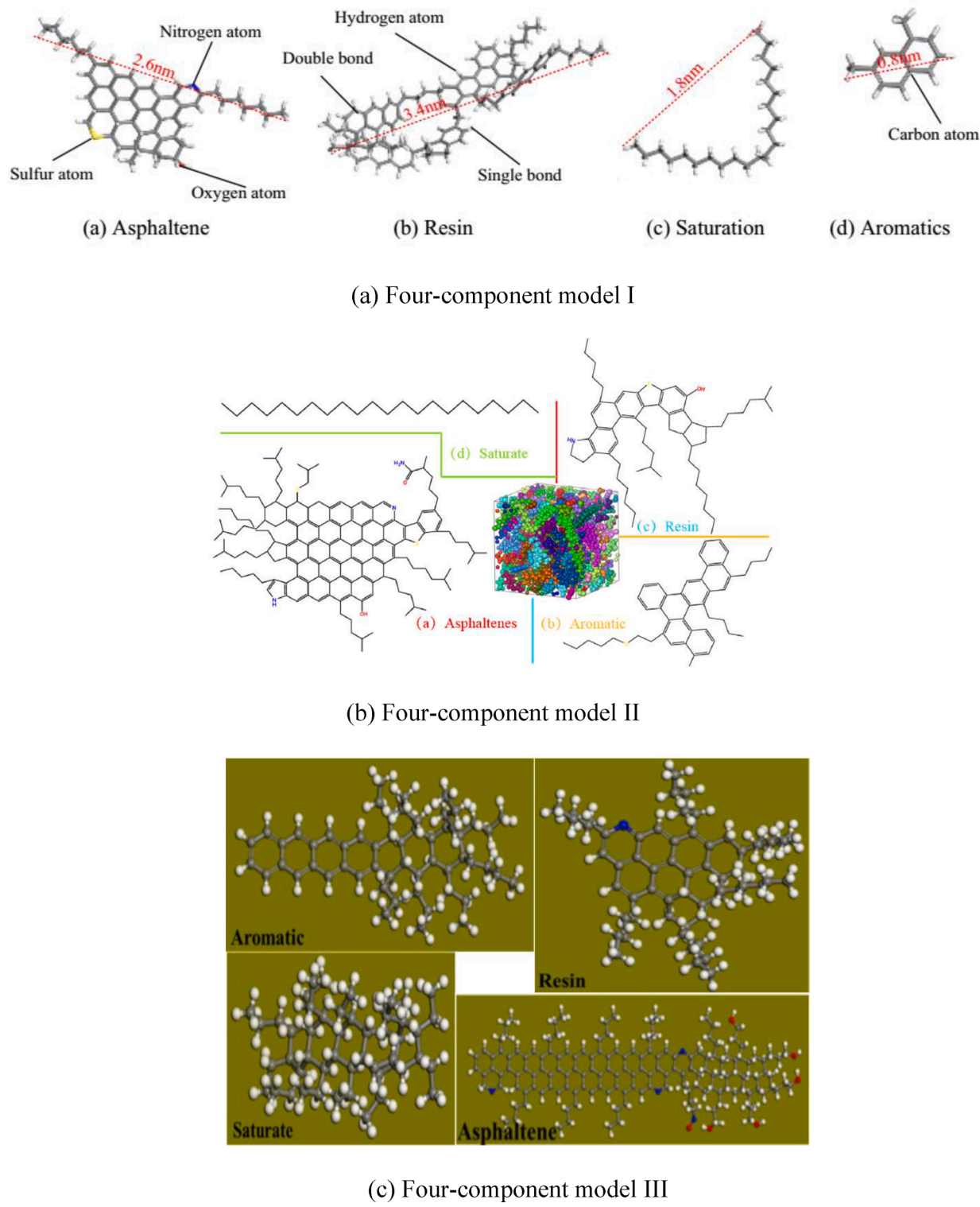


**Fig. 8.** Different four-component molecular models of virgin bitumen.

previous models in characterizing the aging influence on bitumen's physical and mechanical properties.

#### 4.2. Forcefield selection

The molecular mobility and distribution in a bitumen model are distinctly determined by the intramolecular and intermolecular interaction between various molecules. The total energy of one simulation

model consists of kinetic and potential energies, and a forcefield is employed to describe the intermolecular force between different atoms and molecules. Therefore, the selection of an appropriate forcefield for one specific bitumen model is crucial to ensure the accuracy and reliability of simulation outputs. However, the conclusion regarding which force field is the best choice for bituminous materials has still not been drawn. The application of MD simulations in the field of bituminous materials is not too long, and thus the forcefield selection is generally

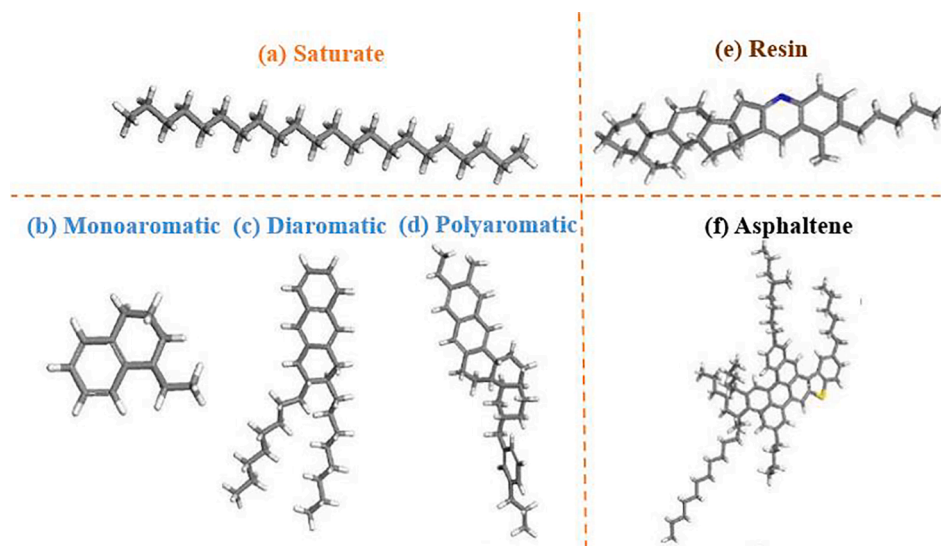


**Fig. 9.** Molecular structure of each fraction in a six-components molecular model.

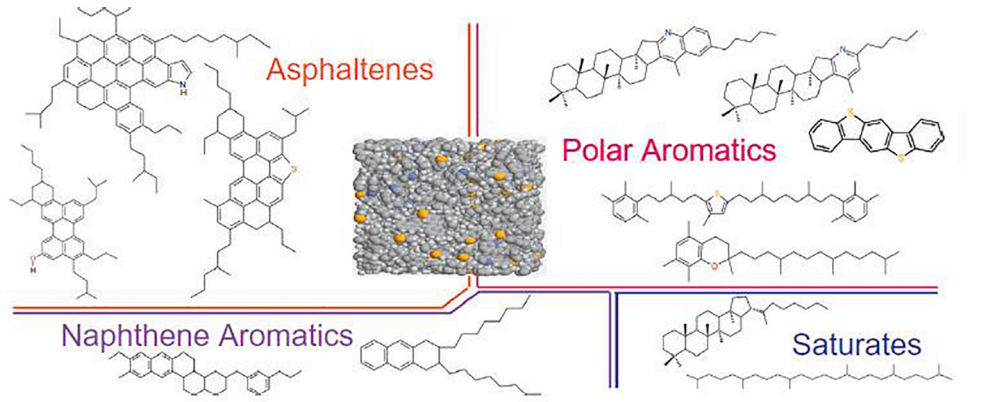


**Fig. 10.** Molecular structures of each fraction in a twelve-components model.

performed based on the existed ones designed for other organics, inorganic matter, polymers, or metals. Therefore, the forcefield types chosen in various MD simulations on bituminous materials are not uniform, and Table 1 summarizes the Forcefield types utilized for MD simulations on bulk bitumen models.

The commonly-used forcefields in bulk bitumen systems contain the Optimized Potential for Liquid Simulation (OPLS), Condensed-phase Optimized Molecular Potential for Atomic Simulation Studies (COMPASS), Amber Cornell Extension Force Field (ACEFF), General Amber Force Field (GAFF), Polymer Consistent Force Field (PCFF), Consistent Valence Force Field (CVFF), Chemistry at Harvard Macromolecular Mechanics (CHARMM), Reaction Force Field (ReaxFF), MARTINI Force Field, as well as DREIDING Force Field. A brief description of each Force Field and corresponding references are also listed in Table 1.

In summary, it is challenging to distinguish the advantages and disadvantages of different Forcefield types utilized in MD simulations on bitumen models on the basis of previous limited comparison work. According to the references' information, the COMPASS (II) Forcefield is the most popular one so far for various bituminous models. Moreover, the OPLS and DREIDING Forcefields were preferred about ten years ago. The forcefields of ACEFF, GAFF, PCFF, CVFF, and CHARMM were selected in a few cases. It should be noted that the ReaxFF and MARTINI Forcefields are available in specific bitumen systems. The ReaxFF effectively detects the chemical reaction pathway of bitumen molecules, such as the oxidative aging mechanism at an atomic level. In addition,

the MARTINI Forcefield was considered a good choice when the research attention was on the microstructures of different phases in bitumen systems at the mesoscale.

You et al. [140] adopted the ACEFF forcefield for an MD simulation on the 12-component bitumen model with the OPLS forcefield. The results revealed a sensational agreement in the MD simulation outputs between the ACEFF and OPLS forcefields. Similarly, Sonibare et al. [100] compared the MD simulations on an ordinary-three-component bitumen model with CHARMM and OPLS-aa forcefields. It was found that all density, diffusion coefficient, and radial distribution function (RDF) parameters from the two forcefields were very similar. However, the CHARMM forcefield could predict the crystallization of *n*-docosane at 300 K more accurately than the OPLS-aa force field. Overall, the difference in MD simulation outputs between various Forcefields is still unclear, which should be further explored and compared to optimize the forcefield for bituminous materials with a sufficient accuracy.

#### 4.3. Validation parameters in MD simulations

It is important to validate the reliability of established molecular bitumen models and the setting parameters in MD simulations; otherwise, the MD simulation outputs would fail to connect with the practical applications. To ensure the similarity between the established molecular models and actual bituminous materials, various chemical characteristics in elemental compositions, SARA fractions, and the functional group

**Table 1**

Commonly-used Forcefields of MD simulations on bulk bitumen systems.

| Forcefield type  | Abbreviation | Brief descriptions   | Ref   |
|--|--------------|--|---|
| Optimized Potential for Liquid Simulation (in all-atom version)                            | OPLS (-aa)   | * The intermolecular interaction is composed of the pairwise repulsive and attractive Lennard-Jones and Coulomb forces;<br>* It works significantly well on many organic functional groups and proteins models;<br>* It is available in both three-component and twelve-component molecular models of bitumen.   | [42,94,96,100–104]  |
| Condensed-phase Optimized Molecular Potential for Atomistic Simulation Studies Force Field | COMPASS (II) | * It was the first forcefield derived from an ab initio calculation method;<br>* It can be utilized to simulate well and predict the structure, conformation, vibration frequency, and thermodynamic properties of a single molecule or condensed matter in a wide range;<br>* COMPASSII is an essential extension to the COMPASS force field;<br>* It has broad and detailed coverage in materials such as most common organics, small inorganic molecules, and polymers;<br>* It is the most popular forcefield applied for bituminous materials models. | [32,33,38,45,46,51,59,60,67,69,79,81,82,86,88,89,103,105–137] |
| Amber Cornell Extension Force Filed  | ACEFF        | * It is based on the Amber Cornell Force Field using some experimental parameters obtained from the General Amber Force Field (GAFF);<br>* It is appropriate for different simulation systems with organic and biological molecules.   | [64,80,138–141]   |
| General Amber Force Field  | GAFF         | * It is an extension of the AMBER force field, and it was parameterized for most of the organic molecules;<br>* It is an entire force field, and all parameters are available for the basic atom types.  | [73,142,143]  |
| Polymer Consistent Force Field   | PCFF         | * It is a class II ab initio force field that comes from CFF91 and is mainly proposed for organic systems and some metallic elements;<br>* It has been extensively parameterized and validated for polymers and organic materials.   | [63,125]  |
| Consistent Valence Force Field   | CVFF         | * It can describe the intra- and intermolecular interactions in bitumen nanocomposite systems;<br>* It cannot fully present the special hydrogen bond functions in bitumen;<br>* It is adopted to simulate the debonding behavior between the bitumen and mineral powder filler.   | [61,144]  |
| Chemistry at Harvard Macromolecular Mechanics  | CHARMM       | * It covers a wide range of organic groups, including bio-molecules and drug-like molecules;<br>* It is well employed in modeling systems containing solvent and bio-molecules.  | [68,100]  |
| Reaction Force Field   | ReaxFF       | * It is a bond-order-dependent Force Field allowing for bond breaking and formation;<br>* It has been parameterized and implemented for various materials and processes, including the polymers, metals, ceramics, and silicon for chemical simulations.   | [31,105,146]  |
| MARTINI Force Field  | MARTINI      | * It is based on parametrizing an extensive library of molecular simulation models against experimental thermodynamic data for coarse-grained molecular dynamics.  | [104]   |
| DREIDING Force Field   | DREIDING     | * It is a simple but versatile and generic all-atom force field to predict thermodynamics and structural properties of organic, biological, and main-group inorganic molecules.  | [144,147–151]   |

distribution of bitumen should be measured. After the MD simulations, several predicted physical or mechanical parameters should be compared with realistic results from experiments or previous studies. Table 2 lists the common validation parameters in MD simulation studies on bituminous materials.

The selected validation parameters in most MD simulations on bulk bitumen systems are the density, glass transition temperature, cohesive energy density, solubility parameter, diffusion coefficient, radial distribution function, shear modulus, viscosity, surface free energy, maximum adhesion force, nano-hardness, and modulus. At the same time, the most popular parameters to validate the reliability of MD simulation outputs are the density, glass transition temperature, cohesive energy density, and solubility parameters. Furthermore, the

colloidal structures of bitumen have been verified through the radial distribution function results of SARA fractions. In addition, the contact angle test was performed to measure the surface free energy of bituminous materials, and the Atomic Force Microscopy (AFM) was employed to examine the maximum adhesion force, nano-hardness, and modulus of bitumen.

#### 4.4. Performance prediction of bulk bitumen systems

It is expected that the MD simulations are able to provide valuable information on the material models at the nanoscale, which is hardly obtained from the macroscale tests. In the meanwhile, the relationships between the molecular structures and material performance could be

**Table 2**

The common validation parameters in MD simulations on bituminous materials.

| Parameters   | Ref   | Parameters   | Ref             |
|--|---|--|-----------------|
| Density<br>( $\text{g cm}^{-3}$ )                    | [38,39,42,44,45,55,57], 58, 62, 67, 73, 78, 80, 87, 94, 95, 103, 107, 116, 120, 121, 127, 128, 132, 133, 136, 137, 140, 144, 147] | Radial distribution function (RDF)                   | [59,86,132,134] |
| Glass transition<br>temperature (K)                  | [44,55,57,59,80,86,87,116,140,144]  | Shear modulus (GPa)                                  | [44,140]        |
| Cohesive energy density<br>( $\text{J m}^{-3}$ )     | [55,57,59,67,82,113,116,121,127,128]  | Viscosity (Pa·s)                                     | [80,140,144]    |
| Solubility parameter<br>( $\text{J m}^{-3})^{0.5}$ ) | [57–59,67,82,86,113], 116, 127, 128, 133, 134, 137]   | Surface free energy / maximum<br>adhesion force (nN) | [62,95,99,126]  |
| Diffusion coefficient<br>( $\text{m}^2/\text{s}$ )   | [140]   | Nanohardness and modulus (MPa)                       | [99]            |

detected according to the MD simulation outputs. It would help us fundamentally understand the atomic-level mechanism and guide the material composition optimization for satisfactory performance. This section overviews the different parameters of bituminous materials predicted from MD simulations. Due to space limitations, Table 3 only lists the standard parameters of bulk bitumen systems together with the corresponding brief descriptions. It should be noted that the detailed definition and calculation formula of each parameter are not presented here, which can be found in the references given. Concerning the bulk bitumen models, the performance parameters originated from MD simulations are divided into four categories: thermo-physical properties, thermo-dynamics properties, thermo-mechanical properties, and structural properties.

#### 4.4.1. Thermo-physical properties

The thermo-physical properties of a bulk bitumen model are composed of the density, cohesive energy density, solubility parameter, thermal expansion coefficient, binding energy, isothermal compressibility, interaction energy, surface free energy, work of cohesion, Flory-Huggins interaction parameter, ductility, flexibility index, thermal conductivity, and heat capacity. Generally, various parameters are utilized together to thoroughly address the research questions from a multi-scale viewpoint.

Density is a fundamental parameter utilized to verify the reliability of MD simulation outputs on bitumen models because of its easy accessibility from laboratory tests or databases mentioned in previous work. For instance, Qu et al. [95] verified the efficiency of their developed six-fraction bitumen model according to the similar density values from MD simulations and experiments. However, the elastic modulus measured by AFM was much lower than the predicted values, which might be related to the scale difference. Likewise, Ding et al. [78] proposed an innovative three-component bitumen model and found that experimental density was closer to the predicted value of the current model than other two models. In addition, a bitumen model's density variation as a function of temperature is always detected to anticipate the glass transition temperature ( $T_g$ ) parameter.

The MD simulation outputs of cohesive energy density (CED) and solubility parameters ( $\delta$ ) are also essential. Apart from the validation role, the CED variation was monitored to estimate the influence factors of aging, modification, and rejuvenation. Moreover, both CED and  $\delta$  parameters strongly depend on the intermolecular interactions in a whole system. The  $\delta$  values of bituminous materials come from the dispersion, polar, and hydrogen bonding interactions, which could be measured through both Hansen's 3-D space fitting and Van Krevelen-Hoftyzer methods. Li and Greenfield conducted a comparison in solubility parameters between the measured and predicted values to validate their proposed 12-component bitumen model [94]. It was revealed that various molecules in one solubility class exhibited the similar solubility parameter values. From the perspective of polymer science, the solubility parameter difference ( $\Delta\delta$ ) between diverse components in one polymer composite is an essential indicator for forecasting the

compatibility and blending potential. Two materials with a lower  $\Delta\delta$  would exhibit a higher compatibility level. Wang et al. [45] calculated the Flory-Huggins interaction parameters between the maltene, resin, and oils according to the solubility parameters, and found that the asphaltene and resin were partly soluble in maltene and oils. There were about 5–10 % negative deviations between the predicted solubility parameters and the measured values, which was associated with the underestimated strength of the attractive interaction terms. Additionally, it was reported that the sulfur dosage negatively influenced the accuracy in solubility parameters prediction of bitumen model.

Energetic parameters of bitumen models can be directly outputted from MD simulations, including the potential, kinetic, van der Waals, and electrostatic terms. All of these energetic parameters are attributed to both intramolecular and intermolecular interactions. Liu et al. [44] investigated the low-temperature performance of various bitumen models using both MD simulations and experimental characterizations (differential scanning calorimetry (DSC) and dynamic shear rheometer (DSR)). They observed that the non-bond energy correlated well with the macroscale parameters of glass transition temperature, creep stiffness, and  $m$ -value at low temperatures. Meanwhile, the increment in aromaticity enlarged the diffusive capacity of bitumen molecules dramatically. Bao et al. [38] implemented the MD simulations to explore the rejuvenation efficiency on the interaction energies of an aged bitumen model, and it was revealed that the rejuvenator contributed more to intermolecular energies than valence interactions.

The binding energy ( $E_{\text{binding}}$ ) is an efficacious indicator to compute the interaction force between diverse molecules and components, which refers to the energy difference between the blend and sum of all individuals. Li et al. [130] utilized the  $E_{\text{binding}}$  parameter to quantitatively estimate the adsorption strength between the bitumen and sodium chloride molecules. The positive  $E_{\text{binding}}$  values implied a strong absorption interaction between sodium chloride and bitumen molecules, which enlarged as temperature increased but reduced with the increment in anti-icing agent dosage. Long et al. [115] calculated the  $E_{\text{binding}}$  parameter between the nano-silica and SARA molecules to evaluate the compatibility level. The results demonstrated that the asphaltene, resin, and aromatic components displayed a greater compatibility than the saturates, while the latter exhibited the best miscible with the nano-SiO<sub>2</sub>. Additionally, oxidative aging adversely influenced the compatibility degree between the nano-silica and bitumen molecules.

Surface free energy ( $\gamma$ ) is the work required to extend the surface area of a solid phase, which results from the disruption of intermolecular interactions. Xu et al. [103] computed the  $\gamma$  values of two bitumen models in the light of the potential energy difference between the film and bulk systems. Moreover, the work of cohesion ( $W_c$ ) of one bitumen model was obtained by doubling the  $\gamma$  parameter, which could effectively assess the cohesion performance and failure potential of bitumen model. The predicted  $\gamma$  and  $W_c$  values of both bitumen models agreed well with experimental results. Cui et al. [124] exploited the same method to forecast the  $\gamma$  and  $W_c$  values of fresh, aged and rejuvenated bitumen models with variable rejuvenator dosages. The aged bitumen

**Table 3**

The summary of different parameters of bulk bitumen systems predicted from MD simulations.

| Categories                    | Parameters                                      | Code          | Brief descriptions   |
|-------------------------------|---|---------------|--|
| a. Thermo-physical properties | Solubility parameter                            | $\delta$      | <ul style="list-style-type: none"> <li>* It is derived from the root square of the cohesive energy density (CED);</li> <li>* It is an efficient indicator to assess the compatibility potential between different molecules or materials;</li> <li>* The closer the solubility parameters of the two materials are, the better the blending effect is.* If the solubility parameter difference between the two materials exceeds 4.1 (<math>J\cdot cm^3)^{0.5}</math>, it is generally tricky to blend uniformly.</li> <li>* It is the energy required per a unit volume to overcome the intermolecular forces when the molecules evaporate from the bulk model;</li> <li>* It can be utilized to evaluate the strength of intermolecular interactions;</li> <li>* It may be associated with the stiffness or strength of materials.</li> <li>* It represents the tightness level of molecules in the whole model.</li> <li>* It is the most popular validation parameter due to its available measurement.</li> <li>* It can be used to track the equilibrium degree of a model during an MD simulation.</li> <li>* It refers to the thermal expansion potential of a molecular model;</li> <li>* It shows the variation rate of the model length or volume as a function of temperature;</li> <li>* It can estimate the temperature susceptibility, and a high thermal expansion coefficient value represents an apparent temperature sensitivity.</li> <li>* It can evaluate the intermolecular interaction level between different groups of molecules;</li> <li>* The amount of binding energy implies how tightly various molecules are combined;</li> </ul> |
|                               | Cohesive energy density                         | CED           | <ul style="list-style-type: none"> <li>* For a blend, the binding energy can be employed to assess the compatibility between different separated phases;</li> <li>* It is defined as the variation rate of model volume under a constant external pressure at a fixed temperature;</li> <li>* It can evaluate the deformation resistance of bitumen models. Meanwhile, a lower isothermal compressibility implies a higher deformation resistance;</li> <li>* It may be related to the molecular components, intermolecular interactions, and free volume fraction of a whole simulation model.</li> <li>* The interaction energy is the primary output from MD simulations, including the kinetic energy, potential energy, van der Waals energy, electrostatic energy, etc.* The potential energy mainly consists of the valence interactions (or bond) and non-bond interactions in the colloidal structure of bitumen;</li> <li>* The interaction energy values may vary during the aging, modification, and rejuvenation procedures.</li> <li>* It equals the work required to peel off the molecules from the bulk bitumen and create a new surface area;</li> <li>* It can estimate the cracking potential and cohesion performance of bulk bitumen system;</li> <li>* It can be experimentally measured with a contact angle test;</li> <li>* It can appraise the adhesion work between two connected phases.</li> <li>* It is derived by doubling the surface free energy;</li> <li>* It refers to the work needed to separate one bitumen model into</li> </ul>  |
|                               | Density   | $\rho$        | <ul style="list-style-type: none"> <li>* It is the most popular validation parameter due to its available measurement.</li> <li>* It can be used to track the equilibrium degree of a model during an MD simulation.</li> <li>* It refers to the thermal expansion potential of a molecular model;</li> <li>* It shows the variation rate of the model length or volume as a function of temperature;</li> <li>* It can estimate the temperature susceptibility, and a high thermal expansion coefficient value represents an apparent temperature sensitivity.</li> <li>* It can evaluate the intermolecular interaction level between different groups of molecules;</li> <li>* The amount of binding energy implies how tightly various molecules are combined;</li> </ul>  |
|                               | Thermal expansion coefficient                   | $\alpha$      | <ul style="list-style-type: none"> <li>* It shows the variation rate of the model length or volume as a function of temperature;</li> <li>* It can estimate the temperature susceptibility, and a high thermal expansion coefficient value represents an apparent temperature sensitivity.</li> <li>* It can evaluate the intermolecular interaction level between different groups of molecules;</li> <li>* The amount of binding energy implies how tightly various molecules are combined;</li> </ul>   |
|                               | Binding energy (Interfacial interaction energy) | $E_{binding}$ | <ul style="list-style-type: none"> <li>* It is derived by doubling the surface free energy;</li> <li>* It refers to the work needed to separate one bitumen model into</li> </ul>  |

**Table 3 (continued)**

| Categories               | Parameters                 | Code  | Brief descriptions  |
|--------------------------|----------------------------|---|---|
| b. Mechanical properties | Isothermal compressibility | $\beta_T$   | <ul style="list-style-type: none"> <li>* For a blend, the binding energy can be employed to assess the compatibility between different separated phases;</li> <li>* It is defined as the variation rate of model volume under a constant external pressure at a fixed temperature;</li> <li>* It can evaluate the deformation resistance of bitumen models. Meanwhile, a lower isothermal compressibility implies a higher deformation resistance;</li> <li>* It may be related to the molecular components, intermolecular interactions, and free volume fraction of a whole simulation model.</li> <li>* The interaction energy is the primary output from MD simulations, including the kinetic energy, potential energy, van der Waals energy, electrostatic energy, etc.* The potential energy mainly consists of the valence interactions (or bond) and non-bond interactions in the colloidal structure of bitumen;</li> <li>* The interaction energy values may vary during the aging, modification, and rejuvenation procedures.</li> <li>* It equals the work required to peel off the molecules from the bulk bitumen and create a new surface area;</li> <li>* It can estimate the cracking potential and cohesion performance of bulk bitumen system;</li> <li>* It can be experimentally measured with a contact angle test;</li> <li>* It can appraise the adhesion work between two connected phases.</li> <li>* It is derived by doubling the surface free energy;</li> <li>* It refers to the work needed to separate one bitumen model into</li> </ul> |
|                          | Interaction energy         | $E$ ( $E_{kinetic}$ , $E_{potential}$ , $E_{vdw}$ , $E_{ele}$ , etc.) | <ul style="list-style-type: none"> <li>* The interaction energy is the primary output from MD simulations, including the kinetic energy, potential energy, van der Waals energy, electrostatic energy, etc.* The potential energy mainly consists of the valence interactions (or bond) and non-bond interactions in the colloidal structure of bitumen;</li> <li>* The interaction energy values may vary during the aging, modification, and rejuvenation procedures.</li> <li>* It equals the work required to peel off the molecules from the bulk bitumen and create a new surface area;</li> <li>* It can estimate the cracking potential and cohesion performance of bulk bitumen system;</li> <li>* It can be experimentally measured with a contact angle test;</li> <li>* It can appraise the adhesion work between two connected phases.</li> <li>* It is derived by doubling the surface free energy;</li> <li>* It refers to the work needed to separate one bitumen model into</li> </ul>   |
| c. Surface properties    | Surface free energy        | $\gamma$  | <ul style="list-style-type: none"> <li>* It equals the work required to peel off the molecules from the bulk bitumen and create a new surface area;</li> <li>* It can estimate the cracking potential and cohesion performance of bulk bitumen system;</li> <li>* It can be experimentally measured with a contact angle test;</li> <li>* It can appraise the adhesion work between two connected phases.</li> <li>* It is derived by doubling the surface free energy;</li> <li>* It refers to the work needed to separate one bitumen model into</li> </ul>   |
|                          | Work of cohesion           | W   | <ul style="list-style-type: none"> <li>* It equals the work required to peel off the molecules from the bulk bitumen and create a new surface area;</li> <li>* It can estimate the cracking potential and cohesion performance of bulk bitumen system;</li> <li>* It can be experimentally measured with a contact angle test;</li> <li>* It can appraise the adhesion work between two connected phases.</li> <li>* It is derived by doubling the surface free energy;</li> <li>* It refers to the work needed to separate one bitumen model into</li> </ul>   |

(continued on next page)

**Table 3 (continued)**

| Categories                           | Parameters      | Code | Brief descriptions  |
|--------------------------------------|-----------------|------|---|
|                                      |                 |      | two parts;<br>* It is firmly attributed to the bulk model's cohesion property and cracking potential.<br>* It is proposed to characterize the compatibility and blending potential of two different materials;<br>* It is calculated based on the solubility parameter difference;<br>* It can be used to measure the strength of intermolecular forces in intimately mixed blends  |
| Flory-Huggins interaction parameter  | $\chi$          |      |   |
| Ductility                            | $D_u$           |      | * It reflects the elastic and tension properties of bitumen;  |
| Flexibility index                    | $\phi$          |      | * It was proposed based on the multiple structural attributes from the molecular size, branching, cycles, and heteroatom content.<br>* It is defined to assess the ability to transmit the heat energy in a diffusive manner based on a Fourier's law;<br>* It may be related to the thermal heating self-healing capacity of bituminous materials;<br>* It may affect the temperature sensitivity of bitumen.  |
| Thermal conductivity                 | $k$             |      |   |
| Heat capacity                        | $C_p$ and $C_v$ |      | * Heat capacity is the absorbed energy from the outside when the temperature increases unit of heat.<br>* It is a temperature below which a material shows glassy (elastic) behavior and above which shows viscous behavior;  |
| Glass transition temperature         | $T_g$           |      | * It results from the movement of molecular chains at one temperature point;<br>* A Differential Scanning Calorimetry can measure it;<br>* It may be attributed to the relaxation and low-temperature performance.<br>* It represents the movement capacity of molecules in bitumen models;<br>* It depends on the molecule size, temperature, and intermolecular interaction;<br>* It may be associated with the macroscale viscosity, low-temperature |
| <b>b. Thermo-dynamics properties</b> |                 |      |   |
| Diffusion coefficient                | $D$             |      |   |

**Table 3 (continued)**

| Categories                             | Parameters | Code | Brief descriptions   |
|--|------------|------|--|
|  |            |      | relaxation, and high-temperature deformation properties.<br>* It measures the position deviation of one molecule from an initial point versus a simulation time;   |
| Mean square displacement               | MSD        |      | * It can be estimated experimentally through a neutron scattering and photon correlation spectroscopy;<br>* The linear correlation between the MSD and time is monitored to calculate the diffusion coefficient D of different molecules;<br>* It can assess the molecular mobility of various molecules in a bitumen model.   |
| Activation energy                      | $E_a$      |      | * It refers to the minimum energy required to activate atoms or molecules for undergoing the chemical transformation or physical transport;<br>* It is always detected through a correlation curve between temperature and diffusion coefficient or viscosity;   |
| Wetting time                           | $t$        |      | * It can estimate the molecular mobility and flowability of bituminous materials.<br>* It is a special indicator from the MD simulations on self-healing behaviors of bituminous materials;<br>* It refers to the time consumed when a microcrack between the separated layers of bitumen disappears;<br>* A smaller wetting time value demonstrates a higher self-healing potential of the bitumen model. |
| Modulus                                | K, G, E    |      | * It contains the bulk modulus (K), shear modulus (G), and elastic modulus (E);<br>* The MD simulation can impose strains in the modes of 1000000, 010000, 001000, 000100, 000010, and 000,001 on the whole bitumen model. Under a strain loading, the corresponding stress and stiffness constant ( $C_{ij}$ ) can be determined, which are utilized to calculate the modulus and Poisson                 |
| <b>c. Thermo-mechanical properties</b> |            |      |  |

(continued on next page)

**Table 3 (continued)**

| Categories                        | Parameters | Code | Brief descriptions  |
|-----------------------------------|------------|------|---|
| Viscosity                         | $\eta$     |      | <p>ratio;</p> <p>* These modulus values can reflect the stiffness and deformation resistance to some extent.</p> <p>* The predicted modulus values will be connected to the experimental modulus results;</p> <p>* Bulk modulus shows the inverse of the isothermal compressibility and can evaluate the resistance of a material to uniform compression.</p> <p>* Low viscosity value of bitumen demonstrates a better flowability and workability;</p> <p>* It is influenced by the molecular structure and intermolecular interaction, temperature, and shear rate;</p> <p>* In a typical equilibrium molecular simulation, a Green-Kubo method or Einstein equation are employed to relate elemental fluctuations of the pressure tensor to a viscosity value.* The shear viscosity can be predicted from a shear flow non-equilibrium molecular dynamics (NEMD) method through applying a shear strain to the whole model.</p> |
| Poisson ratio                     | $\nu$      |      | <p>* It is defined as the material deformation in directions perpendicular to the specific direction of loading;</p> <p>* It can be outputted from MD simulations through a shearing mode.</p> <p>* The interaction energy is able to evaluate the interfacial adhesion.</p>  |
| Pull-out force                    |            |      |   |
| Rotational relaxation time        | $\gamma$   |      | <p>* It is analyzed via the rotational correlation functions and self-diffusion coefficients;</p> <p>* It depends on the molecular size, and the large molecule exhibit an extended relaxation time.</p> <p>* The total volume is a sum of occupied volume and free volume;</p> <p>* The occupied volume comes from an</p>  |
| Total volume/<br>Occupied volume/ |            |      |   |

**Table 3 (continued)**

| Categories               | Parameters                                      | Code                                      | Brief descriptions  |
|--------------------------|---|---|---|
|                          | Free volume/<br>Fractional free<br>volume       | V/V <sub>0</sub> /V <sub>f</sub> /<br>FFV | <p>inherent volume of molecules, while the free volume refers to the space between molecules;</p> <p>* When the free volume reduces to a certain extent, the bitumen would present a glass state;</p> <p>* The FFV can estimate the proportion of available volume in the bitumen model;</p> <p>* The free volume distribution is an essential factor in influencing the molecular diffusion capacity.</p>  |
| d. Structural properties |   |   |   |
|                          | Radial distribution<br>function                 | RDF                                       | <p>* It illustrates the occurrence probability of a particle from another particle at a distance r;</p> <p>* It can evaluate a specific molecule's molecular distribution and aggregation level.</p> <p>* It computes the profile of atom density within the evenly spaced slices;</p> <p>* To obtain this parameter, a specific direction is divided into several bins, and the related atoms are counted;</p> <p>* It allows us to deeply analyze the spatial distribution of different molecules in the whole model.</p> |
|                          | Concentration<br>profile                        | RC  | <p>* R<sub>g</sub> is the inertial radius of the molecular coils rotating around the center of mass;</p> <p>* It refers to the distance between the hypothetical concentration point of the differential object mass and the axis of rotation;</p> <p>* It reflects the dimensions of one molecule chain, as well as the rigidity and tightness of molecules.</p>   |
|                          | Radius of gyration                              | R <sub>g</sub>                            | <p>* The probability density equals the ratio of molecule number having their orientation in each bin to the total possible number of orientations, divided by the bin width;</p> <p>* The intermolecular orientation between the similar and different molecules can be calculated;</p> <p>* A random orientation probability density</p>  |
|                          | Molecular<br>orientation<br>probability density | P   | (continued on next page)  |

**Table 3 (continued)**

| Categories | Parameters | Code | Brief descriptions  |
|------------|------------|------|---|
|            |            |      | follows the function $\sin(\theta)^*$ ; If the orientation density curve is very close to $\sin(\theta)$ , there will be few correlations in orientation. |

exhibited lower  $\gamma$  and  $W_c$  values than the fresh one, indicating that aging showed a reduction effect on the  $\gamma$  and  $W_c$  parameters, leading to an increment in the cracking potential of bitumen. Nevertheless, as the rejuvenator content rose, both  $\gamma$  and  $W_c$  values of rejuvenated bitumen models enlarged. In other words, the incorporation of rejuvenator molecules displayed a positive influence on improving the cohesion performance of the aged bitumen model.

The variations of volumetric indicators for bitumen models at different temperatures and pressures could be detected. The model volume generally expands as the temperature increases and reduces under an external force. Two indicators, thermal expansion coefficient (CET) and isothermal compressibility, can be outputted from MD simulations, which are strongly related to the intermolecular interactions and nanoscale deformation potential of a bitumen model. Yang et al. [90] evaluated the impacts of aging and rejuvenation on the CET value of a bitumen model, and found that the aged bitumen exhibited the lowest CET value, which enlarged remarkably with the increment in rejuvenator content. In detail, the addition of 5 wt% bio-oil molecules increased the CET value of aged bitumen by 13.4 %, which was even higher than that of fresh bitumen. Nevertheless, the CET parameter demonstrated an apparent increment when the bio-oil dosage exceeded 10 wt%. Thus, excessive bio-oil rejuvenator would deteriorate the thermal stability and induce a thermal expansion of the rejuvenated bitumen model. Zhang and Greenfield compared the isothermal compressibility of 3-component bitumen models with variable asphaltene types and polystyrene molecules [42]. At low temperatures, the bitumen models were rigid and not easily compressed, implying that the isothermal compressibility may be associated with the stiffness and deformation resistance of bitumen models. Moreover, the bitumen model with a higher aromaticity displayed a lower isothermal compressibility and a higher bulk modulus.

#### 4.4.2. Thermo-dynamics behaviors

Several parameters predicted from MD simulations are attributed to the molecular mobility in a whole simulation model, named thermo-dynamics behaviors. Herein, these thermo-dynamics parameters of the glass transition temperature ( $T_g$ ), mean square displacement (MSD), diffusion coefficient (D), activation energy (Ea), and wetting time reported from MD simulations on bituminous materials are overviewed.

The glass transition temperature is defined as the temperature value at an intersection point where the physical state of one system changes from a glassy to a viscoelastic solid because of the movement of molecular chains. It is generally recognized that the variation rates of thermo-physical properties (such as free volume, density, heat capacity, etc.) before and after the  $T_g$  point are different. For instance, Kang et al. [105] predicted the  $T_g$  parameter of AAA-1 bitumen through detecting the temperature dependence of the free volume, fractional free volume, specific volume, and thermal expansion coefficient at a temperature region of 50–575 K. The predicted  $T_g$  value of 250 K for AAA-1 bitumen was consistent with the experiment result, below which the bitumen model presented a genuinely frozen glassy state. Besides, another transition temperature was observed at around 400 K, which was responsible for the liquid–liquid transition behavior of bitumen from a viscoelastic liquid state to a Newtonian fluid. At the same time, Farshad et al. [143] investigated the aging influence on the  $T_g$  values of bitumen with MD simulations. All bitumen models were subjected to a cooling

procedure from 600 K to 80 K with a cooling speed of 5 K/ns, and the corresponding  $T_g$  values were obtained based on the volume-temperature curve. There was no significant difference in  $T_g$  values between the virgin and aged bitumen models. Moreover, a high cooling rate in MD simulations led to a massive difference in the  $T_g$  parameter between the predicted and measured values.

The relaxation behavior of the whole bitumen model is strongly associated with the molecular mobility of bitumen molecules. During the MD simulations, the movement trajectory of bitumen molecules can be recorded as a function of simulation time, which is represented as an indicator of mean square displacement (MSD). Based on the Einstein's diffusion law, the diffusion coefficient (D) values of molecules approximate the one-sixth values of the slope of MSD-time curves. Luo et al. [128] studied the aging impact on the diffusion capacity of bitumen molecules at two temperatures of 300 and 500 K. It was summarized that the aged bitumen exhibited a lower molecular mobility than the virgin bitumen due to the limitation in free volume, which enlarged as an increment in temperature. Similar findings were reported by Xu and Wang [37], revealing that the increase in molecular size of the asphaltene, resin, and aromatic molecules also contributed to the weakened diffusive capacity of the aged bitumen. Su et al. [113] utilized the MSD and D parameters to explore the influence of nano-ZnO and styrene-butadienestyrene (SBS) modifiers on the diffusion behaviors of bitumen molecules. The increase in nano-ZnO size tended to reduce the diffusion coefficient value, which was further weakened after adding the SBS molecules. Sun et al. [66] drawn a conclusion that the diffusion coefficient, activation energy, and pre-exponential factor (A) are efficient parameters to estimate the self-healing capacity of bitumen models. In addition, Ren et al. [119] employed an MD simulation to investigate the influence of lignin molecules on the diffusive and self-healing performance of bitumen molecules. It was found that all SARA molecules in lignin-modified bitumen exhibited the lower diffusion coefficient and larger wetting time values than that in virgin bitumen.

#### 4.4.3. Thermo-mechanical performance

The thermo-mechanical parameters from MD simulations mainly contain the viscosity, modulus, and pull-off energy (strength). For instance, You et al. [140] conducted a reverse non-equilibrium molecular dynamic (rNEMD) simulation to predict the shear viscosity values of a 12-component bitumen model at different temperatures, which were compared with the viscometer results. In detail, the predicted viscosity values of bitumen model were 200 mPa·s (438.15 K), 300 mPa·s (408.15 K), and 660 mPa·s (374.15 K), which agreed well with experimental results. Similarly, Ding et al. [152] forecasted the shear viscosity of a 3-component bitumen model with the rNEMD method considering the influence of chemical components. The shear viscosity of bitumen model was extremely dependent on the chemical components, which enlarged with the increase in the molecular weight, aromatic carbon proportion, and heteroatom concentration. Moreover, the molecular weight played a more significant role in affecting the shear viscosity of the bitumen model than other influence factors.

When an elastic strain was imposed, several modulus parameters of a bitumen model could be obtained from MD simulations, including the Young's modulus, shear modulus, bulk modulus, and Poisson ratio. Hou et al. [106] performed an MD simulation on a 3-component bitumen model to estimate its thermo-mechanical parameters for further Multi-physics simulations. The predicted Young's modulus, shear modulus, and bulk modulus values were 1.054 GPa, 0.9 GPa, and 1.4 GPa with a Poisson ratio of 0.36. Li et al. [153] reported these mechanical parameters of various colloid, saturated phenol, and asphaltene systems. The asphaltene molecules exhibited the highest Young's modulus of 2.8 GPa, followed by the colloid model. At the same time, the saturated phenol displayed the lowest Young's modulus of 0.52 GPa but the largest Poisson's ratio of 0.45. Yao et al. [154] focused on the bulk modulus prediction of a 3-component bitumen model through applying a slight strain. The MD simulation output was closer to the laboratory data than

the reference values. They also carried out the modulus simulation on an exfoliated multi-layered graphite nanoplatelets (xGNP) modified bitumen model under the minor volumetric strains [138]. The predicted bulk modulus and shear modulus agreed well with the measured values, but Young's modulus from MD simulations was larger than the experimental results. The reasons may be related to several factors of the selected time step, simulation time, molecular number, and calculation methods. Nevertheless, the high consistency of Poisson's ratio suggested that the stress response of the bitumen model with a minor strain was reliable.

The tension test was also implemented on bitumen models to evaluate their cohesive performance at an atomic level. Hou et al. [155] observed that the molecular structure of bitumen was generally stretched, and a hole in the microstructure occurred under a tension force. Similarly, Guo et al. [46] conducted a MD tension simulation on a bitumen model with a tension rate of 10 Å/fs. During the stretching process, the total energy of the whole bitumen system increased progressively, and the van der Waals interaction played an important role. When a large deformation was generated, the total and potential energy values both reduced distinctly, which referred to a fracture or fatigue cracking in the bitumen model. Xu et al. [156] employed the MD method in simulating an atomic force microscopic (AFM) procedure between the silicon tip and bitumen molecules. It was found that the predicted hardness and modulus remarkably relied on the loading rate, leading to a noticeable difference between the simulation outputs and experimental results. It was worth noting that the aging influence on the adhesion performance of bitumen could be reflected well in MD simulations.

#### 4.4.4. Structural characteristics

According to the quantitative structure–activity relationship, the structural characteristics reflect the physical and mechanical performance of bitumen model to some extent, which is mainly influenced by the chemical components and environmental conditions. This section summarizes the main structural properties of bitumen models predicted from MD simulations, including the volumetric parameters, relative concentration, radial distribution function, and radius of gyration. The total volume of bitumen model is a sum of occupied volume and free volume. Afterwards, a critical volumetric indicator, fractional free volume (FFV), is obtained by calculating the ratio of free volume to total volume. It was reported that FFV parameter was strongly correlated with the glass transition temperature and low-temperature performance of bitumen. Xiao and Fan [132] explored the ultraviolet aging mechanism at the nanoscale, and observed that the ultraviolet (UV)-aged bitumen model exhibited a lower free volume expansion rate than a virgin bitumen. It was because the UV-aging degraded the chain segments and reduced the movement capacity of bitumen molecules. Other studies reported the similar findings in terms of the aging influence on the volumetric parameters of bitumen models [103,107]. For instance, Jiao et al. [127] concluded that the fractional free volume of bitumen models displayed a decreasing trend with the increment in probe radius. Moreover, the molecular mobility and permeability of crumb rubber modified bitumen (CRMB) models were enhanced as the temperature increased on the basis of the enlarged FFV values. Nevertheless, there was no apparent correlation between the FFV value with the degradation degree of crumb rubber.

The relative concentration (RC) is another crucial structural indicator to assess the molecular distribution level by calculating the density ratio of molecule in a tiny unit volume to the whole system. Li et al. [104] implemented the coarse-grained MD simulation to observe the microstructure of bitumen at the mesoscopic scale. According to the relative concentration profile, the aggregation behaviors of asphaltene molecules were quantified. In addition, the reduction in temperature promoted the agglomeration potential between asphaltene molecules. Liu et al. [44] measured the relative density distribution of SARA fractions in various bitumen models. The increased aromatic carbon number

in resin and aromatic molecules weakened the agglomeration level of asphaltene molecules and promoted the molecular dispersion of resin-asphaltene aggregates. Yu et al. [59] utilized the relative concentration profile to examine the influence of oxidative aging on molecular distribution of SBS and bitumen molecules in an SBS modified bitumen model at the X, Y, and Z directions. The significant peak value in a relative concentration (RC) curve revealed that SBS and asphaltene molecules were aggregated easily, while the resin, aromatic, and saturate molecules were uniformly dispersed in the whole bitumen model. Meanwhile, there was a remarkable competition between SBS and asphaltene molecules, and chemical components of the aged bitumen hindered the adsorption of SBS to the light-weight molecules.

The relative distribution level between different molecules in a bitumen model can also be estimated by the radial distribution function (RDF) parameter, which refers to the probability of occurrence for one molecule to a reference molecule. Eventually, RDF curves of the occurrence probability  $g(r)$  versus an intermolecular distance  $r$  can be drawn. Guo et al. [141] performed the MD simulations on interaction behaviors between rubber and bitumen molecules using RDF curves. The incorporation of rubber molecules remarkably influenced the agglomeration state of bitumen molecules, and rubber molecules exhibited a more substantial interaction potential with naphthalene aromatics and saturates than the asphaltene molecules. The intermolecular RDF curves illustrated that the BR molecules presented the best adsorption potential to light fractions of bitumen, followed by the SBR and NR molecules. Furthermore, bitumen with a higher naphthalene aromatic and saturate dosage exhibited a robust interaction with a rubber modifier. Tang et al. [157] adopted a dissipative particle dynamics method to explore the nanostructure and asphaltene agglomeration in a bitumen model. The RDF results demonstrated that the agglomeration degree between asphaltene molecules was significant when the molecular structures of asphaltenes were the same, which was related to the asphaltene proportion and bitumen viscosity. Interestingly, the  $g(1.39)$  and  $g(1.53)$  peak values showed a high connection with the low-temperature parameters of  $T_g$ , stiffness ( $S$ ), and  $m$ -value from experimental tests.

It was reported that the molecular model's radius of gyration ( $R_g$ ) could evaluate the stiffness, elasticity, and ductility of polymers, denoting the distance between the hypothetical concentration point of molecular differential mass and the axis of rotation [109]. Yu et al. compared the  $R_g$  curves of virgin bitumen, polyurethane modified bitumen, and polyurethane/graphene oxide modified bitumen models [158]. The probability density in the  $R_g$  curve of bitumen enlarged after adding polymers, implying that the bitumen's regularity and degree of functionality were improved. The active functional groups in a polyurethane molecule and the oxygen-containing functional groups in a graphene oxide molecule both contributed to the improved regularity and rigidity of bitumen model. Su et al. compared the  $R_g$  curves of SARA fractions in a bitumen before and after adding SBS molecules [60]. These  $R_g$  curves of SARA molecules were significantly different due to the difference in molecular weight and size. Moreover, involving SBS molecules changed the peak position and  $R_g$  width for bitumen components. It denoted that the flexibility of branched chains in bitumen molecules was reinforced by SBS molecules, resulting in a tighter molecular structure of SBS-modified bitumen than the virgin bitumen.

## 5. MD simulations on aged bitumen systems

Bitumen is composed of different heavy-weight and high-polarity molecules, which are easy to be oxidized. It would significantly affect the mechanical properties of asphalt pavement, and thus the low-temperature and fatigue cracking damage would occur. It is important to understand the aging influence and mechanism of bitumen at different scales to seek solutions to effectively prolong the service life of asphalt pavement. From the viewpoint of macroscale evaluation, the ratios of mechanical properties of bitumen before and after aging are

usually utilized to quantitatively assess the performance deterioration level of bitumen due to aging effect. These mechanical parameters contain the viscosity, complex modulus, and rutting parameter from the DSR test, elastic recovery and creep compliance from a multiple stress creep and recovery (MSCR) method, stiffness and m-value from the bending beam rheometer (BBR) test. On the other hand, the chemical and morphological methods are also conducted to explain the aging mechanisms from a microscale perspective. The FTIR and GPC tests are the most popular chemical characterization methods to estimate the aging influence on the functional group components and molecular weight distributions, respectively. Moreover, the comparison between the SARA fractions of bitumen before and after aging was made to investigate the variety of chemical compositions of bitumen during the aging process. The commonly-used indices from macroscale experiments to evaluate the aging performance of bitumen are summarized in **Table 4**.

From previous experimental results, the aging significantly enlarged the softening point, complex modulus, viscosity, rutting parameter, and stiffness of bitumen. On the contrary, the ductility, penetration, m-value, and phase angle decreased. In addition, the aging effects on bitumen's mechanical and rheological properties were related to the internal changes of chemical compositions and microstructures. From the FTIR and GPC results, oxidation aging accelerated the formation of both carbonyl and sulfoxide functional groups and remarkably increased the molecular weight and surface roughness of bitumen. Moreover, the

asphaltene and aromatic content in bitumen increased and decreased dramatically during the aging process. Nevertheless, it is difficult to investigate the aging mechanism at the nanoscale level and its influence on the thermodynamics properties of bitumen only using these macro-scale experiments. Meanwhile, the microscopic reasons for these mechanical, rheological, or chemical performance variations of bitumen during the aging process are still unclear.

### 5.1. Oxidative reaction mechanism and kinetics of bitumen molecules

Although it is well-known that oxidative aging would increase the polar functional groups in bitumen, such as ketone and sulfoxide, however, the dynamic oxidation reactions and corresponding products of each SARA molecule in bitumen are still controversial, which inhibits the molecular model establishment of aged bitumen and understanding the aging influence on essential thermodynamic properties of bitumen from a nanoscale perspective. Currently, a reaction molecular dynamic simulation (MD) method has been proposed to explore the chemical oxidation reaction pathways of bitumen molecules. The atomistic-based chemo-physical forcefield, named ReaxFF, was developed to address the problem that most common forcefields are only appropriate for the systems without chemical reactions. It should be noted that the ReaxFF forcefield is based on the Density Functional Theory (DFT) [31,160]. During the atomic-based molecular dynamics simulation, the interaction energy terms between different C—H—S—O atoms were calculated to determine the break and formation potentials of old and new chemical bonds. Afterward, the atomistic-level chemical oxidative kinetic characteristics and reaction pathways of bitumen molecules were tracked, and thus the aging mechanisms and bitumen's chemical products during the oxidation aging process could be proposed. This section reviews previous reactive MD simulation studies on the oxidation reaction of bitumen molecules. **Table 5** lists the relevant molecular models of bitumen and simulation conditions (temperature and oxygen levels).

Additionally, all molecular models in reactive MD simulations were established through mixing the bitumen molecules with atomic or molecular oxygen, as illustrated in **Fig. 11**. The oxygen molecules would attach and collide with bitumen molecules under the interaction forces from ReaxFF force field. The potential energy was calculated to identify the break or formation potentials of various chemical bonds. Pan et al. [147] utilized the reactive MD simulation and quantum chemistry theory to explore the oxidative reaction details of the saturate, resin, and asphaltene molecules as well as the average molecule of bitumen. The molecular models of fractional bitumen molecules before and after the oxidation aging are displayed in **Fig. 12a**. The results revealed that the aromatic and asphaltene molecules were partially oxidized with sulfoxidation and ketonization, while the saturate molecules exhibited a

**Table 4**  
Commonly-used characterization methods and aging indicators [159].

| Characterization methods      | Aging indicators                       | Abbreviation | Formula  |
|-------------------------------|--|--------------|--|
| Penetration                   | The change rate of penetration         | CRP          | $P_{\text{aged}}/P_{\text{fresh}}$                               |
| Softening point               | The change rate of softening point     | CRS          | $SP_{\text{aged}}/SP_{\text{fresh}}$                             |
| Ductility                     | The change rate of ductility           | CRD          | $D_{\text{aged}}/D_{\text{fresh}}$                               |
| Viscosity                     | The change rate of viscosity           | CRV          | $\eta_{\text{aged}}/\eta_{\text{fresh}}$                         |
| SARA fractions                | The change rate of asphaltenes content | CRAC         | $AC_{\text{aged}}/AC_{\text{fresh}}$                             |
|                               | The change rate of colloidal index     | CRCI         | $CI_{\text{aged}}/CI_{\text{fresh}}$                             |
|                               | The change rate of complex modulus     | CRCM         | $G_{\text{aged}}/G_{\text{fresh}}$                               |
| Dynamic Shear Rheometer (DSR) | The change rate of phase angle         | CRPA         | $\delta_{\text{aged}}/\delta_{\text{fresh}}$                     |
|                               | The change rate of the rutting factor  | CRRF         | $(G^*/\sin\delta)_{\text{aged}}/(G^*/\sin\delta)_{\text{fresh}}$ |
|                               | The change rate of the fatigue factor  | CRFF         | $(G^*\sin\delta)_{\text{aged}}/(G^*\sin\delta)_{\text{fresh}}$   |
| Bending beam rheometer (BBR)  | The change rate of stiffness           | CRS          | $S_{\text{aged}}/S_{\text{fresh}}$                               |
|                               | The change rate of m-value             | CRM          | $m_{\text{aged}}/m_{\text{fresh}}$                               |
| Spectrophotometry             | The change rate of absorbance area     | CRAA         | $AA_{\text{aged}}/AA_{\text{fresh}}$                             |
| Fluorescence spectroscopy     | The change rate of integral area       | CRIA         | $IA_{\text{aged}}/IA_{\text{fresh}}$                             |
| Atomic force microscopy (AFM) | The change rate of surface roughness   | CRSR         | $SR_{\text{aged}}/SR_{\text{fresh}}$                             |
|                               | The change rate of adhesion force      | CRAF         | $AF_{\text{aged}}/AF_{\text{fresh}}$                             |
| FTIR spectroscopy             | The change rate of carbonyl index      | CRC          | $C_{\text{aged}}/C_{\text{fresh}}$                               |
|                               | The change rate of sulfoxide index     | CRS          | $S_{\text{aged}}/S_{\text{fresh}}$                               |
|                               | The change rate of butadiene index     | CRB          | $B_{\text{aged}}/B_{\text{fresh}}$                               |
| Fluorescence microscopy       | Fluorescent images                     | —            | —  |
| Gel permeation chromatography | The change of $M_w/M_n$                | —            | —  |

**Table 5**  
The reactive MD simulation conditions on oxidative aging of bitumen molecules.

| Bitumen model                    | Force field        | Temperature                | Oxygen level*   | Ref   |
|----------------------------------|--------------------|----------------------------|---|-------|
| 12-component AAA-1 bitumen model | ReaxFF force field | 300, 400, 500, 600 (K)     | 500 oxygen molecules  | [31]  |
|                                  |                    | 200, 300, 400, 500 (K)     | 800 oxygen atoms  |       |
|                                  |                    | 1200, 1400, 1600, 1800 (K) | Molecular oxygen; Equivalent O <sub>2</sub> level of 0.25, 0.5 and 1* | [146] |
|                                  |                    | 130 (°C)                   | Oxygen molecules with one standard atmospheric pressure (1 ATM)       | [148] |
| 3-component bitumen model        |                    |                            |   | [147] |
| Average bitumen model            |                    |                            |   |       |

\*The oxygen level is the ratio of the amount of oxygen to the oxygen dosage required to completely oxidize the bitumen molecules into CO<sub>2</sub>, HO<sub>2</sub>, SO<sub>2</sub>, and NO<sub>2</sub>.

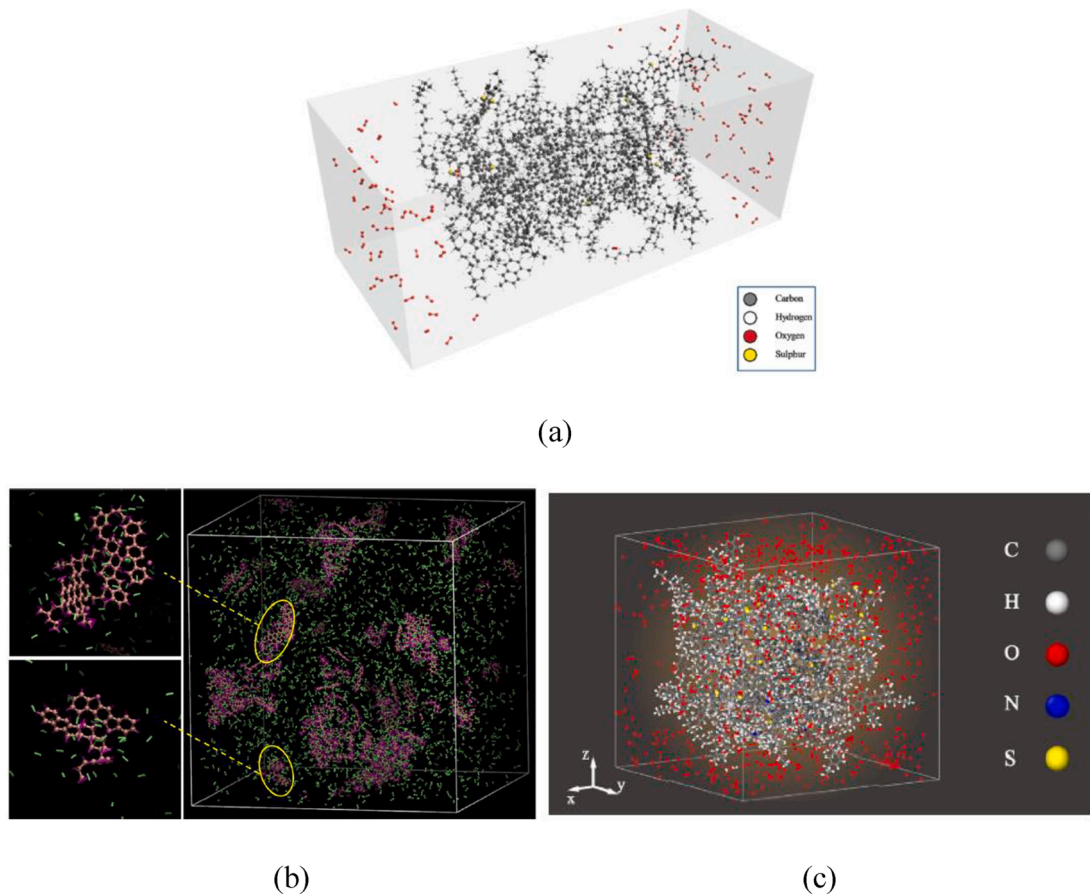


**Fig. 11.** The bitumen-oxygen molecular models in reactive MD simulations.

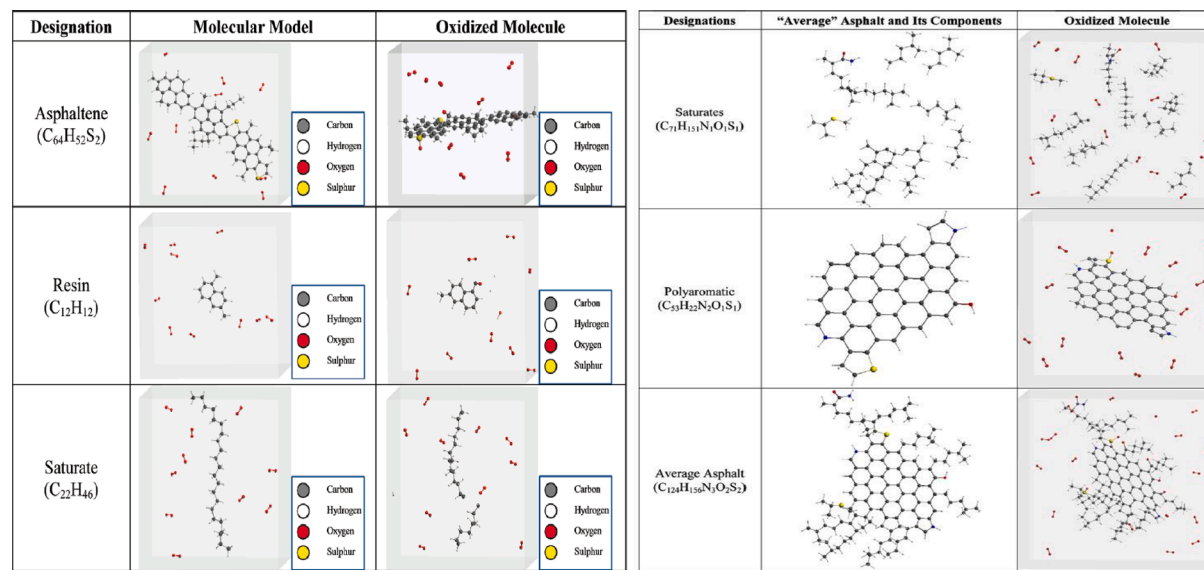
good oxidation resistance. Moreover, the saturated alkane chain would be separated into several shorter chains, and the sulfoxide formation was earlier than the carbonyl groups. Fig. 12b illustrates the chemical kinetics of the breaking, sulfoxidation, and ketonization of alkane chains during an oxidation reactive MD simulation. The conclusion was drawn that the sulfoxides were mainly generated in the initial spurt, followed by the immediate product of ketones when the oxidation time was long enough [31]. Furthermore, the ratio of sulfoxide to carbonyl functional groups depended on the sulfur dosage in bitumen.

Based on the 12-component molecular model of bitumen, Yang [146] and Hu [31] performed the reaction MD simulation to probe the oxidative aging mechanisms of the AAA-1 bitumen model considering the influence of both simulation temperature and oxygen content. Yang et al. [146] simulated the chemical reaction pathways between 12 types of bitumen molecules and aromatic or molecular oxygen. The normal finding was observed that the ketones and sulfoxides were the main products of bitumen molecules during an oxidation MD simulation. In addition, the ketones were more easily generated on the cyclic benzyl carbons than on the branched benzyl carbons. Besides, the environmental temperature significantly affected the reaction thermodynamics and aging products of bitumen molecules. When the temperature was lower than 300 K, no reaction product could be detected, which was associated with the low collision possibility between reactant molecules. The system energy was lower than the reaction activation energy. However, at the high temperature of 600 K, the C–C, C–H, or C–S chemical bonds in bitumen molecules were massively broken, resulting in the significant generation of harmful gaseous molecules (i.e., SO<sub>3</sub>, H<sub>2</sub>O<sub>2</sub>, CO, CO<sub>2</sub>, and O<sub>2</sub>).

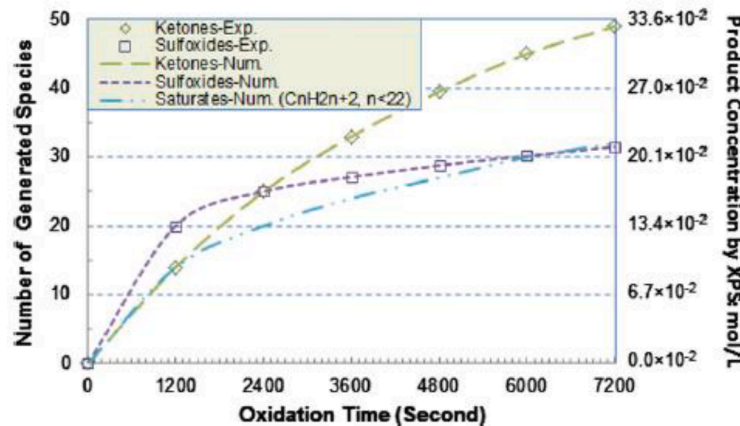
Similarly, the generation of sulfoxide groups was earlier than the ketones because the sulfur atoms were easily connected with oxygen atoms through forming stable and strong S=O bonds. The primary

chemical reactions, main products, and polymerization mechanisms of bitumen molecules during the oxidative aging MD simulations are demonstrated in Fig. 13. It was reported that the molecular or atomic oxygen was attached to the α-C atom to form the hydroperoxides, followed by a generation of the sulfoxide and carbonyl functional groups. Importantly, the hydroperoxides (C—O—O<sup>·</sup>) was the critical intermediate product to determine the occurrence potential for the oxidative aging of bitumen molecules. Meanwhile, the polymerization phenomenon would occur when the aromatics and free radicals were formed through the “dehydrogenation” oxidation reactions [31].

More recently, the effects of reaction temperature and oxygen level on the oxidative aging kinetics and pathway of AAA-1 bitumen molecules were investigated by Hu et al. using a reactive MD simulation with a ReaxFF forcefield [31]. The yield of oxygen-containing functional groups in bitumen was accelerated by the increased temperature and oxygen concentration. Fig. 14 illustrates the representative molecular structures of the aged bitumen molecules in MD simulations. It was found that the aromatic rings were decomposed, which resulted in the aromaticity reduction of aged bitumen. It was due to the high temperature (higher than 1200 K) of simulation system, which allowed the ring-opening and condensation reactions. Although it has been proved that the reactive MD simulation method is able to explore the oxidative reaction pathways of bitumen molecules, more work still needs to be done for completely and accurately explaining the oxidative aging mechanisms and chemical products of bitumen molecules, which could be beneficial in establishing the representative molecular models of aged bitumen with different aging degrees. Meanwhile, chemical characterization methods should be performed to validate the reactive MD simulation outputs, such as the FTIR, GPC, NMR, X-ray photoelectron spectroscopy (XPS), and Elementary analysis [145].



(a) Molecular structures of bitumen molecules during the oxidation reaction MD simulations



(b) Chemical kinetics of alkane chain breaking, sulfoxidation, and ketonization

Fig. 12. Molecular models of bitumen molecules before and after oxidative aging reactions.

### 5.2. Aging influence on bitumen properties at the nanoscale

Although different kinds of experimental tests can be employed to directly investigate the aging influence on the physical, rheological and mechanical properties of bitumen, the aging mechanism regarding the intrinsic molecular-level compositions and intermolecular interaction has not been interpreted clearly. Additionally, these laboratory tests are time-consuming and strongly dependent on the instrument availability, which distinctly hinders the full-scale understanding on the aging behaviors of bituminous materials. Moreover, the MD simulation could be employed to efficiently predict the essential physical, thermodynamic, and mechanical properties of virgin and aged bitumen.

Before running an MD simulation, the key issue is to establish an accurate molecular model of an aged bitumen. In line with the previous findings from both macroscale characterization and microscale reactive MD simulations, it was believed that the oxygen molecules would react with the benzyl carbon and sulfur atoms in bitumen molecules easily, and the ketones and sulfoxides functional groups were generated, which is illustrated in Fig. 15. Afterward, researchers proposed the representative oxidized molecular structures of SARA molecules in aged bitumen

through involving the C=O and S=O functional groups on the potential benzyl carbon and sulfur atoms in virgin bitumen molecules. Fig. 16 demonstrates the molecular structures of the 12-component bitumen model before and after aging process, which is the most-popular molecular model for an aged bitumen when the aging behavior is fundamentally studied through MD simulations [103]. However, the full-oxidized molecular model of the aged bitumen has not considered the influence of aging level on the molecular structures' variation of bitumen molecules. Therefore, Qu et al. [33] tried to establish the molecular structures of SARA fractions for a short-term aged bitumen, and the amount of carbonyl and sulfoxide groups is in the middle between the virgin and full-oxidized bitumen models. The oxidized asphaltene, resin, and aromatic molecules for the short-term aged bitumen are displayed in Fig. 17.

After determining the molecular structures of SARA fractions in virgin and aged bitumen, a comparison work on various physical and thermodynamics properties between the virgin and aged bitumen models have been conducted after the MD simulations. Table 6 lists the detailed input parameters in previous MD simulation studies on the aging influence on bitumen performance, including the molecular

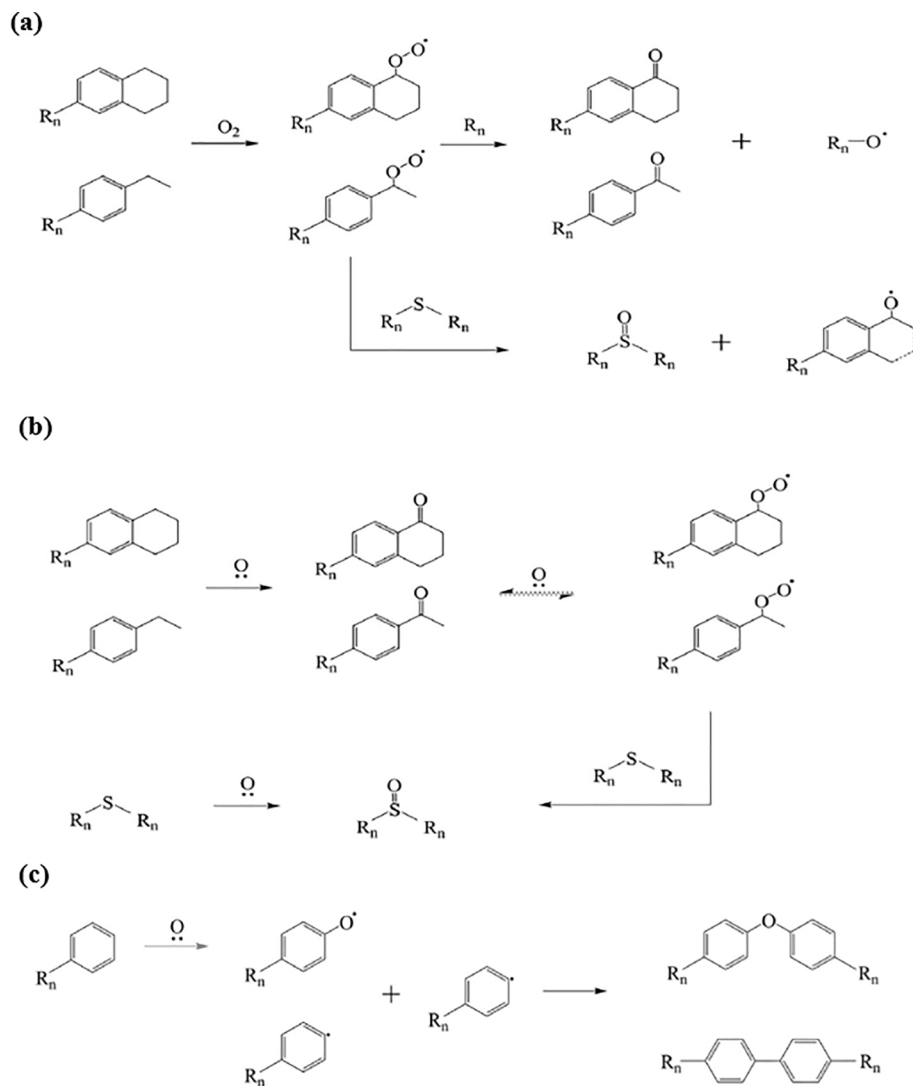


**Fig. 13.** The primary oxidation reactions and polymerization pathway of bitumen molecules during the reaction MD simulations, (a) molecular oxygen, (b) atomic oxygen, and (c) polymerization.

models of aged bitumen and these selected forcefields. Besides, the main physical and thermodynamics parameters outputted from MD simulations are also displayed herein. In view of the MD simulation results, the formation of polar oxidized functional groups (mainly C=O and S=O) significantly increased the density, bulk modulus, and viscosity, which was attributed to the enhancement in intermolecular and intramolecular forces between aged bitumen molecules. That's why the oxidative aging tended to improve the hardness and resistance to uniform compression or tension of bitumen. Pan et al. found that the oxidized bitumen was compressed and tensioned slower than the virgin bitumen due to the stronger intermolecular bonds. Besides, the aged bitumen model exhibited more remarkable temperature insensitivity and moisture sensitivity than a pure bitumen. Xu [103] and Luo [107] adopted the same molecular models of virgin and aged bitumen as well as the force field to evaluate the aging influence on the physical, thermodynamics, and interfacial adhesion properties of bitumen or bitumen-aggregate systems. It was revealed that the aged bitumen model exhibited a higher cohesive energy density and glass transition temperature. At the same time, bitumen aging deteriorated the surface free energy, mean square distance, self-healing rate, fractional free volume, and diffusion coefficient. It was expected that the involvement of polar functional groups enhanced the intermolecular interactions and accelerated the shrinkage of the whole bitumen system. The bitumen molecules'

diffusive capacity showed a decreasing trend because of the increased molecular size and the reduced free volume.

These conclusions were also obtained by Qu [33] and Farshad et al. [73], who built the molecular models of virgin and aged binders according to the experimental results of the functional groups distribution, SARA fractions, and oxygen dosage. Furthermore, the oxidative aging distinctly decreased the energy ratio and increased the moisture damage potential of the bitumen-aggregate interfacial model. Interestingly, although the surface free energy of aged bitumen was lower than the virgin bitumen, Luo et al. [107] observed that the adhesion performance of aged bitumen was superior because the presence of polar groups would enhance the bonding strength between the bitumen and aggregates. The opposite results were reported in a previous study [33], and the reason was related to the different molecular models of aged bitumen utilized for MD simulations.

In addition, MD simulation technology could help researchers detect the concentration gradient of oxygen molecules in a bitumen model during the diffusion process, which affected the oxidative aging kinetics and thermodynamics properties of bitumen layer [148]. To this end, Liu et al. [108] combined the experimental extraction and MD simulation methods to monitor the aging gradient of bitumen layer during a thin film oven (TFO) test. Fig. 18 shows the bitumen-oxygen interfacial molecular model. The parameters of mean square distance, diffusion

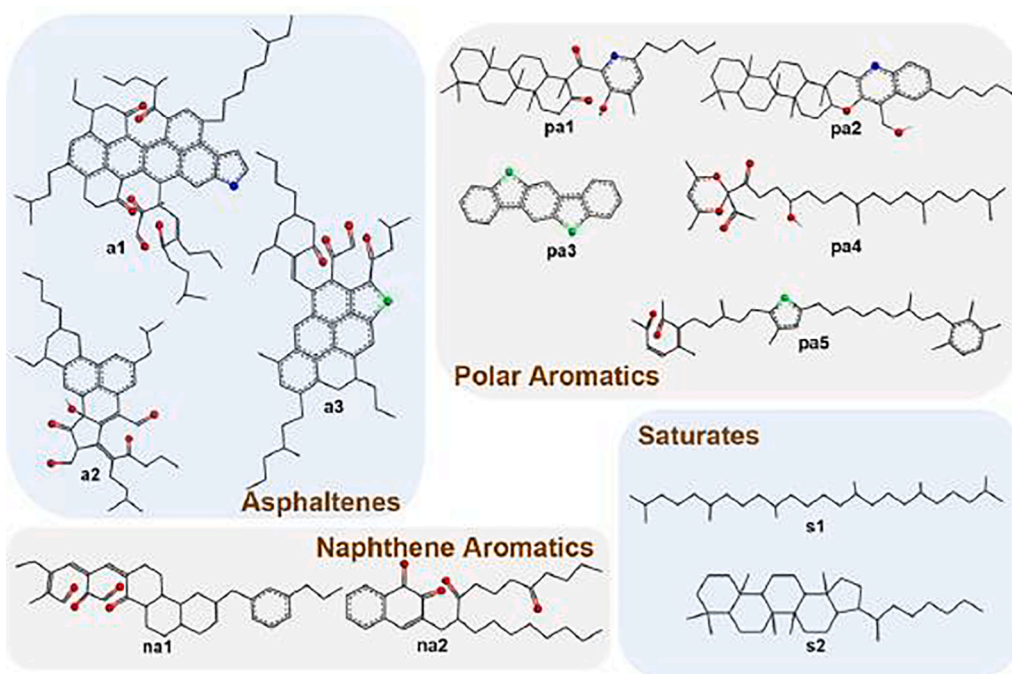


**Fig. 14.** Representative molecular structures of the aged bitumen molecules (Black atoms are carbon, red refers to the oxygen atom, blue is the nitrogen atom, and green represents the sulfur atom). (For interpretation of the references to colour in this figure legend, the reader is referred to the web version of this article.)

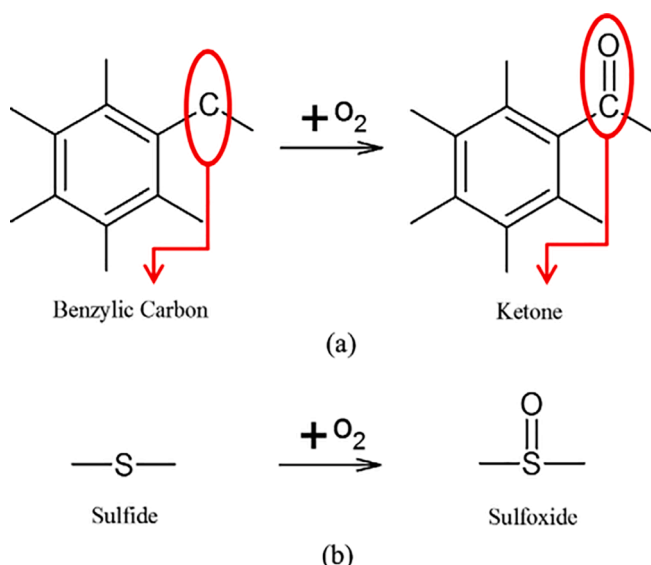


**Fig. 15.** The formation of (a) ketone and (b) sulfoxide functional groups in bitumen molecules during oxidative aging.

coefficient, and concentration distribution of oxygen molecules were calculated to validate the existence of the concentration gradient of oxygen molecules in different bitumen layers during the TFOT aging procedure. Nevertheless, the coupled effects of oxygen diffusion and oxidative reaction kinetics during the bitumen aging should be further investigated to deeply understand the aging behaviors of bitumen molecules from both static and dynamic perspectives.

## 6. MD simulations on modified bitumen systems

Asphalt pavements always suffer from the coupled effects of heating, light, heavy loading, and moisture, which accelerate the occurrence of diseases, such as rutting and cracking. Hence, improving the rheological

and mechanical properties of the bitumen binder is essential, which directly determines the engineering performance of asphalt roads. The modification technology was proposed to achieve this goal by adding polymers, fillers, or other effective additives into bitumen. Furthermore, much work has been conducted to evaluate the influence of different modifiers on enhancing the macroscale mechanical properties of bitumen using experimental methods. However, the microscale modification mechanism and the effects of these modifiers on the physical and thermodynamics properties of bitumen are challenging to investigate in the pavement engineering laboratory, which is vital to determine the macroscale properties of modified and optimize the effective modifiers for bitumen. Most recently, the MD simulation method has been applied to investigate the interaction mechanism between bitumen molecules and various modifiers, which is beneficial to the multiscale study of the underlying modification mechanism of polymer-modified bitumen, asphalt mastic as well as bio-bitumen binders.

### 6.1. Polymer-modified bitumen models

Regarding the modified bitumen, the commonly-used polymers are the segmented copolymers, such as the styrene-butadienestyrene (SBS) [151] and styrene-butadiene rubber (SBR) [143]. Moreover, the crumb rubber powder is another popular waste polymer of bitumen modification due to the significant economic and environmental benefits [122,141]. The SBS-modified bitumen is the most popular binder in asphalt roads because of its excellent dynamic performance, which was strongly dependent on the interaction between SBS and bitumen molecules from the molecular level [91]. Thus, it is necessary to fully understand the modification mechanism of SBS-modified bitumen from the molecular level. The MD simulations are beneficial for detecting the interfacial interaction between different kinds of molecules and predicting the overall thermodynamics, physical, and mechanical properties of a whole complex system. Due to the development of the representative molecular structure of bitumen, the interaction mechanism between bitumen and SBS molecules started to be studied by molecular dynamics simulation. It is well-known that the molecular weight of SBS copolymer is more considerable than 20000 g/mol, which would

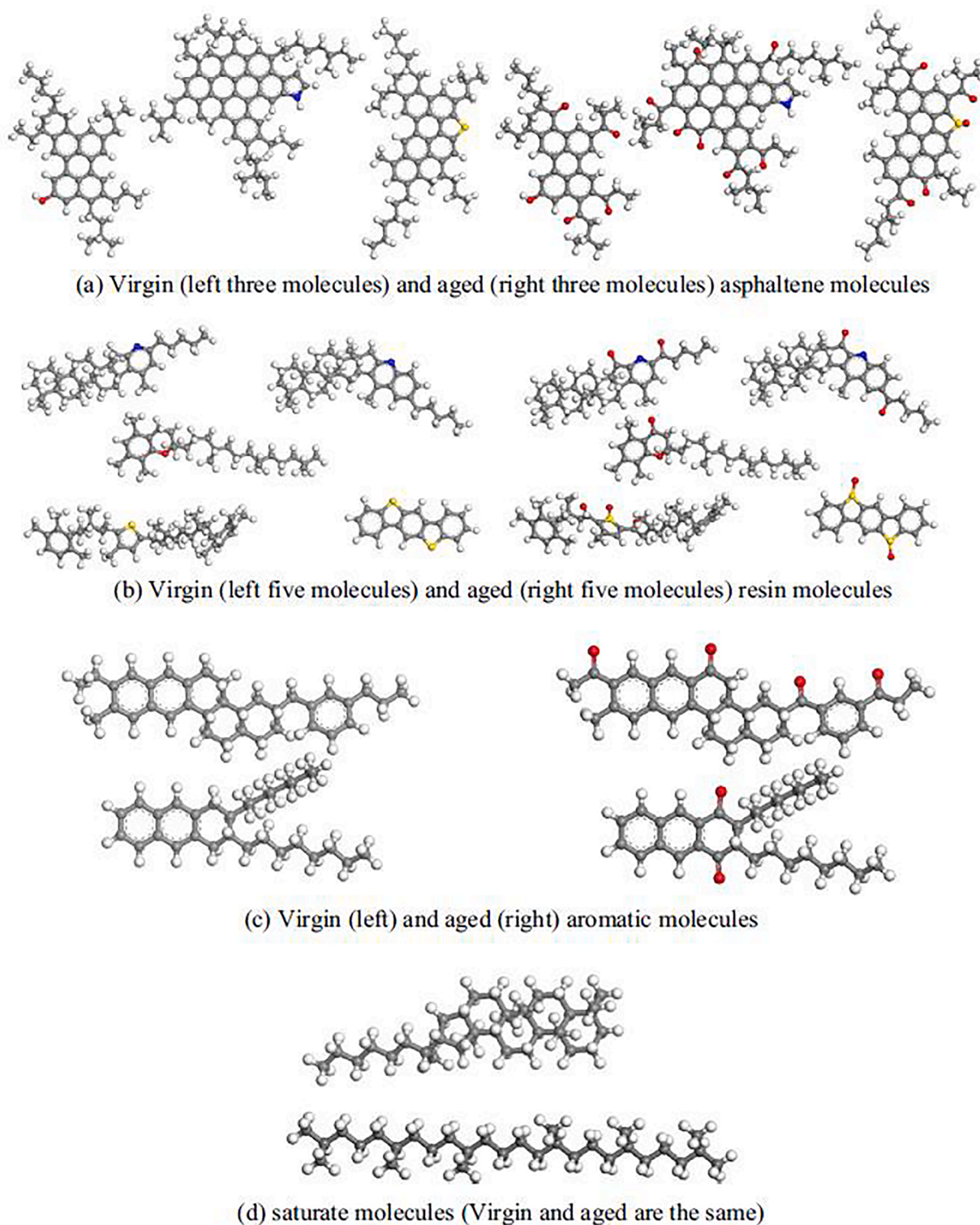


**Fig. 16.** Molecular structures of SARA fractions in bitumen before and after oxidative aging.

adversely affect the computational efficiency. Thus, several typical molecular structures of SBS copolymer were proposed to establish the molecular model of SBS modified bitumen, summarized in Fig. 19. It can be found that the polymerization degree in the molecular structures of the SBS modifier selected in MD simulations is all lower than 15, which are slightly varies in different studies. It has been validated that these simplified molecular structures of SBS copolymer can meet the computational limitation and efficiently show significant influence on the

molecular structure and thermodynamics properties of bitumen.

With the MD or quantum atomic simulation based on the density functional theory (DFT), the nanoscale interaction between SBS copolymer and the SARA fraction molecules in bitumen can be quantified. Ding et al. [151] focused on the effects of adding SBS on the molecular agglomeration behaviors of bitumen molecules according to the RDF curves from MD simulation. The classical colloidal structure of bitumen at the molecular scale was visualized, and the colloidal nucleus was

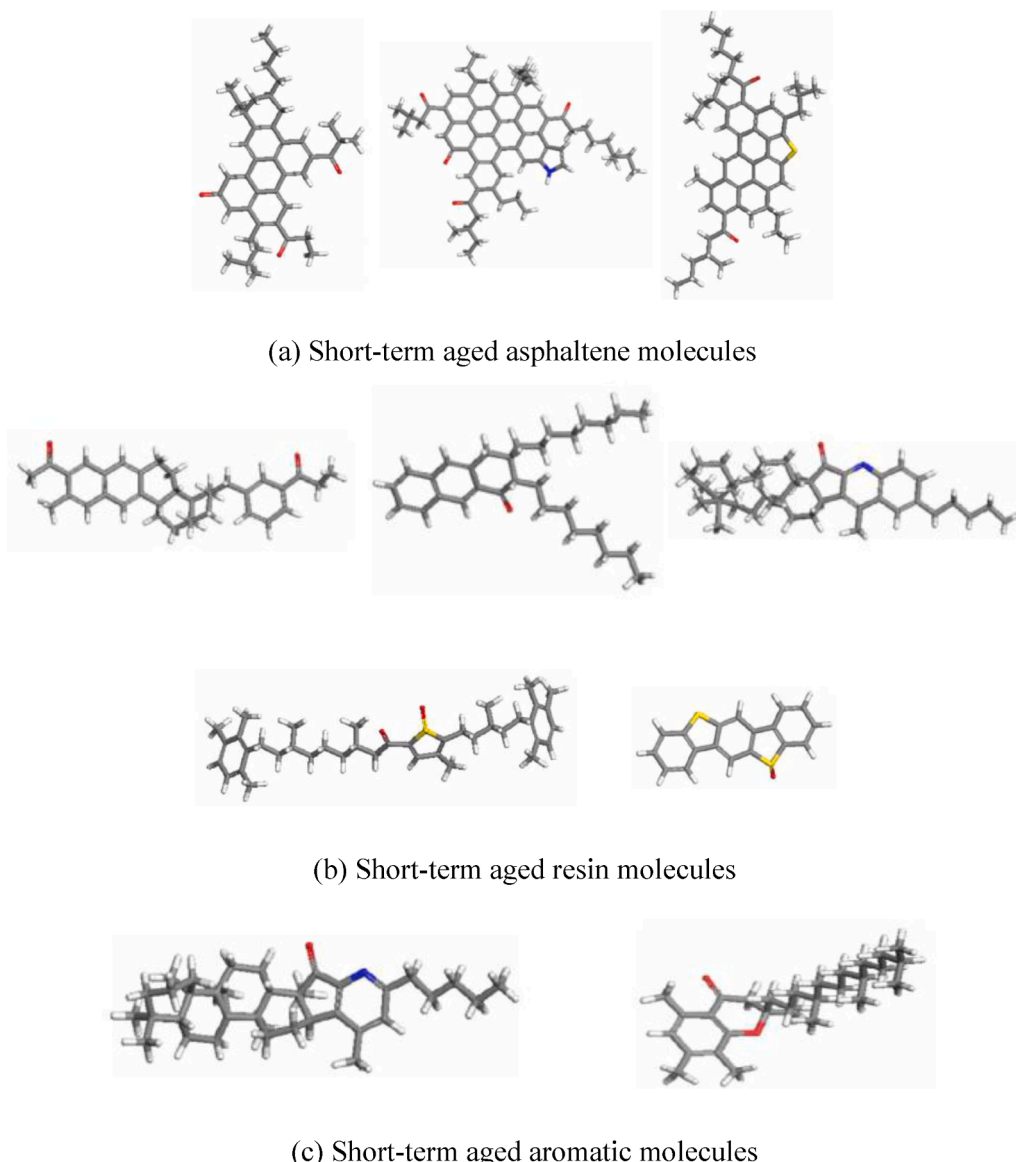


**Fig. 17.** Molecular structures of SARA fractions for short-term aged bitumen.

composed of asphaltenes and resins. Moreover, the colloidal characteristic of bitumen was more susceptible to SBS when the asphaltenes' alkane side branches were longer. To further figure out the interaction mechanism of SBS and various SARA molecules in bitumen, Feng et al. [32] calculated the binding energy ( $E_{\text{binding}}$ ) and charge transfer number ( $Q_{\text{transfer}}$ ) during the mixing of SBS copolymer with 12-component bitumen molecules and the difference in interaction forces between SBS and different types of bitumen molecules were found. The physically mixing mechanism of SBS-modified bitumen was indicated with no chemical reaction because the  $E_{\text{binding}}$  value of the SBS and bitumen molecules were all harmful. The same conclusion was reported by Zeng et al. [91]. They applied DMol3 with the DFT method to measure the change of vibration peak intensity before and after adding an SBS molecule into a four-component bitumen system. Moreover, it was reported that the interactions between the SBS modifier with aromatic, resin and asphaltene molecules were more stable and more predominant than the saturate, which resulted from the formation of  $\pi$ - $\pi$  stacking interaction. Hence, the nanoscale interaction between SBS copolymer and bitumen dramatically depends on their molecular structure. For instance, oxidative aging would significantly affect SBS-modified bitumen's rheological and mechanical properties. The main reason is the

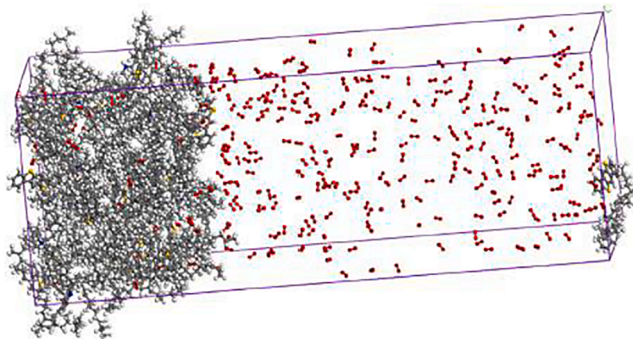
interaction deterioration due to the change in the molecular structure of SBS and bitumen molecules.

Crumb rubber (CR) is also an essential modifier of bitumen, which can not only improve the high-and-low temperature properties of bitumen but also be beneficial to environment protection and cost-saving. Although many experimental tests have been conducted to investigate the influence of crumb rubber on bitumen's chemical, rheological and mechanical properties, the interaction mechanism between crumb rubber and bitumen is still unclear. From the macro-scale experimental characterizations, it is difficult to detect the modification mechanism of crumb rubber modified bitumen (CRMB) from the molecular-level perspective. Therefore, researchers used the MD simulation method to explore the thermodynamics, self-healing, interface properties, compatibility, interaction behaviors, mechanical performance, and the aging behavior of the CRMB binder. It is well-known that the crumb rubber comes from waste tires and has quite complicated components, hindering the determination of its detailed molecular structure for MD simulation. It was reported that the CR powder was composed of three main polymers, including natural rubber (NR), *cis*-polybutadiene (BR), and styrene-butadiene rubber (SBR). Fig. 20 illustrates the representative molecular structures of these three crumb

**Table 6**

The input and output parameters in MD simulations on the aged bitumen.

| Molecular models of SARA fractions in aged bitumen     | Aided-Experimental tests          | Selected force field | MD simulation output parameters  | Ref   |
|--|-----------------------------------|----------------------|--|-------|
| Full-oxidized 12-component molecular model             | SHARP AAA-1 bitumen model         | DREIDING             | Potential energy; Density; Bulk modulus (isothermal compressibility); Viscosity; Compression and tension strength;   | [33]  |
| Full-oxidized 12-component molecular model             | SHARP AAA-1 bitumen model         | COMPASSII            | Density; Surface free energy; Viscosity; Cohesive energy density; Radial distribution functions; Mean square distance; Self-healing density; Diffusion coefficient; Energy ratio | [103] |
| Full-oxidized 12-component molecular model             | SHARP AAA-1 bitumen model         | COMPASSII            | Cohesive energy density; Glass transition temperature; Fractional free volume; Mean square distance; Adhesion energy; Energy ratio   | [107] |
| Partial and full-oxidized 12-component molecular model | Functional groups; SARA fractions | COMPASS              | Density; Cohesive energy density; Surface free energy; Fractional free volume; Work of adhesion;   | [73]  |
| Full-oxidized 12-component molecular model             | SARA fractions; oxygen content    | -                    | Density; Bulk modulus; Viscosity; Glass transition temperature   | [148] |

**Fig. 18.** The interfacial molecular model of a bitumen-oxygen system.

rubber components, proposed by Hu et al. [121] and Guo et al. [122,123,141]. To meet the computational ability, the polymerization degree of NR and BR was 16 and 20, respectively. Regarding the SBR molecule, the number of styrene and butadiene was selected as 3 and 16.

Guo et al. [122,123] established the molecular models of crumb rubber modified bitumen with various CR dosages from 5 to 30 wt% by incorporating the three CR mentioned earlier components into the typical three-components bitumen molecular model. The CRMB binders' compatibility and mechanical properties were estimated based on the solubility parameter, binding energy, and modulus outputted from MD simulation with the COMPASS force field. The results showed that the compatibility between BR and bitumen is better than the SBR and NR

components. Moreover, with the increase of CR dosage, the modulus of the CRMB system enhances firstly, followed by decreasing later and increasing at last. Finally, the optimum dosage of crumb rubber was proposed.

Additionally, Hu et al. [121] applied some molecular models of crumb rubber and bitumen and the force field to evaluate the influence of additional CR modifiers on the self-healing and interface properties of bitumen. After MD equilibrium simulation, it was found that the high rubber content would result in the prolongation of wetting time and decrease of molecular diffusivity of CRMB models, which indicated that the self-healing capacity of CRMB binder was deteriorated with the increase of crumb rubber dosage, while the cohesion strength was enhanced. On the other hand, the Al<sub>2</sub>O<sub>3</sub>-CRMB and SiO<sub>2</sub>-CRMB interfacial systems were built, and the thermodynamics parameters of work of adhesion, work of de-bonding, and energy ratio were calculated to study the effects of rubber dosage on the adhesion and moisture damage of the aggregate-CRMB system. They found that the CR influence on interface properties depended on the aggregate type. Furthermore, the high CR dosage improved the adhesion and moisture stability of the Al<sub>2</sub>O<sub>3</sub>-CRMB model, which showed no evident influence on the SiO<sub>2</sub>-CRMB model.

To further deeply understand the interaction behaviors between crumb rubber components (NR, BR, and SBR) and bitumen molecules (saturate, naphthalene aromatic, and asphaltene), Guo et al. [141] used MD simulation. They evaluated the influence of rubber and bitumen type on the agglomeration interaction based on the radial distribution function (RDF) curve. Regarding the virgin bitumen model, the agglomeration phenomenon of asphaltene adsorbing the naphthalene aromatic and saturate could be observed, which further validated the colloidal structure theory of bitumen. It was found that the addition of crumb rubber significantly affected the agglomeration degree of bitumen molecules, which could explain the CR modifier absorbing the light components from the bitumen matrix. Besides, the accumulation of rubber-naphthalene aromatic was more clustered than rubber-saturate. The order for the molecular agglomeration between rubber constituents and light fractions of bitumen was found as BR > SBR > NR. Further, MD simulation results revealed that the higher proportion of naphthalene aromatic and saturate would accelerate the agglomeration degree of rubber-bitumen molecules. Wang et al. [81] studied the influence of aging on the thermodynamics properties of crumb rubber modified bitumen system with MD simulation technology. They found that the aging would enhance the molecular dynamics energy of the CRMB model, which caused an increment in the hardness of the aged CRMB binder. Fardin and Rajesh [143] applied the MD simulation to explore bitumen's volumetric, structural, and dynamic properties. The results manifested that the addition of SBR molecules reduced the mobility of bitumen molecules dramatically. Meanwhile, the aggregation degree of the asphaltene molecules in SBR-modified bitumen was more evident than in a virgin binder. Hence, the influence of the SBR molecule in these thermodynamic and structural parameters of bitumen directly affects its viscosity and viscoelastic properties at the macroscale level.

## 6.2. Asphalt mastic models

The fillers are always incorporated into the bitumen matrix to manufacture the mastic binder and enhance the asphalt mixture's mechanical and interfacial properties. Apart from these organic polymer modifiers, inorganic fillers are also essential materials used to improve the performance of bitumen. Currently, nano-particles are popular due to their excellent stiffness and superficial area. Thence, a lot of experiments have been performed to evaluate the influence of nano-modifiers on the rheological properties, adhesion, and aging behaviors of bitumen, such as the nano-SiO<sub>2</sub>, nano-ZnO, nano-TiO<sub>2</sub>, nano-size graphene, and carbon nanotubes. The experimental results revealed that the addition of nano-modifiers positively affected the improvement of stiffness, anti-aging, adhesion strength, and moisture resistance of bitumen binders.

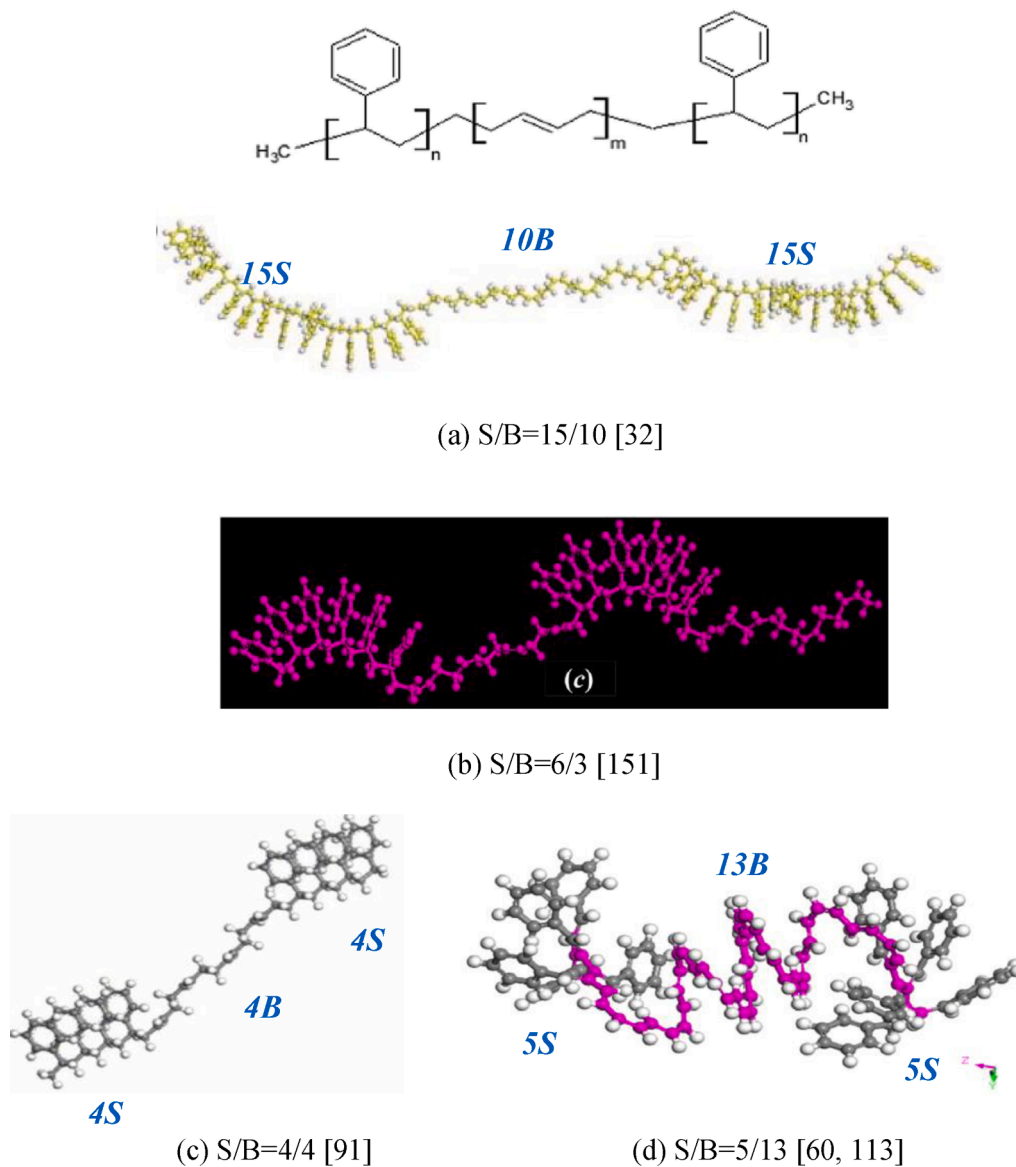


**Fig. 19.** Molecular structures of styrene–butadienestyrene copolymer.

Meanwhile, due to the sizeable superficial area, the nano-materials were also utilized to enhance the compatibility of polymer-modified bitumen.

Most recently, molecular dynamics (MD) simulation technology has been employed as an effective tool to investigate the modification mechanism and influence of the inorganic nano-particles on the molecular structure, thermodynamics properties, and interfacial adhesion of bitumen from the viewpoint of the nanoscale. The supplement of microscale findings would be beneficial to explain the macroscale phenomenon and design the optimum nano-particles/bitumen systems, which exhibit sufficient engineering characteristics. However, not all types of nano-modifiers in bitumen have been studied practically from a nanoscale perspective. Moreover, the MD simulation is a new-developed technology, and its application in bituminous materials didn't last long. Hence, this paper only summarized the MD simulation results from the existing studies. Fig. 21 displays the molecular structures of different types of nano-modifiers as a basis of MD simulation, including the nano-silica, ZnO cluster, TiO<sub>2</sub>, and CaCO<sub>3</sub> photocatalysts, nanometer-sized graphene, and carbon nanotube. These molecular structures of nanoparticle clusters of surfaces could be established with the MD simulation tool by cleaving, hydroxylation, collection, or supercell operations.

To investigate the effects of nano-SiO<sub>2</sub> filler on bitumen mastic's

thermodynamic and mechanical properties, Zhu et al. [116] built the bitumen/silica molecular models with different nano-silica concentrations of 3.3, 6.7, 9.8, and 20.2 wt%. After MD simulation, it could be found that the involvement of SiO<sub>2</sub> molecules deteriorated the molecular interaction but accelerated the mobility of bitumen molecules. The reason was attributed to the light fractions adsorption of silica nanoparticles and increased free volume because of the additional silica molecules. Meanwhile, the MD simulation results showed that with the increase of Nano-SiO<sub>2</sub> molecules, the glass transition temperature of the mastic system decreased and the Young's, shear, and bulk moduli all enhanced, which may be related to the formation of particle-aggregation and structural skeletons in the bitumen mastic system with high Nano-SiO<sub>2</sub> concentration.

Like the polymer-modified bitumen, the nano-filler/bitumen is also a complicated binary system. Hence, it is essential to evaluate the compatibility of bitumen mastic to prevent the occurrence of phase separation. A macroscale storage stability test can effectively assess the compatibility between bitumen and modifiers. The compatibility of binary or ternary systems depends on the molecular interaction between different matters. The compatibility mechanism of nano-silica modified bitumen was analyzed by Long et al. [120] based on the parameters of

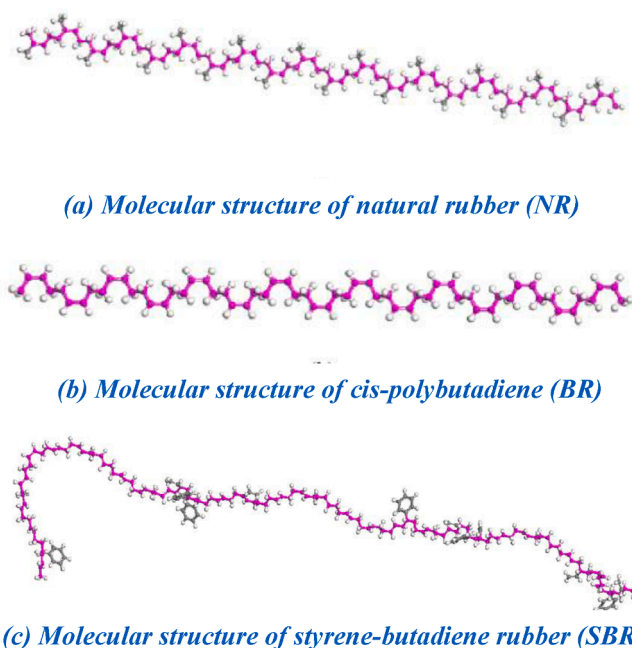


**Fig. 20.** Representative molecular structures of crumb rubber components.

solubility, the Flory-Huggins parameters, and interaction energy outputted from MD simulation. The results revealed that the interaction between silica and saturate molecules was stronger than aromatic, resin, and asphaltene components, which hindered the volatilization of saturate molecules and improved bitumen's aging resistance. However, Li et al. [118] drew the opposite conclusion that polar molecules were closer to the surface of silica molecules than non-polar fractions (saturate) (Fig. 22b). The reason may be due to the difference in evaluation indexes. The former used the thermodynamic parameter (solubility parameter and interaction energy), while the latter considered the relative concentration of bitumen molecules around the silica molecule. The two studies reported that adding silica molecules would destroy the original colloidal structure of bitumen molecules, which was significantly affected by environmental temperature and related to the rheological-mechanical properties of asphalt mastic.

Apart from physicochemical properties of bulk silica-bitumen mastic system, Long et al. [115] also analyzed the interfacial adhesion behavior and moisture damage resistance of nano-silica modified bitumen by establishing the bitumen-moisture-aggregate interfacial models and calculating the adhesion energy with MD simulation technology (Fig. 22a). The microstructure analysis showed that the nano-silica could significantly hinder the asphaltene agglomeration on the aggregate surface and enhance the bitumen's oxidative aging resistance. Furthermore, it was proved that adding nano-silica improved the work of adhesion and water damage resistance in the bitumen-aggregate system.

The molecular interactions between bitumen and different nano-filters (Titanium dioxide  $TiO_2$ , Calcium carbonate  $CaCO_3$ , and Silica  $SiO_2$  shown in Fig. 21c) have been studied by Cao et al. [117] with MD simulation to investigate the influence of inorganic photocatalysts on microstructure and physical properties of bitumen. Compared with the  $CaCO_3$ , the  $TiO_2$  molecules presented a special modification effect because of the robust interaction with bitumen molecules. Recently, nanoscale carbon materials attracted much attention because of their excellent surface and electrical properties. The representative molecular structure of graphene and carbon nanotube is displayed in Fig. 21d. Zhou et al. [86] utilized MD simulation and reported the influence of adding graphene and carbon nanotubes on bitumen's thermal and mechanical properties. Based on the experimental and MD simulation results of glass transition temperature and modulus, the optimum content

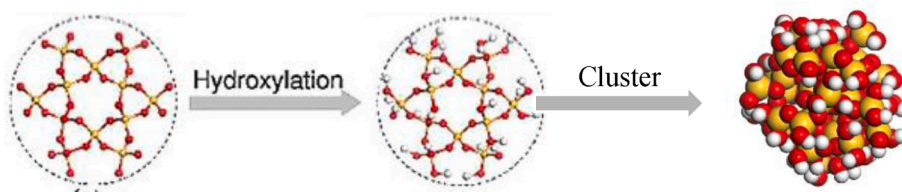
of graphene and carbon nanotubes was recommended as 6.3 and 3.8 %, respectively. Meanwhile, the positive effects of exfoliated graphite nanoplatelets on increasing the density, viscosity, and thermal conductivity of bitumen were found by Yao et al. [138]. They established the three-components bitumen model and ran the MD simulation with the Amber Cornell Extension Force Field (ACEFF).

In addition, other inorganic nano-filters have been applied to improve the rheological and mechanical properties of bitumen and reuse the solid waste, such as the red mud, a waste residue of the aluminum industry. Although experimental results reported that red-mud would improve the mechanical performance of asphalt binder and mixture, the detailed modification mechanism of red mud-modified bitumen is still unclear. Fu et al. [161] used the MD simulation method to explore the interfacial energy between red mud components ( $Fe_2O_3$  and  $Al_2O_3$ ) with asphaltene molecules. The results revealed that the asphaltene molecule could naturally absorb on the surface of red mud. Therefore, increasing  $Al_2O_3$  dosage or decreasing  $Fe_2O_3$  content in red mud filler would be beneficial to improve the adsorption strength of asphaltene. Furthermore, due to the unique layered structure and radical shielding functions, the layered double hydroxides (LDHs) could be used as an effective anti-aging agent of bitumen. Zhao et al. [150] built the LDHs-modified bitumen model and performed the MD simulation to further understand the influence of LDHs on the thermo-physical properties and ultraviolet aging resistance of bitumen according to the outputted parameters of isothermal compressibility, heat capacity, diffusion coefficient, and relaxation time. They concluded that the addition of LDHs molecules improved the heat capacity and thermal stability of the bitumen system dramatically, and there was no chemical reaction during the mixing of layered double hydroxides and bitumen. Further, their group combined the experimental and MD simulation methods and reported that incorporating surface-active additives (dodecyl benzene-sulfonic acid DBSA and polyvinyl alcohol PVA) distinctly enhanced the low-temperature cracking resistance and compatibility of the LDHs-modified bitumen system.

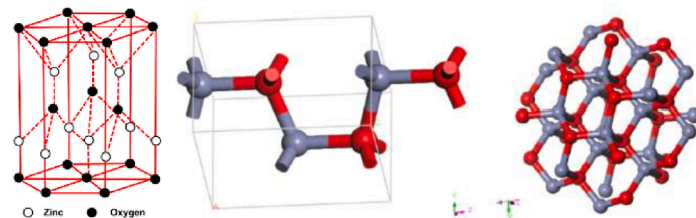
In order to solve the issue of lousy compatibility of polymer-modified bitumen, the nano-materials are proposed to be added into modified bitumen because of their advantageous specific area. Therefore, several researchers started to explore the interaction mechanism of the multi-components system and study the influence of polymers and nano-filters on the thermodynamic properties and microstructure of bitumen from the nanoscale perspective. It was found that the nano-ZnO could increase the interaction force between polymerized styrene-butadiene (PSB) and bitumen molecules due to the hydroxyl modification effect, which improved the structural stability of PSB-modified bitumen [162]. Likewise, Su et al. [113] studied the physical properties and molecular structure of nano-ZnO/SBS compound-modified bitumen models through MD simulation. As expected, the solubility parameter of SBS-modified bitumen decreased when the nano-ZnO was incorporated, indicating the nano-ZnO could enhance the miscibility between SBS and bitumen molecules. Meanwhile, adding ZnO enlarged the bulk, shear, and elastic modulus and improved the high-temperature properties of SBS-modified bitumen while the molecular diffusion mobility deteriorated. It should be mentioned that the influence of nano-ZnO depends on its particle size. Further, the nano-ZnO and SBS molecules increased the bitumen molecular structure's tightness and colloidal structure stability.

### 6.3. Bio-bitumen models

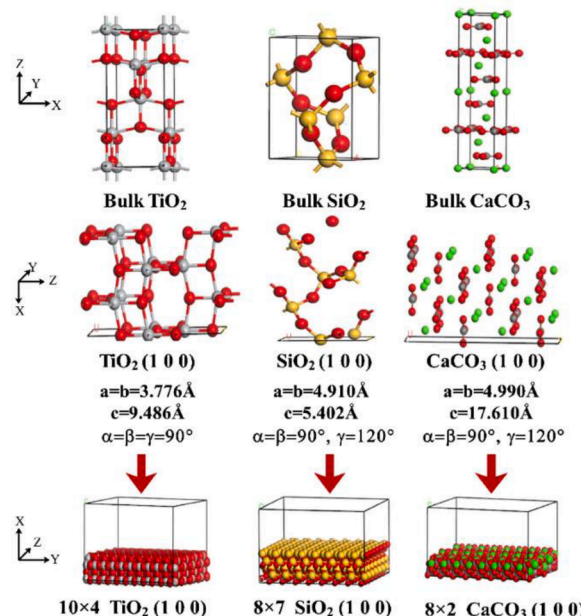
To reduce the consumption of base bitumen and manufacture environmental and sustainable binder, the bio-bitumen is proposed by adding the bio-oils derived from microalgae, waste wood, and swine manure during the fast pyrolysis process. It has been verified that bio-oils could partially replace the petroleum-based bitumen and improve the rheological properties of oxidized bitumen. A considerable study has explored the interaction mechanism between bio-oils and bitumen with



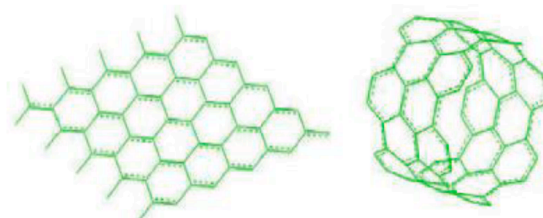
(a) Molecular structure of silica filler particles



(b) Molecular structure of ZnO cluster



(c) Molecular layer structures of different photocatalysts



(d) Molecular structure of graphene and carbon nanotube

**Fig. 21.** The molecular structures of nano-filler modifiers.

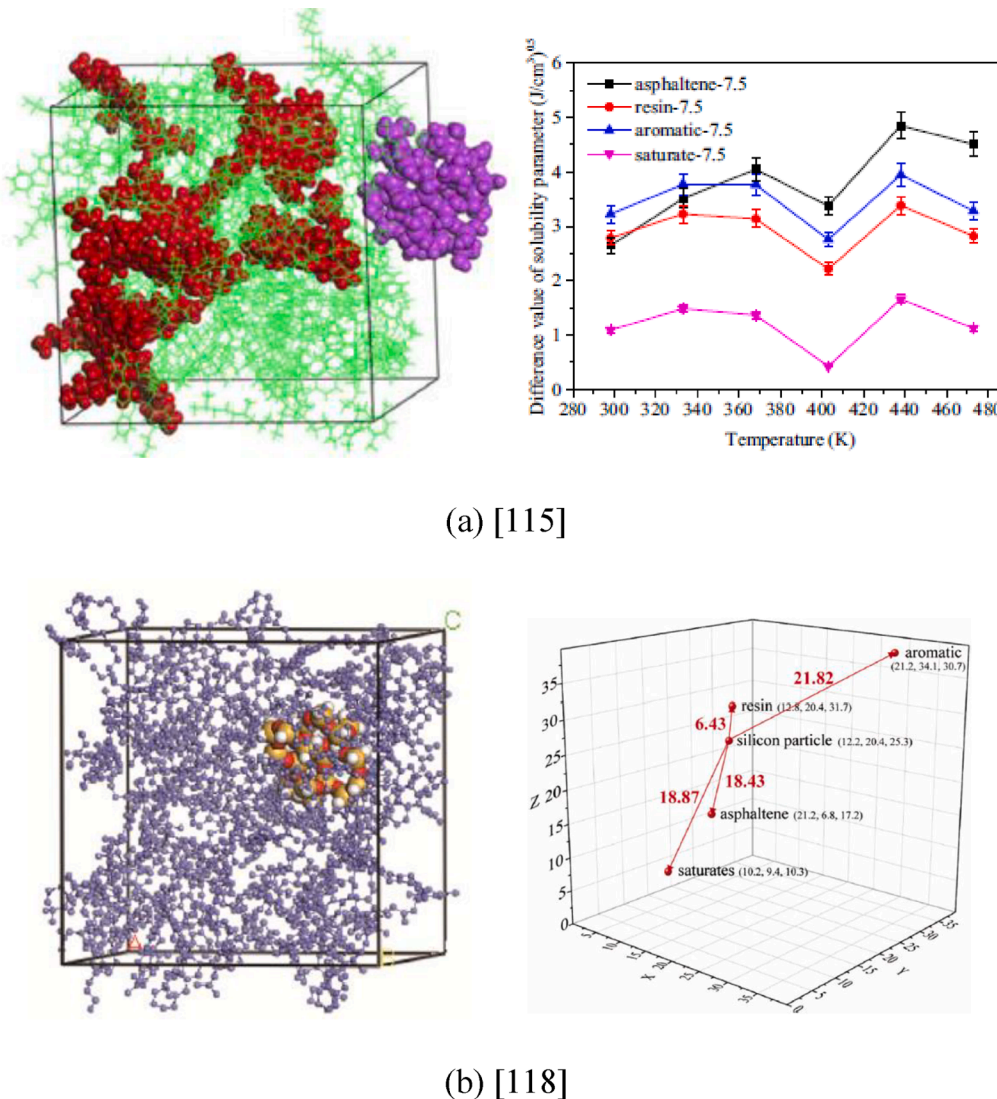


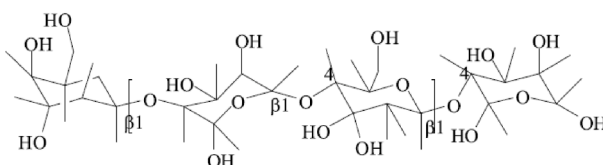
Fig. 22. The silica-bitumen system and related MD simulation results.

MD simulations. However, it is difficult to determine the exact molecular formula of bio-oil because of its complex components and different resource types. Fig. 23 summarizes several typical molecular structures of various bio-oils, such as cellulose (a), triglyceride (b), paraffin (c), and fatty acids (d). Although the molecular structures are different, the long-chain aliphatic hydrocarbons, carbonyl, ester, or amide groups are the main elements of bio-oil molecules. Hence, the molecular structures of bio-oils are similar to that of saturates, which would soft the bitumen and restore its rheological properties by changing the molecular interaction and colloidal structure of bitumen molecules.

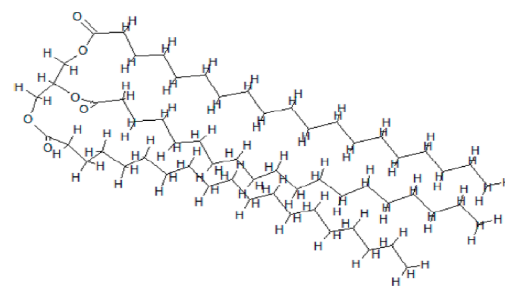
The bio-oil effects on bitumen have been investigated using MD simulations to predict the thermodynamics and diffusion properties of bio-bitumen binder without extra experimental tests and deeply understand the interaction mechanism of bio-oils and bitumen at the molecular and atomic levels. Qu et al. [110] applied MD simulation (with COMPASS force field) to study the influence of bio-oil (waste cooking oil) and paraffin (wax) molecules on the physical properties of bitumen. Compared to the virgin bitumen model, the bio-oil modified bitumen systems showed a lower density, surface free energy, and cohesive energy density, consistent with the low modulus and good fatigue resistance from experimental results. In addition, MD simulation results revealed that the addition of paraffin would deteriorate the stiffness and molecular mobility of bitumen, and that's why the wax adversely

influenced the fatigue and low-temperature cracking resistance of the binder and its dosage should be controlled.

Further, Sonibare et al. [102] established a representative molecular model of waste vegetable oil by mixing three types of fatty acids with the molar ratio of oleic acid to palmitic acid to linoleic acid as 7:6:2. The three-components molecular model of bitumen was utilized in this study. The structure, molecular interaction, and thermodynamic properties of vegetable oil-modified bitumen were predicted based on the MD simulation trajectories with the OPLS-aa forcefield. Notably, the density, molecular diffusion behaviors, and thermal conductivity of vegetable oil molecular models were not dependent on the type of fatty acid. The reason may be related to the similar molecular structures of linoleic, palmitic, and oleic fatty acids when the incorporated vegetable oil molecules could enhance the density and relaxation of bitumen. The influence of vegetable oil molecules on decreasing the viscosity of bitumen is significant at low temperatures, which converted to a negligible effect at high temperatures. Regarding the molecular structure, the fatty acids molecules could be uniformly distributed in bitumen and facilitate the molecular interactions between bitumen components. The dynamic mobility of bitumen was accelerated by adding vegetable oil molecules, which was attributed to its low molecular weight and high diffusion ability. Similar conclusions in terms of the dynamic properties of bio-bitumen were reported by Sun and Zhou [109]. They found that



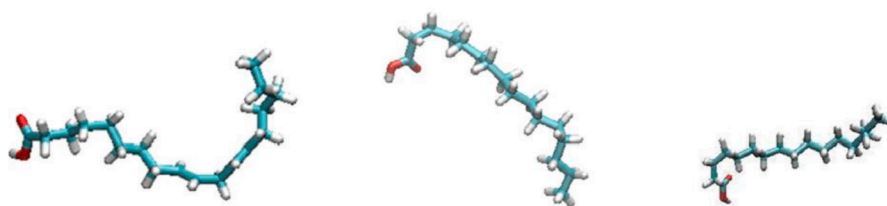
(a) Molecular structure of cellulose



(b) Molecular structure of bio-oil



**(c) Molecular structure of paraffin**



(d) Molecular structures of the fatty acids (Linoleic acid, Palmitic acid, Oleic acid)

**Fig. 23.** The representative molecular structures of bio-materials for bio-bitumen [102,109–111].

the bio-bitumen model's diffusion coefficient improved with the cellulose molecule content increase.

The compatibility between bio-oil and saturate molecules was better than resin and asphaltene due to their similar chemical structures. Therefore, the bio-oil could be used as the saturate fraction of bitumen, which significantly strengthened the diffusion driving force and flexibility of bitumen. Additionally, no chemical reaction was observed while mixing waste wood bio-oil and bitumen. Due to the softening effect, the bio-oils are always used as rejuvenators to restore the colloidal structure and physio-rheological properties of aged bitumen by supplementing the light constitute. The rejuvenation function of bio-oil will be discussed in the following section. It could be speculated that the interaction mechanism of bio-oil should be the same, no matter in the modification or rejuvenation cases. The only difference is the molecular variety of bitumen systems.

## 7. MD simulations on rejuvenated bitumen systems

From the viewpoints of environmental protection and economic benefit, researchers have concentrated on reusing the waste reclaimed asphalt pavement material during the maintenance and reconstruction of damaged asphalt pavements. The performance deterioration of asphalt mixture is mainly due to the quality degradation of bitumen under the complex environmental conditions of heat, light, oxygen, and moisture. Based on the aging mechanisms of bitumen, the aged bitumen is generated by the oxidation of bitumen molecules and the increase in the ratio of heavy and light components, which alters the molecular interaction and colloidal structure of the virgin bitumen system. Theoretically, the oxidized molecules with considerable molecular weight in aged bitumen could be restored and transformed into the original bitumen molecules through the deoxidization and cracking reactions.

However, it is difficult for pavement engineers and researchers to realize the objective due to the high reaction energy and efficient catalyst required. Hence, most rejuvenation cases of the aged bitumen are achieved by replenishing the light-weight oil fractions decreased during the aging process of bitumen, such as the saturates and aromatics.

According to the experimental results, different rejuvenators could be used to restore and improve the rheological and mechanical properties of the aged bitumen, such as bio-oils (vegetable oils), paraffinic oil, engine oil, naphthenic oil, and aromatic oil. Although the rejuvenation effectiveness depends on the rejuvenator type and dosage, rejuvenators are expected to improve the low-temperature cracking and fatigue resistance of aged bitumen. To understand the underlying rejuvenation mechanism and evaluate the rejuvenator effects on nanoscale properties of the aged bitumen, molecular dynamic (MD) simulation technology has been proven to be effective. However, it is challenging to determine the molecular models of different rejuvenators because most of them are composed of multiple molecules, especially those derived from petroleum-refining products. Fig. 24. lists the proposed molecular models of various rejuvenators. Considering the chemical characteristics of aromatic oil, naphthenic and paraffinic oils, a single molecular formula  $C_{12}H_{16}$  containing polar benzene ring, saturate naphthenic and alkyl hydrocarbons is the standard model used as the molecular structure of rejuvenator (see Fig. 24a) [124]. As mentioned, the bio-oil is also a critical rejuvenator, consisting of long-chain alkane, carbonyl, and ester functional groups. For instance, Shu et al. [88] established sunflower oil's molecular structure (shown in Fig. 24b). The molecular structures of fatty acids discussed in Section 6.3 were also applied to establish the molecular models of vegetable oil or waste cooking oil. Besides, other scholars found that the amide functional group also existed in rejuvenators. Xiao et al. [89] suggested the formula of  $C_{13}H_{15}NO_3$  and  $C_{11}H_{13}NO_2$  to represent the molecular structures of two

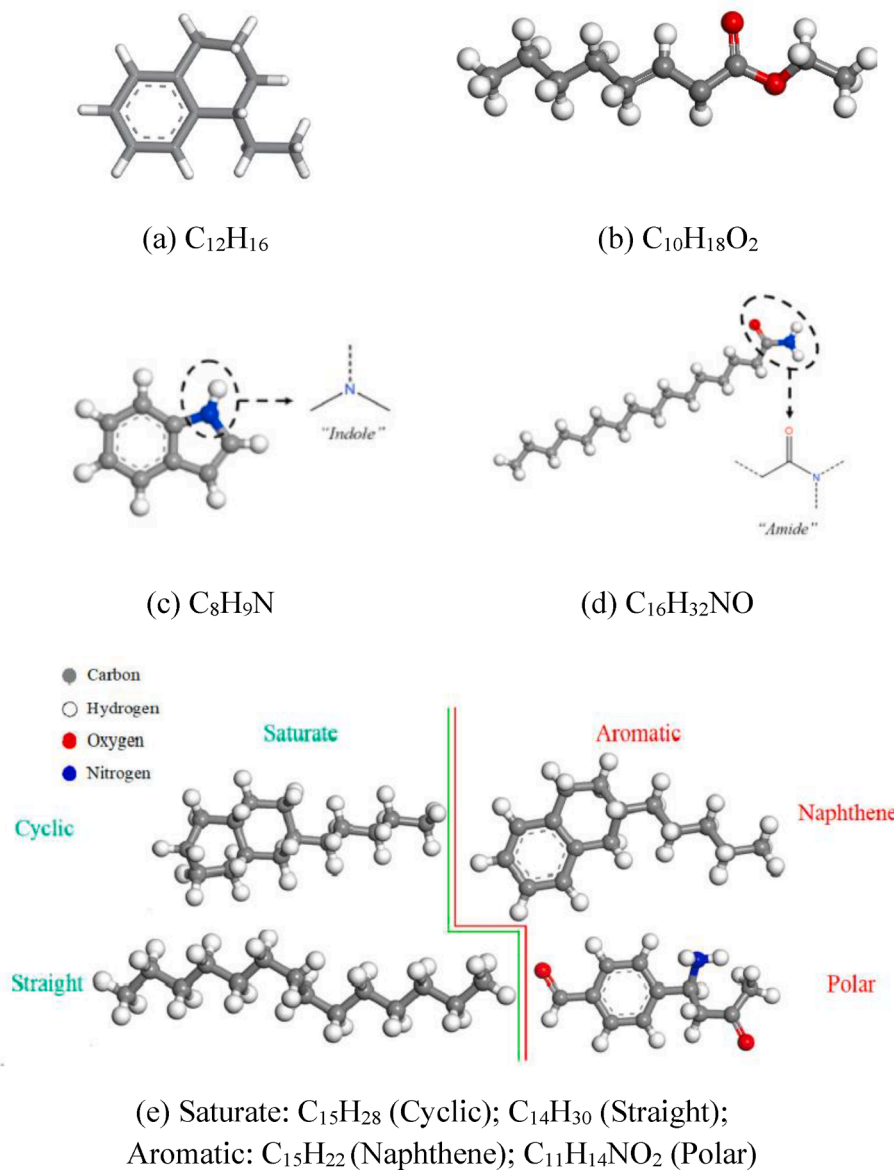


Fig. 24. Typical molecular structures of rejuvenators.

rejuvenators used in their study. Meanwhile, the aromatic-based model with indole group ( $C_8H_9N$ ) and alkyl-based model containing amide ( $C_{16}H_{32}NO$ ) were built, shown in Fig. 24c and d, respectively. From these established molecular models, the polar aromatic cyclic and long-chain alkyl hydrocarbons are the main body of rejuvenator molecules, which connect with various polar functional groups, such as carbonyl, ester, indole, or amide. Thus, the hydrocarbon and the functional group types should be mainly considered when building the molecular models of rejuvenators.

To determine the molecular structures of rejuvenators, the average molecular weight, elemental components, functional groups, carbon-hydrogen types, and chemical components need to be measured through several chemical characterization methods, such as GPC, Elementary analysis, FTIR, NMR, and gas chromatography-mass spectrometry (GC-MS). Sun and Wang [65] divided the molecular structures of rejuvenators into four categories, i.e., cyclic saturates, straight saturate, naphthalene aromatics, and polar aromatic. Their developed molecular models are displayed in Fig. 24e. Obviously, during the establishment of molecular structures of rejuvenators, they paid attention to the types of central hydrocarbon bodies and functional groups.

However, these four types of rejuvenator molecules were proposed based on previous works without any experimental measurement. Hence, these molecular models should be further modified to better represent the real rejuvenators on the basis of their chemical properties.

Although there are still research gaps between the results from MD simulations and experiments because of the estimated molecular structures of rejuvenators and the selected common-used forcefield, the application of MD simulation technology could predict the fundamental effects of rejuvenators on the thermodynamics and mechanical properties, dynamic behaviors, and molecular structures of the aged bitumen. Meanwhile, rejuvenation mechanisms of the rejuvenated bitumen could be detected at the molecular and atomic scales using MD simulation. Notably, the combination of rejuvenation technology and MD simulation could be beneficial in designing effective rejuvenators of the aged bitumen with different aging degrees and chemical properties. For example, Cui et al. [124] conducted an MD simulation to investigate the impacts of rejuvenator ( $C_{12}H_{16}$ ) dosage on restoring the thermodynamics, adhesion properties, and microstructure of the aged bitumen considering the temperature and moisture factors with the classic 12-component bitumen model and COMPASSII force field. As a result, it

was revealed that the rejuvenator molecules would improve the cracking resistance based on the increase of cohesion work while weakening the rutting resistance due to the decreased modulus and viscosity of the aged bitumen.

Regarding the microstructure, the addition of a rejuvenator would hinder the self-agglomeration of asphaltenes and restore the colloidal structure to some extent, which could be fully close to that of virgin bitumen. Moreover, the rejuvenated bitumen showed better moisture damage resistance than the aged bitumen. The temperature and moisture would also significantly affect the adhesion properties of bitumen on aggregates. Yang et al. [90] studied the thermodynamic properties of bio-oil regenerated bitumen with a ternary rejuvenator model containing acetic acid, 1-carboxy-2-propanone, and methanol. The MD simulation demonstrated that adding bio-oil molecules could restore the thermal expansion coefficient, modulus, and flexibility of the aged bitumen. However, the excessive bio-oil molecules would adversely influence the high-temperature properties and thermal stability of bitumen.

The aged bitumen always presents higher viscosity due to the strong molecular interaction and low molecular mobility, which would lead to the inhomogeneity and high mixing temperature needed. Using a rejuvenator aims to restore the thermodynamics and rheological properties of aged bitumen and activate the diffusion ability of bitumen molecules. However, it is impossible to observe the function of the rejuvenator in increasing the dynamic nature of aged bitumen molecules. Hence, several researchers implemented the MD simulations to capture the difference in diffusion behaviors between aged and rejuvenated binders. Xiao et al. [89] established the molecular models of rejuvenated binders to characterize the effects of rejuvenator type and bitumen aging degree on the actual movement of rejuvenators in the aged bitumen. The simulation results of the mean square distance (MSD) and diffusion coefficient showed that rejuvenators diffused faster in long-term aged bitumen, which was also reported by Shu et al. [88] that the aging of bitumen would increase the diffusion rate of sunflower oil molecules in the bitumen model. In addition, the diffusion characteristic of a rejuvenator depends on its components. The high temperature would accelerate the dynamic molecular diffusion due to strong Brownian molecular movement and large free volume fractions in the bitumen system. Moreover, it was demonstrated that rejuvenator molecules would improve the self-healing performance of bitumen, and the sunflower oil diffusion process consisted of the quick contact and stable diffusion stages. A similar MD simulation of rejuvenator diffusion in aged binders has also been performed by Xu et al. [37]. They found that the molecular interaction also contributed to the diffusion force between rejuvenator and aged bitumen molecules apart from the thermal motion. Besides, the microscale free voids in the bitumen model could increase the contact area and accelerate the rejuvenator diffusion.

All the studies above estimated the diffusion behaviors of rejuvenators and bitumen in the molecular models of rejuvenated binders. The diffusion of a molecule results from its self-motion and molecular interaction, which is called "self-diffusion" considering the rejuvenated bitumen model is homogeneous (no concentration gradient). In practice, the rejuvenator is always incorporated into the reclaimed asphalt mixture (aged bitumen covers on the aggregate) and the rejuvenator diffuses into the aged bitumen gradually, which is influenced by mixing temperature and time [163]. In the practical case, the existed concentration gradient dominates the diffusion behavior of rejuvenators in the aged binders. To detect the diffusion coefficient of the rejuvenator, multiple extraction methods were used after a while from mixing the rejuvenator with RAP material. Meanwhile, the FTIR or storage stability tests were also introduced to directly put the rejuvenator on the surface of aged bitumen and determine the concentration variety of rejuvenator in an aged binder as a function of diffusion time. To observe and predict the diffusion process of rejuvenator in aged bitumen, the two-layer molecular model consisting of pure rejuvenator and aged bitumen layers was established. An MD simulation was run to measure the

diffusion coefficient of rejuvenator molecules derived from the concentration gradient [164].

## 8. Further discussion: Potential connections between nanoscale and macroscale performance

According to previous review points, it has been proved that MD simulation is an effective and powerful tool for multi-scale investigations on various virgin, aged, modified, and rejuvenated bitumen systems. Meanwhile, several essential thermodynamics performance of these bitumen models can be predicted from MD simulations. However, most existing research is merely focused on the nanoscale evaluations or mechanism explanations on bituminous materials using MD simulations, and the potential correlations between the chemical, thermodynamics, and rheological properties of bituminous materials are always ignored. Moreover, it is challenging but valuable to address the practical and engineering problems regarding the performance deterioration of bitumen binder in asphalt pavement during its service life. Besides, the macro-and-microscale evaluation parameters from both experiments and MD simulations, as well as their potential correlations in bulk, dynamic and interfacial systems are remarkably miscellaneous. Herein, the possible connections between diverse nanoscale and macroscale performance are discussed for bulk bitumen systems briefly, which is beneficial in facilitating the multiscale and systematic study on bituminous materials in the future.

**Fig. 25** illustrates the chemo-rheological and thermodynamics parameters of bitumen, which are obtained from the experimental measurements and MD simulations. The involvement of thermodynamics properties predicted from MD simulations significantly improves the completeness of multi-scale characterizations on bituminous materials. Based on the working principles of MD simulation, it is necessary to figure out the molecular structures of research objects, such as the SARA fractions of virgin and aged bitumen, rejuvenators, polymer modifiers, and fillers. Therefore, a series of chemical characterizations are prerequisite before implementing an MD simulation program. To determine the chemical structures of bitumen molecules, the chemical characteristics of SARA fractions, elementary components, average molecular weight, and functional group distribution are always investigated using the chromatographic separation, elemental analysis, GPC, and FTIR tests. If necessary, other chemical characterization methods can be supplemented, such as the NMR, X-ray diffraction (XRD), GC-MS, and Time-of-flight spectrum (TOF) [165,166]. Overall, the chemical characteristics of bitumen are essential for the accuracy of MD simulation outputs. The inaccurate molecular structures of bituminous materials would result in the increment in unreliability of simulation results.

In addition, many previous studies reported that the variations in chemical properties of bitumen distinctly affected its rheological and mechanical performance during the modification, aging, and rejuvenation procedures. Essentially, the change of chemical components of bitumen binders directly influences their thermodynamic properties and viscoelastic behaviors. Therefore, it is possible and important to establish some potential connections between the mechanical performance measured by experimental tests at the macroscale and thermodynamics properties outputted from MD simulations and. Generally, we expect the bitumen to exhibit sufficient resistance to deformation and cracking. To this end, the complex modulus ( $G^*$ ), rutting parameter ( $G^*/\sin\delta$ ), recovery percentage (R%), and non-recovery creep compliance (Jnr) are frequently selected to evaluate the high-temperature properties of bitumen. At the same time, bitumen's low-temperature and fatigue cracking resistance can be estimated with the macroscale indicators of G-R parameter, relaxation time ( $t$ ), and fatigue life ( $N_f$ ). Furthermore, the flow activation energy ( $E_a$ ) derived from a viscosity-temperature correlation formula is associated with the workability of bitumen.

It is of great importance to consider the potential correlations between the microscale parameters from MD simulations with the macroscale high-and-low temperature properties, fatigue life, and

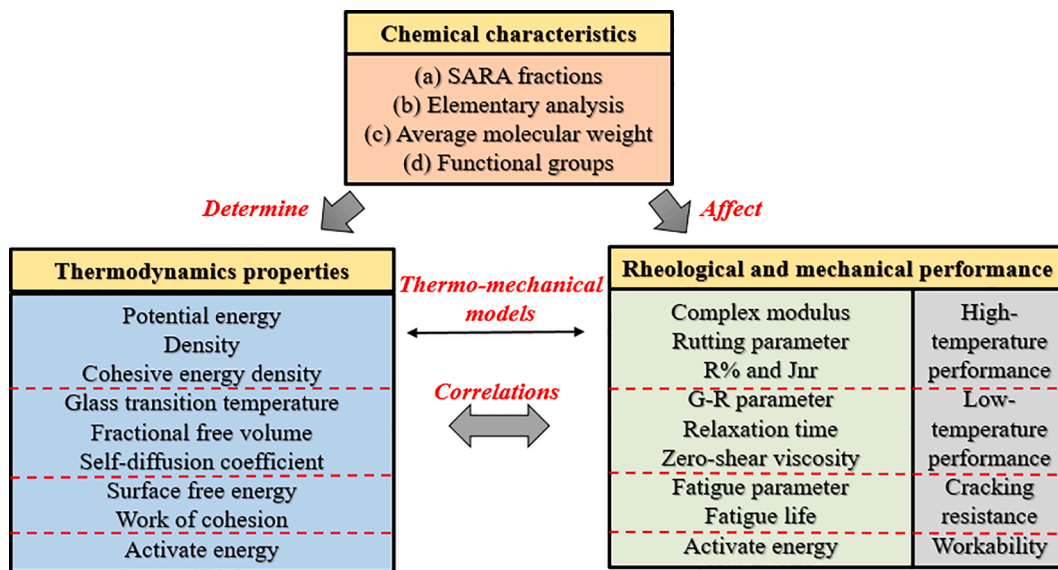


Fig. 25. Potential relationships between chemo-physio-rheological parameters of bitumen.

workability from experiments. Only in this way we can use the MD simulation outcomes to predict the macroscale performance of bituminous materials and enhance the mechanical properties through molecular design and optimization. Fig. 25 also lists the main thermodynamics parameters of bulk bitumen systems from MD simulations, including the potential energy, density, cohesive energy density (CED), glass transition temperature, fractional free volume (FFV), self-diffusion coefficient (D), surface free energy ( $\gamma$ ), work of cohesion (Wc), and activation energy (Ea). Similar to macroscale performance, these thermodynamics parameters are initially divided into high-temperature deformation, low-temperature and fatigue cracking, and workability. It should be mentioned that the potential correlations are determined according to the physical definition of thermodynamic parameters, and these microscale and macroscale properties may be cross-correlated. The possible relationships are discussed in detail as follows:

a. The bitumen model with substantial molecular interactions indicated by higher potential energy, density, and cohesive energy density would exhibit a high stiffness [167]. In the macroscale evaluations, the bitumen stiffness is distinctly correlated with its high-temperature deformation and rutting resistance [168]. There may be potential relevance between these thermodynamic indicators (potential energy, density, and cohesive energy density) and macroscopic high-temperature properties ( $G^*$ ,  $G^*/\sin\delta$ , R%, and Jnr);

b. Regarding the low-temperature shrink and fatigue cracking resistance of bitumen, the rheological indices of G-R parameter, relaxation time ( $t$ ), fatigue factor ( $G^*\sin\delta$ ), and fatigue life ( $N_f$ ) are universally characterized. On the one hand, the cracking possibility of bituminous material is strongly related to both molecular flexibility and free volume fraction, which instantly accelerates the relaxation and stress release of bitumen molecules. From a nanoscale perspective, the molecular flexibility could be estimated with the thermodynamics parameters of glass transition temperature ( $T_g$ ), fractional free volume (FFV), and self-diffusion coefficient (D). In general, the bitumen system with a lower  $T_g$ , higher FFV, and D value would exhibit a higher flexibility. On the other hand, the interfacial chemistry theory proposed the energy-based parameters (surface free energy and work of cohesion) to assess the cracking potential of simulated systems. The bitumen binder with lower  $\gamma$  and Wc values would display a higher cracking risk.

c. The temperature sensitivity of macroscale properties (i.e., viscosity and modulus) can be estimated with the activation energy (Ea) parameter. Similarly, the Ea parameter can be derived from the correlation equations between the temperature and microscale indicators

(diffusion coefficient, thermal expansion coefficient, modulus, or viscosity) from MD simulations.

Herein, the potential relationships between the micro-and-macroscopic performance of bituminous materials are discussed for the first time. Moreover, the idea that the combination of molecular dynamics simulation and experimental methods is recommended to comprehensively multiscale evaluate the rutting, cracking, and fatigue resistance of bituminous materials. However, there are still research gaps and challenges regarding the correlations between MD simulation outputs and experimental results, and some of them are listed as follows:

- The above-discussed potential correlations between microscale and macroscopic parameters should be further validated and strengthened based on future simulation and experimental results;
- More useful parameters from MD simulations and the corresponding potential correlations will be developed, including the statistics (potential energy, pressure, temperature, and solubility parameter), dynamic (mean square displacement (MSD), diffusion coefficient (D), and isothermal compressibility ( $\beta$ )), and structural properties (radius distance function (RDF), the radius of gyration ( $R_g$ ) and relative concentration (RC) analysis);
- This review paper only discussed the potential connections between micro-and-macroscales indicators of bulk bitumen systems. It is important and meaningful to further explore the possible relationships between thermodynamics parameters from MD simulations and macroscopic performance in terms of both dynamics (diffusion and self-healing) [169] and interfacial systems (adhesion and moisture damage) [170] of bituminous materials.

## 9. Conclusions and recommendations

### 9.1. Main conclusions

This review summarizes the application cases regarding the molecular dynamics (MD) simulation method in the field of different virgin, aged, modified, and rejuvenated bitumen systems. It enables researchers to comprehensively understand the main functions of MD simulations on bituminous materials and further develop its potential values in addressing the research issues of asphalt pavement materials. Some main conclusions are listed as follows:

(1) Different molecular models of bitumen have been proposed, including the average, 3-component, 4-component, 6-component, and 12-component molecular models. Nowadays, the 12-component model is the most popular because of the high accuracy. Nevertheless, more accurate molecular models of bitumen with different chemical components from variable sources should be further developed to improve the reasonability of MD simulation outputs.

(2) Although different forcefields have been employed in MD simulation investigations of bituminous materials, the COMPASS (II) forcefield is the most commonly-used. Moreover, the general parameters for model validation contain the density, glass transition temperature, cohesive energy density, and solubility parameter.

(3) From the MD simulations, various thermo-physical, thermo-dynamics, thermo-mechanical, and structural parameters of bulk bitumen systems at the atomic scale could be predicted, which is extremely difficult to be obtained from the macroscale experimental characterizations.

(4) MD simulation is an effective tool to explore the influence of aging, modification, and rejuvenation on the molecular-scale properties of bituminous materials, and explain the underlying mechanisms from the viewpoints of intermolecular interaction, molecular structure, and molecular mobility. In addition, the oxidative paths and products of bitumen molecules can be predicted from MD simulations with a specific reaction forcefield. However, it is still necessary to optimize the molecular structures of aged bitumen, polymers (SBS, SBR, CR), fillers, bio-oil, and rejuvenators to enlarge the reliability of MD simulation outputs.

(5) There may be some potential relationships between these nanoscale parameters of bulk bitumen systems outputted from MD simulations and the mechanical performance from macroscale experimental measurements. In the future, more efforts should be made to establish the connection bridge at different scales, which is essential to develop an integral multiscale evaluation method from the molecular design, performance prediction, and model validation to material optimization and synthesis of bituminous materials without lots of experimental attempts.

## 9.2. Recommendations for future works

- The molecular models of virgin and aged bitumen, modifiers, and rejuvenators should be further optimized to strengthen the accuracy of MD simulation results. Before implementing MD simulations, a series of chemical characterizations on bituminous materials are necessary rather than randomly choosing the standard model from previous studies. Although the molecular structures of bitumen strongly depend on the material type and resource, the relevant standards and recommendations for chemical characterization methods of bituminous materials can be discussed and formulated.
- More works should be made to exploit and optimize the setting parameters of MD simulations on bituminous materials, including the forcefield, ensemble, thermostat (temperature control), barostat (pressure control), time step, and simulation time.
- Although these basic parameters of density, glass transition temperature, and solubility parameter could be used to validate the reliability of MD simulation outcomes, more key indicators should be measured and compared to further ensure the reasonability of both molecular models and MD simulation settings.
- The long-term aging reaction mechanism on the molecular structure variation of various bitumen molecules should be explored, which is beneficial to establishing the molecular model of aged bitumen and designing the more efficacious rejuvenators for reclaimed asphalt pavement.
- The MD simulation will be further developed and employed in investigating the modification and rejuvenation mechanisms of multi-component bitumen systems at an atomic level.
- The potential connections between these outputted parameters from MD simulations and macroscale properties measured from experiments should be further explored with data analysis tools, and thus

MD simulation will play an essential role in predicting the rheological and mechanical properties of bituminous materials without performing laboratory tests.

## Declaration of Competing Interest

The authors declare that they have no known competing financial interests or personal relationships that could have appeared to influence the work reported in this paper.

## Data availability

Data will be made available on request.

## Acknowledgements

The first author would thank China Scholarship Council for the funding support (CSC, No., CSC201901530025). Meanwhile, the corresponding author would thank the European Union's Horizon 2020 Research and Innovation Programme under the Marie Skłodowska-Curie grant agreement (No.101030767).

## References

- [1] Rocha Segundo I, Freitas E, Castelo Branco VTF, Landi Jr S, Costa MF, Carneiro JO. Review and analysis of advances in functionalized, smart, and multifunctional asphalt mixtures. *Renew Sustain Energy Rev* 2021;151:111552.
- [2] Capitao SD, Picado-Santos LG, Martinho F. Pavement engineering materials: Review on the use of warm-mix asphalt. *Constr Build Mater* 2012;36:1016–24.
- [3] Xu X, Luo Y, Sreeram A, Wu Q, Chen G, Cheng S, et al. Potential use of recycled concrete aggregate (RCA) for sustainable asphalt pavements of the future: A state-of-the-art review. *J Cleaner Prod* 2022;344:130893.
- [4] Polacco G, Filippi S, Merusi F, Stastna G. A review of the fundamentals of polymer-modified asphalts: Asphalt/polymer interactions and principles of compatibility. *Adv Colloid Interface Sci* 2015;224:72–112.
- [5] Choudhary J, Kumar B, Gupta A. Utilization of solid waste materials as alternative fillers in asphalt mixes: A review. *Constr Build Mater* 2020;234:117271.
- [6] Al-Sabaei AM, Napiah MB, Sutanto MH, Alalouf WS, Usman A. A systematic review of bio-asphalt for flexible pavement applications: coherent taxonomy, motivations, challenges and future directions. *J Cleaner Prod* 2020;249:119357.
- [7] Cheraghian G, Falchetto AC, You Z, Chen S, Kim YS, Westerhoff J, et al. Warm mix asphalt technology: An up to date review. *J Cleaner Prod* 2020;268:122128.
- [8] Zhang K, Huchet F, Hobbs A. A review of thermal processes in the production and their influences on performance of asphalt mixtures with reclaimed asphalt pavement (RAP). *Constr Build Mater* 2019;206:609–19.
- [9] Moghaddam TB, Baaj H. The use of rejuvenating agents in production of recycled hot mix asphalt: A systematic review. *Constr Build Mater* 2016;114:805–16.
- [10] Du Y, Chen J, Han Z, Liu W. A review on solutions for improving rutting resistance of asphalt pavement and test methods. *Constr Build Mater* 2018;168:893–905.
- [11] G., White.. State of the art: Asphalt for airport pavement surfacing. *Int J Pavement Res Technol* 2018;11(1):77–98.
- [12] Hajj R, Bhasin A. The search for a measure of fatigue cracking in asphalt binders – a review of different approaches. *Int J Pavement Eng* 2018;19(3):205–19.
- [13] Kogbara RB, Masad EA, Kassem E, Scarpa A, Anupam K. A state-of-the-art review of parameters influencing measurement and modeling of skid resistance of asphalt pavements. *Constr Build Mater* 2016;114:602–17.
- [14] Wang W, Wang L, Xiong H, Luo R. A review and perspective for research on moisture damage in asphalt pavement induced by dynamic pore water pressure 2019;204:631–42.
- [15] Morian N, Hajj EY, Glover CJ, Sebaaly PE. Oxidative aging of asphalt binders in hot-mix asphalt mixtures. *Transportation Research Record: Journal of the Transportation Research Board* 2011;2207:107–16.
- [16] Ding H, Zhang H, Liu H, Qiu Y. Thermoreversible aging in model asphalt binders. *Constr Build Mater* 2021;303:124355.
- [17] Jamieson S, White G. Review of stone mastic asphalt as a high-performance ungrooved runway surfacing. *Road Materials and Pavement Design* 2020;21(4):886–905.
- [18] Habbouche J, Hajj EY, Sebaaly PE, Piratheepan M. A critical review of high polymer-modified asphalt binders and mixtures. *Int J Pavement Eng* 2020;21(6):686–702.
- [19] Pan P, Wu S, Xiao F, Pang L, Xiao Y. Conductive asphalt concrete: A review on structure design, performance, and practical applications. *J Intell Mater Syst Struct* 2015;26(7):755–69.
- [20] Wu W, Jiang W, Yuan D, Lu R, Shan J, Xiao J, et al. A review of asphalt-filler interaction factors. *Constr Build Mater* 2021;299:124279.

- [21] Chen M, Geng J, Xia C, He L, Liu Z. A review of phases structure of SBS modified asphalt: Affecting factors, analytical methods, phase models and improvements. *Constr Build Mater* 2021;294:123610.
- [22] Liu S, Shukla A, Nandra T. Technological, environmental and economic aspects of asphalt recycling for road construction. *Renew Sustain Energy Rev* 2017;75: 879–93.
- [23] Wang S, Cheng D, Xiao F. Recent developments in the application of chemical approaches to rubberized asphalt. *Constr Build Mater* 2017;131:101–13.
- [24] Siebri-Acevedo C, Lastra-Gonzalez P, Pascual-Munoz P, Castro-Fresno D. Mechanical performance of fibers in hot mix asphalt: A review. *Constr Build Mater* 2019;200:756–69.
- [25] Yu X, Burnham NA, Tao M. Surface microstructure of bitumen characterized by atomic force microscopy. *Adv Colloid Interface Sci* 2015;218:17–33.
- [26] Tauste R, Moreno-Navarro F, Sol-Sanchez M, Rubio-Gamez MC. Understanding the bitumen ageing phenomenon: A review. *Constr Build Mater* 2018;192: 593–609.
- [27] Zhu J, Birgisson B, Kringsos N. Polymer modification of bitumen: Advances and challenges. *Eur Polym J* 2014;54:18–38.
- [28] A. Abouelsaad, G. White. Review of asphalt mixture raveling mechanisms, causes and testing. *International Journal of Pavement Research and Technology*. <https://doi.org/10.1007/s42947-021-00100-7>.
- [29] Xu S, Garcia A, Su J, Liu Q, Tabakovic A, Schlangen E. Self-healing asphalt review: from idea to practice. *Adv Mater Interfaces* 2018;5:1800536.
- [30] Behnood A. Application of rejuvenators to improve the rheological and mechanical properties of asphalt binders and mixtures: A review. *J Cleaner Prod* 2019;231:171–82.
- [31] Hu D, Gu X, Cui B, Pei J, Zhang Q. Modeling the oxidative aging kinetics and pathways of asphalt: a ReaxFF molecular dynamics study. *Energy Fuels* 2020;34: 3601–13.
- [32] Feng Y, Yu C, Hu K, Chen Y, Liu Y, Zhang T. A study of the microscopic interaction mechanism of styrene-butadiene-styrene modified asphalt based on density functional theory. *Mol Simul* 2021. <https://doi.org/10.1080/08927022.2021.1876874>.
- [33] Qu X, Liu Q, Guo M, Wang D, Oeser M. Study on the effect of aging on physical properties of asphalt binder from a microscale perspective. *Constr Build Mater* 2018;187:718–29.
- [34] Zheng C, Shan C, Liu J, Zhang T, Yang X, Lv D. Microscopic adhesion properties of asphalt-mineral aggregate interface in cold area based on molecular simulation technology. *Constr Build Mater* 2021;121151.
- [35] Ma L, Vareri A, Jing R, Erkens S. Comprehensive review on the transport and reaction of oxygen and moisture towards coupled oxidative ageing and moisture damage of bitumen. *Constr Build Mater* 2021;283:122632.
- [36] He L, Zhang Y, Alexiadis A, Falchetto AC, Li G, Valentini J, et al. Research on the self-healing behavior of asphalt mixed with healing agents on molecular dynamics method. *Constr Build Mater* 2021;295:123430.
- [37] Xu G, Wang H. Diffusion and interaction mechanism of rejuvenating agent with virgin and recycled asphalt binder: a molecular dynamics study. *Mol Simul* 2018; 44(17):1433–43.
- [38] Bao C, Xu Y, Zheng C, Nie L, Yang X. Rejuvenation effect evaluation and mechanism analysis of rejuvenators on aged asphalt using molecular simulation. *Mater Struct* 2022;55:52.
- [39] Ren S, Liu X, Lin P, Erkens S, Xiao Y. Chemo-physical characterization and molecular dynamics simulation of long-term aging behaviors of bitumen. *Constr Build Mater* 2021;302:124437.
- [40] T. Yu, H. Zhang, J. Sun, D. Chen, H. Wang, Y. Feng. Influence of freezing and thawing on drainage behaviour for porous asphalt pavement based on molecular dynamics simulation. *International Journal of Pavement Engineering*. <https://doi.org/10.1080/10298436.2021.1984476>.
- [41] Gao Y, Zhang Y, Yang Y, Zhang J, Gu F. Molecular dynamics investigation of interfacial adhesion between oxidised bitumen and mineral surfaces. *Appl Surf Sci* 2019;479:449–62.
- [42] Zhang L, Greenfield ML. Analyzing properties of model asphalts using molecular simulation. *Energy Fuels* 2007;21:1712–6.
- [43] Pan T, Lu Y, Wang Z. Development of an atomistic-based chemophysical environment for modelling asphalt oxidation. *Polym Degrad Stab* 2012;97: 2331–9.
- [44] S. Liu, X. Qi, L. Shan. Effect of molecular structure on low-temperature properties of bitumen based on molecular dynamics. *Construction and Building Materials*.
- [45] Wang P, Dong Z, Tan Y, Liu Z. Investigation the interactions of the saturate, aromatic, resin, and asphaltene four fractions in asphalt binders by molecular simulations. *Energy Fuels* 2015;29:112–21.
- [46] Guo M, Huang Y, Wang L, Yu J, Hou Y. Using atomic force microscopy and molecular dynamics simulation to investigate the asphalt micro properties. *Int J Pavement Res Technol* 2018;11:321–6.
- [47] Yildirim Y. Polymer modified asphalt binders. *Constr Build Mater* 2007;21(1): 66–72.
- [48] Kheradmand B, Muniandy R, Hua LT, Yunus RB, Solouki A. An overview of the emerging warm mix asphalt technology. *Int J Pavement Eng* 2014;15(1):79–94.
- [49] Zaumanis M, Mallicks RB, Frank R. Determining optimum rejuvenator dose for asphalt recycling based on Superpave performance grade specifications. *Constr Build Mater* 2014;69:159–66.
- [50] Chen Z, Pei J, Li R, Xiao F. Performance characteristics of asphalt materials based on molecular dynamics simulation-A review. *Constr Build Mater* 2018;189: 695–710.
- [51] Zhu L, Chen X, Shi R, Zhang H, Han R, Cheng X, et al. Tetraphenylphenyl-modified damping additives for silicone rubber: Experimental and molecular simulation investigation. *Mater Des* 2021;202:109551.
- [52] Yao H, Liu J, Xu M, Ji J, Dai Q, You Z. Discussion on molecular dynamics (MD) simulations of the asphalt materials. *Adv Colloid Interface Sci* 2021. <https://doi.org/10.1016/j.cis.2021.102565>.
- [53] Guo M, Liang M, Fu Y, Seeram A, Bhasin A. Average molecular structure models of unaged asphalt binder fractions. *Mater Struct* 2021;54:173.
- [54] Tian Y, Zheng M, Liu Y, Zhang J, Ma S, Jin J. Analysis of behavior and mechanism of repairing agent of microcapsule in asphalt micro crack based on molecular dynamics simulation. *Constr Build Mater* 2021;305:124791.
- [55] Li M, Min Z, Wang Q, Huang W, Shi Z. Effect of epoxy resin content and conversion rate on the compatibility and component distribution of epoxy asphalt: A MD simulation study. *Constr Build Mater* 2022;319:126050.
- [56] Lu P, Huang S, Shen Y, Zhou C, Shao L. Mechanical performance analysis of polyurethane-modified asphalt using molecular dynamics method. *Polym Eng Sci* 2021;61:2323–38.
- [57] Wu M, Xu G, Luan Y, Zhu Y, Ma T, Zhang W. Molecular dynamics simulation on cohesion and adhesion properties of the emulsified cold recycled mixtures. *Constr Build Mater* 2022;333:127403.
- [58] Hu D, Gu X, Dong Q, Lyu L, Cui B, Pei J. Investigating the bio-rejuvenator effects on aged asphalt through exploring molecular evolution and chemical transformation of asphalt components during oxidative aging and regeneration. *J Cleaner Prod* 2021;329:129711.
- [59] Yu C, Hu K, Yang Q, Chen Y. Multi-scale observation of oxidative aging on the enhancement of high-temperature property of SBS-modified asphalt. *Constr Build Mater* 2021;313:125478.
- [60] Su M, Zhou J, Lu J, Chen W, Zhang H. Using molecular dynamics and experiments to investigate the morphology and micro-structure of SBS modified asphalt binder. *Materials Toady Communications* 2022;30:103082.
- [61] Li H, Chen P, Wang H, Luo X, Zhang Y. Pseudo energy-based crack initiation criterion for asphalt-filler composite system under a fatigue shear load. *Theor Appl Fract Mech* 2022;119:103333.
- [62] Shan K, Bao C, Li D, Zheng C. Microscopic analysis of the rejuvenation mechanism and rejuvenation effect of asphalt binders. *Adv Mater Sci Eng* 2021;1958968.
- [63] Gao Y, Zhang Y, Zhang C, Liu X, Jing R. Quantifying oxygen diffusion in bitumen films using molecular dynamics simulations. *Constr Build Mater* 2022;331: 127325.
- [64] Qiu Q, Zhang J, Yang L, Zhang J, Chen B, Tang C. Simulation of the diffusion behavior of water molecules in palm oil and mineral oil at different temperatures. *Renewable Energy* 2021;174:909–17.
- [65] Sun W, Wang H. Molecular dynamics simulation of diffusion coefficients between different types of rejuvenator and aged asphalt binder. *Int J Pavement Eng* 2020; 21(8):966–76.
- [66] Sun D, Lin T, Zhu X, Tian Y, Liu F. Indices for self-healing performance assessments based on molecular dynamics simulation of asphalt binders. *Comput Mater Sci* 2016;114:86–93.
- [67] Cui W, Huang W, Hassan HMZ, Cai X, Wu K. Study on the interfacial contact behavior of carbon nanotubes and asphalt binders and adhesion energy of modified asphalt on aggregate surface by using molecular dynamics simulation. *Constr Build Mater* 2022;316:125849.
- [68] Wang J, Bai Y, Sui H, Li X, He L. Understanding the effects of salinity on bitumen-calcite interactions. *Fuel Process Technol* 2021;213:106668.
- [69] Long Z, Tang X, Ding Y, Miljkovic M, Khanal A, Ma W, et al. Influence of sea salt on the interfacial adhesion of bitumen-aggregate systems by molecular dynamics simulation. *Constr Build Mater* 2022;336:127471.
- [70] Hansson T, Oostenbrink C, Gunsteren W. Molecular dynamics simulations. *Curr Opin Struct Biol* 2002;12(2):190–6.
- [71] Hollingsworth S, Dror R. Molecular dynamics simulation for all. *Neuron* 2018;99 (6):1129–43.
- [72] Zhang L, Greenfield ML. Molecular orientation in model asphalts using molecular simulation. *Energy Fuels* 2017;21:1102–11.
- [73] Fallah F, Khabaz F, Kim YR, Kommidi SR, Haghshenas HF. Molecular dynamics modeling and simulation of bituminous binder chemical aging due to variation of oxidation level and saturate-aromatic-resin-asphaltene fraction. *Fuel* 2019;237: 731–80.
- [74] Huang M, Zhang H, Gao Y, Wang L. Study of diffusion characteristics of asphalt-aggregate interface with molecular dynamics simulation. *Int J Pavement Eng* 2021;22(3):319–30.
- [75] Jennings PW, Pribanic JAS, Desando MA, Raub MF, Frederick S, Hoberg J. Binder characterization and evaluation by nuclear magnetic resonance spectroscopy. *Report* 1993.
- [76] Pauli AT, Miknis FP, Beemer AG, Miller JJ. Assessment of physical property prediction based on asphalt average molecular structures. *Preprints-American Chemistry Society Division Petroleum Chemistry* 2005;50:255–9.
- [77] Zhang L, Greenfield ML. Effects of polymer modification on properties and microstructure of model asphalt systems. *Energy & Fuel* 2008;22:3363–75.
- [78] Ding Y, Huang B, Shu X. Investigation of functional group distribution of asphalt using liquid chromatography transform and prediction of molecular model. *Fuel* 2018;227:300–6.
- [79] Yu X, Wang J, Si J, Mei J, Ding G, Li J. Research on compatibility mechanism of biobased cold-mixed epoxy asphalt binder. *Constr Build Mater* 2020;250:118868.
- [80] Yao H, Dai Q, You Z. Molecular dynamics simulation of physicochemical properties of the asphalt model 2016;164:83–93.

- [81] Wang L, Liu Y, Zhang L. Micro/nanoscale study on the effect of aging on the performance of crumb rubber modified asphalt. *Mathematical Problems in Engineering* 2020;1924349.
- [82] Yu T, Zhang H, Wang Y. Multi-gradient analysis of temperature self-healing of asphalt nano-cracks based on molecular simulation. *Constr Build Mater* 2020; 250:118859.
- [83] Zhang M, Hao P, Li Y. Interfacial adhesive property in "asphalt mixture-PMA copolymer-steel plate" system: Experimental and molecular dynamics simulation. *Constr Build Mater* 2021;281:122529.
- [84] Chu L, Luo L, Fwa TF. Effects of aggregate mineral surface anisotropy on asphalt-aggregate interfacial bonding using molecular dynamics (MD) simulation. *Constr Build Mater* 2019;225:1–12.
- [85] Guo M, Tan Y, Wang L, Hou Y. Diffusion of asphaltene, resin, aromatic and saturate components of asphalt on mineral aggregates surface: molecular dynamics simulation. *Road Materials and Pavement Design* 2017;18(3):149–58.
- [86] Hu K, Yu C, Yang Q, Chen Y, Chen G, Ma R. Multi-scale enhancement mechanisms of graphene oxide on styrene-butadiene-styrene modified asphalt: An exploration from molecular dynamics simulations. *Mater Des* 2021;208:109901.
- [87] Zhou X, Zhang X, Xu S, Wu S, Liu Q, Fan Z. Evaluation of thermo-mechanical properties of graphene/carbon-nanotubes modified asphalt with molecular simulation. *Mol Simul* 2017;43(4):312–9.
- [88] Shu B, Zhou M, Yang T, Li Y, Ma Y, Liu K, et al. The properties of different healing agents considering the micro-self-healing process of asphalt with encapsulations. *Materials* 2021;14:16.
- [89] Xiao Y, Li C, Wan M, Zhou X, Wang Y, Wu S. Study of the diffusion of rejuvenators and its effect on aged bitumen binder. *Applied Sciences* 2017;7:397.
- [90] Yang T, Chen M, Zhou X, Xie J. Evaluation of thermal-mechanical properties of bio-oil regenerated aged asphalt. *Materials* 2018;11:2224.
- [91] Zhang X, Zhou X, Ji W, Zhang F, Otto F. Characterizing the mechanical properties of Multi-layered CNTs reinforced SBS modified asphalt-binder. *Constr Build Mater* 2021;296:123658.
- [92] Zeng Y, Liu Q, Zeng Q, He Y, Xu Z. Research on the mechanism of interaction between styrene-butadiene-styrene (SBS) and asphalt based on molecular vibration frequency. *Materials* 2021;14:358.
- [93] Ramezani MG, Rickgauer J. Understanding the adhesion properties of carbon nanotube, asphalt binder, and mineral aggregates at the nanoscale: a molecular dynamics study. *Pet Sci Technol* 2020;38(1):28–35.
- [94] Li DD, Greenfield ML. Chemical compositions of improved model asphalt systems for molecular simulations. *Fuel* 2014;115:347–56.
- [95] Qu X, Fan Z, Li T, Hong B, Zhang Y, Wei J, et al. Understanding of asphalt chemistry based on the six-fraction method. *Constr Build Mater* 2021;311: 125241.
- [96] Li DD, Greenfield ML. Viscosity, relaxation time, and dynamics within a model asphalt of larger molecules. *J Chem Phys* 2014;140:034507.
- [97] Mullins OC. The modified Yen model. *Energy Fuels* 2010;24:2179–207.
- [98] Mullins OC, Sabbah H, Eyssaoutier J, Pomerantz AE, Barre L, Andrews AB, et al. Advances in asphaltene science and the Yen-Mullins model. *Energy Fuels* 2012; 26:3986–4003.
- [99] Xu M, Yi J, Qi P, Wang H, Marasteanu M, Feng D. Improved chemical system for molecular simulations of asphalt. *Energy Fuels* 2019;33:3187–98.
- [100] Sonibare K, Rathnayaka L, Zhang L. Comparison of CHARMM and OPLS-aa forcefield predictions for components in one model asphalt mixture. *Constr Build Mater* 2020;236:117577.
- [101] Zhang L, Greenfield ML. Rotational relaxation times of individual compounds within simulations of molecular asphalt models. *J Chem Phys* 2010;132:184502.
- [102] Sonibare K, Rucker G, Zhang L. Molecular dynamics simulation on vegetable oil modified model asphalt. *Constr Build Mater* 2021;270:121687.
- [103] Xu G, Wang H. Molecular dynamics study of oxidative aging effect on asphalt binder properties. *Fuel* 2017;188:1–10.
- [104] Li G, Han M, Tan Y, Meng A, Li J, Li S. Research on bitumen molecule aggregation based on coarse-grained molecular dynamics. *Constr Build Mater* 2020;263: 120933.
- [105] Kang Y, Zhou D, Wu Q, Liang R, Shangguan S, Liao Z, et al. Molecular dynamics study on the glass forming process of asphalt. *Constr Build Mater* 2019;214: 430–40.
- [106] Hou Y, Wang L, Wang D, Guo M, Liu P, Xu J. Characterization of bitumen micro-mechanical behaviors using AFM, phase dynamics theory and MD simulation. *Materials* 2017;10:208.
- [107] Luo L, Chu L, Fwa TF. Molecular dynamics analysis of oxidative aging effects on thermodynamic and interfacial bonding properties of asphalt mixtures. *Constr Build Mater* 2021;269:121299.
- [108] Liu Q, Wu J, Xie L, Zhang Z, Ma X, Oeser M. Micro-scale investigation of aging gradient within bitumen film around air-binder interface. *Fuel* 2021;286:119404.
- [109] Sun B, Zhou X. Diffusion and rheological properties of asphalt modified by bio-oil regenerator derived from waste wood. *J Mater Civ Eng* 2018;30(2):04017274.
- [110] Qu X, Liu Q, Wang C, Wang D, Oeser M. Effect of co-production of renewable biomaterials on the performance of asphalt binder in macro and micro perspectives. *Materials* 2018;11:244.
- [111] Qu X, Wang D, Hou Y, Oeser M, Wang L. Influence of paraffin on the microproperties of asphalt binder using MD simulation. *J Mater Civ Eng* 2018;30(8):04018191.
- [112] Ding G, Yu X, Si J, Mei J, Wang J, Chen B. Influence of epoxy soybean oil modified nano-silica on the compatibility of cold-mixed epoxy asphalt. *Mater Struct* 2021; 54:16.
- [113] Su M, Si C, Zhang Z, Zhang H. Molecular dynamics study on influence of Nano-ZnO/SBS on physical properties and molecular structure of asphalt binder. *Fuel* 2020;263:116777.
- [114] Wang P, Zhai F, Dong Z, Wang L, Liao J, Li G. Micromorphology of asphalt modified by polymer and carbon nanotubes through molecular dynamics simulation and experiments: role of strengthened interfacial interactions. *Energy Fuels* 2018;32:1179–87.
- [115] Long Z, You L, Tang X, Ma W, Ding Y, Xu F. Analysis of interfacial adhesion properties of nano-silica modified asphalt mixtures using molecular dynamics simulation. *Constr Build Mater* 2020;255:119354.
- [116] Zhu X, Du Z, Ling H, Chen L, Wang Y. Effect of filler on thermodynamic and mechanical behaviour of asphalt mastic: a MD simulation study. *Int J Pavement Eng* 2020;21(10):1248–62.
- [117] Cao X, Deng M, Ding Y, Tang B, Yang X, Shan B, et al. Effect of photocatalysts modification on asphalt: investigations by experiments and theoretical calculation. *J Mater Civ Eng* 2021;33(5):04021083.
- [118] Li F, Yang Y. Understanding the temperature and loading frequency effects on physicochemical interaction ability between mineral filler and asphalt binder using molecular dynamic simulation and rheological experiments. *Constr Build Mater* 2020;244:118311.
- [119] Ren S, Liu X, Zhang Y, Lin P, Apostolidis P, Erkens S, et al. Multi-scale characterization of lignin modified bitumen using experimental and molecular dynamics simulation methods. *Constr Build Mater* 2021;287:123058.
- [120] Long Z, Zhou S, Jiang S, Ma W, Ding Y, You L, et al. Revealing compatibility mechanism of nanosilica in asphalt through molecular dynamics simulation. *J Mol Model* 2021;27:81.
- [121] Hu D, Pei J, Li R, Zhang J, Jia Y, Fan Z. Using thermodynamic parameters to study self-healing and interface properties of crumb rubber modified asphalt based on molecular dynamics simulation. *Front Struct Civ Eng* 2020;14(1):109–22.
- [122] Guo F, Zhang J, Pei J, Ma W, Hu Z, Guan Y. Evaluation of the compatibility between rubber and asphalt based on molecular dynamics simulation. *Front Struct Civ Eng* 2020;14(2):425–45.
- [123] Guo F, Zhang J, Pei J, Zhou B, Hu Z. Study on the mechanical properties of rubber asphalt by molecular dynamics simulation. *J Mol Model* 2019;25:365.
- [124] Cui B, Gu X, Hu D, Dong Q. A multiphysics evaluation of the rejuvenator effects on aged asphalt using molecular dynamics simulations. *J Cleaner Prod* 2020;259: 120629.
- [125] Xu M, Yi J, Feng D, Huang Y. Diffusion characteristics of asphalt rejuvenators based on molecular dynamics simulation. *Int J Pavement Eng* 2019;20(5):615–27.
- [126] Bao C, Zheng C, Xu Y, Nie L, Luo H. Microscopic analysis of the evolution of asphalt colloidal properties and rejuvenation behavior in aged asphalt. *J Cleaner Prod* 2022;339:130761.
- [127] Jiao B, Pan B, Che T. Evaluating impacts of desulfurization and depolymerization on thermodynamics properties of crumb rubber modified asphalt through molecular dynamics simulation. *Constr Build Mater* 2022;333:126360.
- [128] Luo H, Zheng C, Liu B, Bao C, Tian B, Liu W. Study on SBS modifier of bio-oil/sulfur compound under dry modification mode. *Constr Build Mater* 2022;326: 127059.
- [129] Zhang X, Zhou X, Chen L, Lu F, Zhang F. Effects of poly-sulfide regenerant on the rejuvenated performance of SBS modified asphalt-binder. *Mol Simul* 2021;47(17): 1423–32.
- [130] Li L, Li H, Tan Y, Yang X, Xu H. Investigation of chloride release characteristic of chlorine-based anti-icing asphalt mixture. *Constr Build Mater* 2021;312:125410.
- [131] Hu K, Yu C, Yang Q, Li Z, Zhang W, Zhang T, et al. Mechanistic study of graphene reinforcement of rheological performance of recycled polyethylene modified asphalt: A new observation from molecular dynamics simulation. *Constr Build Mater* 2022;320:126263.
- [132] Xiao MM, Fan L. Ultraviolet aging mechanism of asphalt molecular based on microscopic simulation. *Constr Build Mater* 2022;319:126157.
- [133] Luo H, Zheng C, Yang X, Bao C, Liu W, Lin Z. Development of technology to accelerate SBS-modified asphalts swelling in dry modification mode. *Constr Build Mater* 2022;314:125703.
- [134] Yu C, Hu K, Chen Y, Zhang W, Chen Y, Chang R. Compatibility and high temperature performance of recycled polyethylene modified asphalt using molecular simulations. *Mol Simul* 2021;47(13):1037–49.
- [135] Xu J, Fan Z, Lin J, Liu P, Wang D, Oeser M. Study on the effects of reversible aging on the low temperature performance of asphalt binders. *Constr Build Mater* 2021; 295:123604.
- [136] Hu C, You G, Liu J, Du S, Zhao X, Wu S. Study on the mechanisms of the lubricating oil antioxidants: Experimental and molecular simulation. *J Mol Liq* 2021;324:115099.
- [137] Chen W, Chen S, Zheng C. Analysis of micromechanical properties of algae bio-based bio-asphalt-mineral interface based on molecular simulation technology. *Constr Build Mater* 2021;306:124888.
- [138] Yao H, Dai Q, You Z, Bick A, Wang M, Guo S. Property analysis of exfoliated graphite nanoplatelets modified asphalt model using molecular dynamics (MD) method. *Applied Sciences* 2017;7:43.
- [139] Yao H, Dai Q, You Z, Zhang J, Lv S, Xiao X. Evaluation of contact angle between asphalt binders and aggregates using molecular dynamics (MD) method. *Constr Build Mater* 2019;212:727–36.
- [140] You L, Spyriouni T, Dai Q, You Z, Khanal A. Experimental and molecular dynamics simulation study on thermal, transport, and rheological properties of asphalt. *Constr Build Mater* 2020;265:120358.
- [141] Guo F, Zhang J, Pei J, Zhou B, Falchetto AC, Hu Z. Investigating the interaction behavior between asphalt binder and rubber in rubber asphalt by molecular dynamics simulation. *Constr Build Mater* 2020;252:118956.

- [142] Khabaz F, Khare R. Molecular simulations of asphalt rheology: application of time-temperature superposition principle. *J Rheol* 2018;62:941.
- [143] Khabaz F, Khare R. Glass transition and molecular mobility in styrene-butadiene rubber modified asphalt. *J Phys Chem B* 2015;119:14261–9.
- [144] Nie F, Jian W, Lau D. An atomistic study on the thermomechanical properties of graphene and functionalized graphene sheets modified asphalt. *Carbon* 2021;182:615–27.
- [145] Pan T, Lu Y, Lloyd S. Quantum-chemistry study of asphalt oxidative aging: an XPS-aided analysis. *Ind Eng Chem Res* 2012;51:7957–66.
- [146] Yang Y, Wang Y, Cao J, Xu Z, Li Y, Liu Y. Reactive molecular dynamic investigation of the oxidative aging impact on asphalt. *Constr Build Mater* 2021;279:121298.
- [147] Pan J, Tarefder RA. Investigation of asphalt aging behaviour due to oxidation using molecular dynamics simulation. *Mol Simul* 2016;42(8):667–78.
- [148] Tarefder RA, Arisa I. Molecular dynamic simulations for determining change in thermodynamic properties of asphaltene and resin because of aging. *Energy Fuels* 2011;25:2211–22.
- [149] Pan J, Hossain MI, Tarefder RA. Temperature and moisture impacts on asphalt before and after oxidative aging using molecular dynamics simulations. *J Nanomech Micromech* 2017;7(4):04017018.
- [150] Zhao Z, Wu S, Zhou X, Liu G, Zheng J. Molecular simulations of properties changes on nano-layered double hydroxides-modified bitumen. *Mater Res Innovations* 2015;19(8):556–60.
- [151] Ding Y, Tang B, Zhang Y, Wei J, Cao X. Molecular dynamics simulation to investigate the influence of SBS on molecular agglomeration behavior of asphalt. *J Mater Civ Eng* 2015;27(8):C4014004.
- [152] Ding Y, Huang B, Shu X. Modeling shear viscosity of asphalt through nonequilibrium molecular dynamics simulation. *Transp Res Rec* 2018;2627(28):235–43.
- [153] Li R, Guo Q, Du H, Pei J. Mechanical property and analysis of asphalt components based on molecular dynamics simulation. *J Chem* 2017;1531632.
- [154] Yao H, Dai Q, You Z, Bick A, Wang M. Modulus simulation of asphalt binder models using molecular dynamics (MD) method. *Constr Build Mater* 2018;162:430–41.
- [155] Hou Y, Wang L, Wang D, Qu X, Wu J. Using a molecular dynamics simulation to investigate asphalt nano-cracking under external loading conditions. *Applied Sciences* 2017;7:770.
- [156] Xie M, Yi J, Feng D, Huang Y, Wang D. Analysis of adhesive characteristics of asphalt based on atomic force microscopy and molecular dynamics simulation. *ACS Appl Mater Interfaces* 2016;8:12393–403.
- [157] Tang J, Wang H. Coarse grained modelling of nanostructure and asphaltene aggregation in asphalt binder using dissipative particle dynamics. *Constr Build Mater* 2022;314:125605.
- [158] Yu R, Wang Q, Wang W, Xiao Y, Wang Z, Zhou X, et al. Polyurethane/graphene oxide nanocomposite and its modified asphalt binder: preparation, properties and molecular dynamics simulation. *Mater Des* 2021;209:109994.
- [159] Wang F, Xiao Y, Cui P, Lin J, Li M, Chen Z. Correlation of asphalt performance indicators and aging degrees: A review. *Constr Build Mater* 2020;250:118824.
- [160] Xue L, Shao Y, Zhong W, Ben H, Li K. Molecular dynamic simulation on the oxidation process of coal tar pitch. *Fuel* 2019;242:50–61.
- [161] Fu T, Wei J, Bao H, Liang J. Multiscale study on the modification mechanism of red mud modified asphalt. *Adv Mater Sci Eng* 2020;2150215.
- [162] Zeng Q, Liu Q, Liu P, Chen C, Kong J. Study on modification mechanism of nano-ZnO/polymerised styrene butadiene composite modified asphalt using density functional theory. *Road Materials and Pavement Design* 2020;21(5):1426–38.
- [163] Liu J, Liu Q, Wang S, Zhang X, Xiao C, Yu B. Molecular dynamics evaluation of activation mechanism of rejuvenator in reclaimed asphalt pavement (RAP) binder. *Constr Build Mater* 2021;298:123898.
- [164] Li M, Liu L, Xing C, Liu L, Wang H. Influence of rejuvenator preheating temperature and recycled mixture's curing time on performance of hot recycled mixtures. *Constr Build Mater* 2021;295:123616.
- [165] Li G, Gu Z, Tan Y, Xing C, Zhang J, Zhang C. Research on the phase structure of Styrene-Butadiene-Styrene modified asphalt based on molecular dynamics. *Constr Build Mater* 2022;326:126933.
- [166] Hu D, Gu X, Lyu L, Wang G, Cui B. Unraveling oxidative aging behavior of asphaltenes using ab initio molecular dynamics and static density functional theory. *Constr Build Mater* 2022;318:126032.
- [167] Sun W, Wang H. Molecular dynamics simulation of nano-crack formation in asphalt binder with different SARA fractions. *Mol Simul* 2022;1–12.
- [168] Guo F, Zhang J, Chen Z, Zhang M, Pei J, Li R. Investigation of friction behavior between tire and pavement by molecular dynamics simulations. *Constr Build Mater* 2021;300:124037.
- [169] Zhu X, Yuan Y, Li L, Du Y, Li F. Identification of interfacial transition zone in asphalt concrete based on nano-scale metrology techniques. *Mater Des* 2017;129:91–102.
- [170] Fini EH, Samieadel A, Rajib A. Moisture damage and its relation to surface adsorption/desorption of rejuvenators. *Ind Eng Chem Res* 2020;59:13414–9.